Scenario-Based Robust Facility Layout Design for Multi-Block Manufacturing: A Data-Driven MILP Framework with an Industrial Application

by

Sadra Shoarinejad

A Dissertation Submitted to the
Graduate School of Sciences and Engineering
in Partial Fulfillment of the Requirements for
the Degree of

Doctor of Philosophy

in

Industrial Engineering

KOÇ ÜNİVERSİTESİ

September, 2025

Scenario-Based Robust Facility Layout Design for Multi-Block Manufacturing: A Data-Driven MILP Framework with an Industrial Application

Koç University
Graduate School of Sciences and Engineering

This is to certify that I have examined this copy of a doctoral dissertation by

Sadra Shoarinejad

and have found that it is complete and satisfactory in all respects,
and that any and all revisions required by the final
examining committee have been made.

Committee Members:

Prof. Metin Türkay (Advisor)

Assoc. Prof. Barış Yıldız

Prof. Sibel Salman

Assoc. Prof. İhsan Yanıkoğlu

Prof. Fadime Üney Yüksektepe

Date:

DEDICATION

To my beloved family...

ABSTRACT

Scenario-Based Robust Facility Layout Design for Multi-Block Manufacturing: A Data-Driven MILP Framework with an Industrial Application
Sadra Shoarinejad
Doctor of Philosophy in Industrial Engineering
September, 2025

This dissertation addresses the Unequal-Area Facility Layout Problem (UA-FLP) under uncertainty, with a particular focus on multi-block manufacturing environments where material flows are complex and subject to disruption. The motivation for this research stems from the limitations of traditional deterministic layout models, which often fail to accommodate the operational variability and spatial constraints characteristic of modern industrial systems. In response, the study proposes a structured and data-driven modeling framework based on mixed-integer linear programming (MILP), progressively incorporating realistic constraints and robustness features to enhance layout feasibility and long-term performance.

The thesis begins with the development of a deterministic MILP model that assigns departments of unequal area to two fixed-size layout blocks. The model minimizes total transportation cost while integrating key industrial features such as AEIOUX-based closeness preferences, ramp-based inter-block material transfer, and capacity-constrained flow routing across multiple ramps. Building on this foundation, the second stage introduces a Gamma-robust optimization model that protects against material flow uncertainty by incorporating worst-case deviation terms. The uncertainty parameters are derived from a three-year historical flow dataset using a weighted two-sigma rule, and a protection level is applied to ensure robust yet cost-efficient layouts.

In the final stage, a scenario-based robust MILP model is developed. Ten disruption scenarios are defined to represent potential operational disturbances, including ramp closures, peak demand surges, and supply shortages. Scenario-dependent flow matrices, ramp capacities, and external transportation costs are incorporated while

maintaining a single, unified layout across all scenarios. The model allows for flexible flow redistribution and evaluates spatial configuration through penalty terms, offering a balanced trade-off between cost minimization and layout resilience. Scenario probabilities are used to assess expected performance and solution stability.

The proposed framework is applied to a real-world case study involving the washing machine production plant of a leading home appliance manufacturer. The layout problem involves assigning 21 departments to two connected blocks under realistic spatial and operational constraints. Historical data from 2022 to 2024 is used to quantify uncertainty and validate the robustness of the proposed solutions. The scenario-based results are analyzed through a detailed cost breakdown, ramp utilization metrics, AEIOUX separation penalties, and layout visualizations. The findings demonstrate that the proposed robust layout configurations maintain feasible and efficient performance across a wide range of disruption scenarios.

This dissertation contributes a comprehensive and implementable framework for solving robust multi-block facility layout problems under uncertainty. By integrating practical layout requirements, historical data-driven uncertainty modeling, and scenario-based robustness, the study advances both the theoretical understanding and industrial applicability of robust facility layout design. The resulting methodology provides a scalable decision-support tool for long-term facility planning in dynamic manufacturing environments.

ÖZETÇE

Çok Bloklu İmalat için Senaryo Odaklı Dayanıklı Tesis Yerleşim Tasarımı: Endüstriyel Uygulamalı Veri Tabanlı Bir Karma Tamsayılı Doğrusal Programlama (MILP) Modeli Çerçevesi

Sadra Shoarinejad
Endüstri Mühendisliği, Doktora
Ağustos 2025

Bu tez, belirsizlik altında çok bloklu üretim ortamlarında karmaşık ve kesintiye açık malzeme akışlarının söz konusu olduğu Unequal-Area Facility Layout Problem (UA-FLP)'yi ele almaktadır. Araştırmanın temel motivasyonu, geleneksel deterministik yerleşim modellerinin, modern endüstriyel sistemlerin karakteristik özellikleri olan operasyonel değişkenlik ve mekânsal kısıtları yeterince dikkate alamaması gerçeğinden kaynaklanmaktadır. Bu kapsamda, çalışmada mixed-integer linear programming (MILP) tabanlı, gerçekçi kısıtları ve dayanıklılık unsurlarını aşamalı olarak içeren yapılandırılmış ve veri odaklı bir modelleme çerçevesi önerilmektedir. Amaç, yerleşim fizibilitesini artırmak ve uzun vadeli performansı güvence altına almaktır.

Tez, ilk olarak iki sabit boyutlu yerleşim bloğuna farklı alan gereksinimlerine sahip departmanların atanmasını amaçlayan deterministik bir MILP modeliyle başlamaktadır. Model, toplam taşıma maliyetini minimize etmeyi hedeflerken, endüstriyel açıdan önemli bazı özellikleri de içermektedir: AEIOUX tabanlı yakınlık tercihleri, bloklar arası malzeme transferinin rampalar üzerinden yönlendirilmesi ve kapasiteye dayalı çoklu rampa akışı gibi. Bu temel üzerine inşa edilen ikinci aşamada, malzeme akışındaki belirsizliğe karşı koruma sağlamak amacıyla Gamma-robust bir optimizasyon modeli geliştirilmiştir. Belirsizlik parametreleri, 2022–2024 yılları arasındaki üç yıllık tarihsel veri seti üzerinden ağırlıklı iki sigma kuralı kullanılarak hesaplanmış ve maliyet etkinliği ile dayanıklılık arasında denge kuracak şekilde bir koruma seviyesi belirlenmiştir.

Son aşamada, scenario-based robust MILP modeli geliştirilmiştir. Bu kapsamda, rampaların kullanılamaması, üretim talebindeki ani artışlar ve tedarik problemleri gibi potansiyel operasyonel bozulmaları temsil eden on farklı senaryo tanımlanmıştır.

Modelde senaryoya bağlı malzeme akış matrisleri, rampa kapasiteleri ve dış taşıma maliyetleri dikkate alınmış; tüm senaryolar için ortak bir yerleşim planı korunmuştur. Akışların farklı senaryolarda rampalar arasında esnek şekilde yeniden dağıtılmasına izin verilmiş, ayrıca yerleşim yapılandırması penalty terimleri ile değerlendirilmiştir. Senaryo olasılıkları, beklenen performansın ve çözüm kararlılığının ölçülmesinde kullanılmıştır.

Önerilen modelleme çerçevesi, önde gelen bir beyaz eşya üreticisinin çamaşır makinesi üretim tesisinde uygulanan bir gerçek dünya vaka çalışmasıyla test edilmiştir. Yerleşim problemi, 21 departmanın mekânsal ve operasyonel kısıtlar altında iki bağlantılı bloğa atanmasını kapsamaktadır. 2022–2024 dönemine ait tarihsel veriler, belirsizliğin nicelenmesinde ve modelin dayanıklılığının doğrulanmasında kullanılmıştır. Senaryo temelli sonuçlar, ayrıntılı maliyet dökümü, rampa kullanım oranları, AEIOUX ayrışma cezaları ve yerleşim görselleştirmeleri ile analiz edilmiştir. Bulgular, önerilen dayanıklı yerleşim konfigürasyonlarının çeşitli bozulma senaryoları altında dahi fizibilitesini ve verimliliğini koruduğunu göstermektedir.

Bu tez, belirsizlik altında robust multi-block facility layout problemlerinin çözümüne yönelik kapsamlı ve uygulanabilir bir çerçeve sunmaktadır. Gerçekçi yerleşim gereksinimlerini, tarihsel veriye dayalı belirsizlik modellemesini ve senaryo tabanlı dayanıklılığı entegre ederek, hem teorik bilgi birikimine hem de endüstriyel uygulamalara önemli katkılar sağlamaktadır. Geliştirilen metodoloji, dinamik üretim ortamlarında uzun vadeli tesis yerleşim planlaması için ölçeklenebilir ve veri destekli bir karar destek aracı olarak öne çıkmaktadır.

ACKNOWLEDGMENTS

I would like to express my deepest gratitude to my advisor, Prof. Dr. Metin Türkay, for his invaluable guidance, support, and encouragement throughout my doctoral studies. His insight, patience, and dedication have been instrumental in shaping both my academic and personal development during this journey. I would also like to thank Assoc. Prof. Dr. Barış Yıldız and Dr. İhsan Yanıkoğlu, members of my thesis monitoring committee, for their insightful comments on my thesis, as well as Prof. Dr. Fadime Üney Yüksektepe and Prof. Dr. Sibel Salman, members of my thesis jury, for being part of my committee.

I would like to extend my heartfelt appreciation to my family for their endless love, patience, and encouragement. Their unwavering support has been my greatest source of strength throughout this journey.

I would also like to thank my friends and colleagues for their understanding, support, and the pleasant moments we shared during this challenging process.

Finally, I gratefully acknowledge the financial support of TÜBİTAK under the BIDEB 2244 Industrial PhD Fellowship Program (Grant No. 118C128), which made this research possible.

TABLE OF CONTENTS

LIST OF TABLES

LIST OF FIGURES

ABBREVIATIONS

FLP	Facility Layout Problem
UA-FLP	Unequal-Area Facility Layout Problem
MILP	Mixed-Integer Linear Programming
RO	Robust Optimization
RCPSP	Resource-Constrained Project Scheduling Problem
AEIOUX	Activity Relationship Ratings (A, E, I, O, U, X)

Chapter 1

INTRODUCTION

Facility Layout Problem (FLP) is a classic and critical issue in industrial engineering and operations research, fundamental for designing efficient manufacturing systems. Essentially, FLP involves deciding the optimal placement of departments, machines, or workstations within a facility to minimize material handling costs and improve overall production efficiency [Deshpande et al., 2016, Sun et al., 2018]. A well-designed facility layout significantly influences the long-term performance of manufacturing operations by reducing unnecessary movements, lowering production time, minimizing resource consumption, and ultimately reducing operating costs [Navidi et al., 2012, Ku et al., 2011]. Conversely, an inefficient layout can lead to increased material transportation, longer cycle times, higher energy consumption, and escalated operational expenses. Even incremental improvements in facility layout can yield substantial cost savings and productivity enhancements, highlighting its strategic importance.

Historically, FLP research has extensively explored various optimization techniques and methods. Traditionally, many of these studies simplified the problem by assuming equal-sized departments and fixed, deterministic flow patterns. Such assumptions made it easier to model mathematically and computationally solve the layout problem. However, these simplified models often failed to reflect realistic industrial conditions, as actual manufacturing departments usually vary significantly in size, shape, and operational constraints [Loiola et al., 2007, Grobelny and Michalski, 2017]. Recognizing this limitation, researchers have shifted their focus to more realistic scenarios, notably the Unequal-Area Facility Layout Problem (UA-FLP). UA-FLPs aim to place departments of varying dimensions without overlaps in constrained facility spaces, adding considerable complexity and computational challenges compared to their equal-area counterparts [Drira et al., 2007].

Beyond handling unequal areas, facility layouts also face complex spatial and operational constraints such as physical barriers, fixed infrastructure, safety regulations, and vehicle movement pathways. These constraints significantly influence the feasibility and practicality of layout solutions. For example, [Besbes et al., 2020] demonstrated that barriers like walls, pillars, and unused spaces could substantially affect feasible department placements and material routing, especially in automated transportation scenarios involving forklifts and Automated Guided Vehicles (AGVs).

Alongside spatial considerations, facility layout models can be classified based on their temporal assumptions: Static Facility Layout Problem (SFLP) and Dynamic Facility Layout Problem (DFLP). SFLP assumes stable operational conditions and fixed material flows, optimizing department positions for a consistent production scenario. While this static assumption simplifies the problem, modern manufacturing environments rarely operate under such stable conditions due to factors like fluctuating demand, product variety, and technological advancements [Singh and Sharma, 2006]. These dynamic production realities necessitate reconfigurations and adaptable layouts to maintain efficiency. Therefore, DFLP has gained traction, aiming to design layouts that can adapt across multiple periods to reflect changing production requirements. However, despite their theoretical advantages, dynamic layouts typically involve substantial rearrangement costs and downtime, limiting their practical applicability [Hosseini-Nasab et al., 2018, Kikolski et al., 2018, Anjos and Vieira, 2017].

Although this thesis does not propose dynamic rearrangements over time, it focuses on developing robust static layouts that remain effective under changing production conditions. The aim is to minimize layout disruptions while improving the long-term performance of the system. This balance between stability and flexibility is achieved by incorporating uncertainty into the layout model, enabling it to handle fluctuations in material flow without frequent reconfiguration.

Additionally, a critical yet under-addressed factor in FLP research is uncertainty.

Traditional models usually assume deterministic, fixed material flows between departments. However, in practical industrial settings, material flows can vary significantly due to seasonality, machine downtime, production changes, and market fluctuations. This uncertainty in material flows can severely impact layout performance if not appropriately accounted for, especially in industries like home appliance manufacturing, characterized by frequent product changes, varied department interactions, and multiple transportation modes. Hence, incorporating uncertainty into FLP models is crucial for designing realistic and resilient layouts [Derakhshan Asl and Wong, 2017].

The literature shows multiple attempts at addressing uncertainty, primarily using probabilistic, interval-based, or scenario-based methods. For example, [Peng et al., 2018] addressed stochastic material flows, while Yazdani et al. (2020) proposed robust optimization models considering diverse uncertainty scenarios. Although these approaches improved theoretical robustness, most studies relied on simplified, hypothetical scenarios that overlooked intricate real-world conditions, detailed operational constraints, and unequal-area departments. Moreover, few studies have systematically measured uncertainty levels from actual historical production data or effectively integrated them into robust optimization frameworks. Consequently, there is a significant gap between theoretical robust layout models and practical industrial applications.

To bridge these critical gaps, this thesis proposes a comprehensive, data-driven robust optimization framework specifically tailored for unequal-area facility layouts under realistic operational conditions. The approach employs Mixed-Integer Linear Programming (MILP) to incorporate detailed spatial constraints, such as department sizes, adjacency preferences, and non-overlapping requirements. Crucially, it systematically captures material flow uncertainty by analyzing real-world historical production data, using statistical methods to quantify variability accurately. This data-driven approach ensures that the resulting facility layout is robust against actual production fluctuations, balancing computational efficiency, layout realism, and practical adaptability.

This research is grounded in a real-world industrial application from a leading home appliance manufacturing company based in Turkey, providing a practical and relevant context for testing and validating the proposed models. The selected production facility operates at high capacity and includes several distinct departments such as plastic injection, metal forming, painting, sub-assembly, and final assembly. These departments are physically distributed across two separate layout blocks, reflecting the structural realities of many modern large-scale manufacturing systems. Material transfer between these blocks is carried out through designated internal transportation ramps, utilizing forklifts and other handling equipment, which introduces logistical challenges related to flow routing, ramp availability, and capacity constraints.

This industrial use case plays a central role in the thesis, as it offers a complex yet realistic operational environment that captures the spatial limitations, flow variability, and functional relationships typical in real production settings. By integrating actual flow data, department dimensions, adjacency preferences, and transportation rules from this facility, the thesis ensures that the developed models are not only mathematically sound but also practically applicable. Furthermore, the collaboration with the industrial partner allowed access to historical production records, enabling a data-driven approach to estimate flow uncertainty and evaluate layout performance under different disruption scenarios. This strong connection between the proposed optimization models and real-world manufacturing requirements significantly enhances the practical value and academic relevance of the research.

Furthermore, this thesis provides an extensive real-world application by implementing the proposed robust optimization framework in a home appliance manufacturing facility belonging to a prominent industry leader. This implementation highlights practical considerations, demonstrates the feasibility of the robust layout model, and offers concrete evidence of its effectiveness. The study specifically examines how robust layouts perform under realistic production variability, illustrating tangible benefits in reducing material handling costs and improving operational resilience.

By addressing the identified gaps—real-world applicability, unequal-area departments, realistic operational constraints, and data-driven uncertainty estimation—this research contributes significantly to the existing FLP literature. It not only extends robust optimization methods into more complex and realistic industrial scenarios but also provides a clear methodological pathway for practitioners aiming to enhance factory layouts in dynamic and uncertain manufacturing environments. The results underscore the practical value of robust optimization approaches and reinforce their potential to transform facility layout planning from theoretical models into actionable, resilient industrial solutions.

1.1 Research Questions

Based on the identified gaps in the literature and the objectives of this study, the following research questions were formulated:

- **RQ1.** How can the unequal-area facility layout problem be modeled in multi-block industrial settings in a way that reflects practical flow structures and spatial constraints?

- **RQ2.** To what extent can a deterministic optimization approach provide feasible and cost-effective layout solutions when applied to a real-world production environment?

- **RQ3.** How can data-driven techniques be integrated into facility layout modeling to account for flow uncertainty and improve the robustness of the solutions?

- **RQ4.** What modeling strategies can be used to address multiple operational disruption scenarios, and how can these strategies contribute to more resilient and adaptable facility layouts?

- **RQ5.** How effective are the proposed robust layout models in delivering practical decision support for long-term facility planning in manufacturing systems?

1.2 Research Objectives

This thesis aims to address the challenges of unequal-area facility layout design in uncertain, real-world production environments. The key objectives of the study are as follows:

- To formulate a deterministic Mixed-Integer Linear Programming (MILP) model for the Unequal-Area Facility Layout Problem (UA-FLP) in multi-block settings, incorporating flow-based cost, ramp-based routing, capacity constraints, and spatial preferences.

- To develop a data-driven robust layout model using historical production data and the robust optimization approach to handle material flow variability.

- To extend the model further by creating a scenario-based robust optimization framework that captures layout performance under multiple operational disruptions, such as ramp failures, peak demand, and supply shortages.

- To implement and validate the proposed models using real industrial data from a home appliance production facility, demonstrating practical feasibility and layout resilience.

- To analyze the trade-offs between cost efficiency, robustness, and operational flexibility across different robust modeling approaches.

1.3 Thesis Statement

The core statement of this PhD dissertation is as follows: This thesis focuses on solving the Unequal Area Facility Layout Problem (UA-FLP) by using a Mixed-Integer Linear Programming (MILP) model under flow uncertainty by leveraging historical production data from a real-world manufacturing plant. The proposed model, formulated as a mixed-integer linear program (MILP), integrates a budgeted uncertainty approach to generate layouts that are efficient, flexible, and practically applicable in dynamic industrial environments. To improve the quality of the layout under uncertain conditions, the MILP model is extended with a robust optimization approach. The aim is to find a layout that performs well even when the flow values are time-varying. For this purpose, historical data from a home appliance factory in Turkey is collected to estimate the variability in material movement between departments.The model incorporates this variability to hedge against worst-case scenarios without resorting to frequent layout rearrangements. The thesis provides a novel application of robust optimization theory in a real production setting, thereby bridging the gap between theory and practice in facility layout research.

To contribute to this gap in the literature, this thesis applies a data-driven robust MILP model to a real use case. The selected factory produces home appliances and includes various departments like plastic injection, metal forming, and assembly. These departments are physically separated, and materials are transferred between them using internal transportation vehicles. Historical data on material flows are collected from the factory database. Then, uncertainty levels are calculated based on observed variations in the data. These levels are added to the optimization model using a budgeted uncertainty method, which allows the model to consider different possible outcomes and avoid overly optimistic solutions.

In this way, the layout model becomes more flexible and realistic. It does not rely on a single flow value for each department pair. Instead, it considers a range of possible flows and tries to find a layout that works well in most cases, including the worst ones. This approach helps the company reduce risks and avoid high costs when unexpected changes happen.

Using a MILP model has some advantages. It allows the model to include various constraints, such as department sizes, distances, and adjacency requirements. Although MILP models are sometimes hard to solve, they give high-quality solutions for layout problems, especially when combined with robust optimization techniques.

This thesis has three main contributions. First, it develops a robust layout model for unequal area departments using real data from a factory. Second, it proposes a method to measure uncertainty in material flows based on historical records. Third, it shows how this model can be applied in practice by solving a real-world problem and analyzing the results.

The structure of the thesis is organized as follows. Chapter 2 reviews the literature on facility layout, covering traditional models as well as robust and dynamic approaches. Chapter 3 explains the mathematical formulation of the proposed model and its components. Chapter 4 describes the data used for the study, including how uncertainty values were calculated from historical production records. Chapter 5 presents the case study, showing how the model was applied to a real home appliance factory and discussing the results. Finally, Chapter 6 concludes the thesis and offers suggestions for future research directions.

In summary, this thesis provides a practical and academically valuable method for solving facility layout problems under uncertainty, especially for large manufacturing systems with complex material flows and real operational limitations.

Chapter 2

LITERATURE REVIEW

2.1 Introduction

Facility layout design is a long-standing yet ever-evolving challenge in industrial engineering, involving the optimal arrangement of departments, machines, or workstations within a facility to enhance efficiency and reduce costs. Traditionally, the focus of most studies has been on minimizing material handling costs under static conditions using deterministic data, particularly in single-floor manufacturing environments. However, recent advances in production technology, the emergence of flexible and reconfigurable systems, and growing sustainability concerns have driven researchers to explore more complex, realistic settings such as dynamic, uncertain, and multi-floor environments.

In particular, layout design has become significantly more intricate with the inclusion of varying material flows, vertical transportation constraints, and the need to accommodate changing demand or product mixes. These aspects have introduced new dimensions to modeling facility layouts—such as dynamic facility layout problems (DFLPs), robust and stochastic formulations, and multi-objective approaches combining cost, energy, and environmental considerations.

Recent surveys have highlighted the expanding scope of this field. [Drira et al., 2007] provided a structured classification of layout problems based on space configuration, decision variables, and solution methods. More recently, [Ahmadi et al., 2017] emphasized the growing relevance of multi-floor layouts, where interactions between departments involve vertical as well as horizontal dimensions, and where elevator design, floor allocation, and travel distance modeling require specialized formulations. [Pérez-Gosende et al., 2021] also reviewed developments in heuristic, metaheuristic, and hybrid optimization techniques tailored for real-world applications, showing how intelligent algorithms are increasingly integrated with simulation and mathematical programming to solve complex layout configurations.

This chapter provides a structured review of the existing literature on facility layout problems, categorized based on methodology. It covers optimization-based models, dynamic and robust layout techniques, simulation-based frameworks, and machine learning approaches. Special attention is given to models that integrate realistic constraints, sustainability metrics, and practical implementation insights, aiming to guide the development of more resilient and adaptive layout designs for modern industrial systems.

2.2 Metaheuristic and Mathematical Optimization-Based Approaches

A significant portion of the literature on facility layout problems (FLPs) has focused on optimization-based techniques, including both mathematical programming and metaheuristics. These methods aim to solve increasingly complex layout challenges—such as unequal-area departments, energy-efficient designs, multi-floor configurations, or dynamic reconfigurations—while improving material handling efficiency, minimizing cost, or maximizing space usage. A wide range of problem-specific models and algorithms have been developed to address the diversity of industrial settings.

Some studies focused on mathematical modeling and hybrid heuristics to improve layout decision-making in specific contexts. For example, [Dorrah and Marzouk, 2021] presented a layout framework for multi-purpose buildings that combines agent-based modeling, queuing theory, and a multi-objective assignment model. Their model captured user movement and comfort, balancing these factors with energy efficiency to optimize the space layout of an administrative facility. In connector assembly problems, where cabling and piping dominate cost, [Zhang and Lin, 2024] proposed a hybrid model that combines multi-agent reinforcement learning with 3D A* search. The MARL framework used Wolf Policy Hill-Climbing and achieved better performance in stability, efficiency, and solution quality than classical genetic algorithms and ant colony optimization. Similarly, [Subulan et al., 2023] tackled unequal-area capability-based FLPs using a heuristic decomposition-based iterative mathematical programming model that incorporated machine capabilities. Their approach optimized facility positions and capability distributions, improving layout efficiency and productivity.

In metaheuristic-based research, a number of innovative algorithms have emerged. A learning-based simulated annealing (LSA) method was proposed by [Lin et al., 2024] to solve UA-FLPs by combining reinforcement learning with a two-stage greedy local search. Their approach offered improved convergence and superior solutions in complex scenarios. In a real manufacturing case, [Guo et al., 2023] applied a modified NSGA-II to optimize both material handling and closeness ratings in an air-conditioner plant. Their results demonstrated improved logistics and safety performance over traditional GA-based methods. For multi-row layouts with through-aisle structures, [Zhang et al., 2024b] combined teaching–learning-based optimization with linear programming to minimize logistics costs. Their hybrid model generated superior designs with better material flow efficiency.

Recent studies have also expanded the scope of optimization to include energy and sustainability metrics. [Zhang et al., 2022] developed an energy-efficient layout model using multi-objective particle swarm optimization. By treating energy consumed by AGVs as a primary criterion along with transport distance, they demonstrated that layout design significantly affects operational energy usage. Similarly, [Peron et al., 2020] argued for transforming layout planning into a dynamic process using 3D mapping, motion capture, and indoor positioning systems, making layouts more adaptive and environmentally conscious. Warehouse layout challenges were addressed by [Mayadunne et al., 2024], who proposed a two-step MILP model for storage maximization and optimal bin sizing. Their solution improved storage capacity while maintaining efficiency and adaptability.

Specialized metaheuristic approaches were applied to other layout variants. [Kim and Chae, 2019] used Monarch Butterfly Optimization (MBO) to minimize loop length in single-loop systems with AGVs. Their model incorporated a slicing tree structure to build efficient paths through departments. In multi-workshop environments, [Guan et al., 2019] proposed a model that minimizes both internal and external transport costs, solved with a discrete MOPSO algorithm that used two optimization stages—layout encoding and refinement via linear programming. [Ji et al., 2023] presented a double-row layout model with fixed loading/unloading points, solved using discrete differential evolution. This model accounted for safety and flow direction and performed well in a real-world reducer workshop.

Several studies explored reinforcement learning and dynamic systems. [Kaven et al., 2024] applied MARL to flexible assembly layouts and scheduling, where mobile units adapt to changing jobs. Their model used proximal policy optimization and outperformed random agents in uncertain conditions. [Liu et al., 2018] introduced a particle swarm optimization method for UA-FLPs, combining material handling, closeness ratings, and space efficiency via an objective space division technique. [Zolfi and Jouzdani, 2023] developed a continuous layout model across multiple floors with dynamic demand and included elevator count and placement as decision variables. They used simulated annealing to solve large instances that exact methods could not handle.

Some models incorporated complex geometric and spatial constraints. [Liu et al., 2020] presented a configuration space evolutionary algorithm for UA-FLPs that respected aspect ratios, material flows, and closeness/distance requirements. [Lotfi et al., 2022] addressed renewable energy facility location under uncertainty using a robust stochastic model with an ε-constraint solution, improving both output and profit in energy planning. Meanwhile, [Hussain et al., 2023] modeled fog computing placement in smart cities as a facility location problem, solved with a hybrid SONG algorithm combining PSO and NSGA-II to balance delay and energy.

In manufacturing environments, [Motahari et al., 2023] optimized both part family scheduling and group layout using an ε-constraint method and NSGA-II. Their model included physical machine size, flexible routing, and machine capacity. [Kubalík et al., 2023] designed a layout model with fixed shape/cost workstation variants and extended their evolutionary algorithm to accommodate these constraints through new mutation operators and a cooling strategy. [Amaral, 2024] addressed double row layouts using an enhanced MILP model with tightened constraints and valid inequalities, solving larger problem instances more efficiently than earlier models.

More complex environments have also inspired new metaheuristic models. [Wei et al., 2019] proposed a chaotic genetic algorithm for reconfigurable manufacturing layouts with relocation costs and material handling, using Tent mapping to boost search diversity. Their approach outperformed standard GAs on real cases. [Rubio et al., 2021] optimized robotic manufacturing layouts by minimizing robot and transport time under energy constraints, using Pareto analysis to support planning. [Das et al., 2024] modeled a two-stage logistics layout problem with carbon constraints and triangular type-2 neutrosophic numbers. Solved via ε-constraint, their model showed superior results in carbon control and customer satisfaction.

Layout planning in multi-floor buildings was addressed by [Che et al., 2017], who required same-department rooms to be adjacent and solved the problem using an exact ε-constraint method. [Liu and Liu, 2019] introduced a multi-objective ant colony algorithm with local search and gradient descent to generate Pareto-optimal layouts in UA-FLP. [Klar et al., 2022] explored DDQN for large-scale layout design with 20 departments, showing that action masking and reward modifications improved learning and layout quality.

Dynamic and uncertain environments received further attention. [Zhun et al., 2021] applied a fuzzy demand-based layout model using pigeon-inspired optimization with elite archiving and fuzzy numbers. [Besbes et al., 2021] combined GA with A* to solve realistic 2D layouts including machine orientation and obstacles. [Jolai et al., 2012] tackled DFLP using a nonlinear model and improved PSO that avoided overlap and improved solution diversity.

Complex constraints were tackled in other advanced formulations. [Liu et al., 2022b] added machine order and adjacency rules into a double-row layout and used discrete differential evolution to solve it. [Seyedi et al., 2024] developed a mixed-integer nonlinear model for dynamic layouts with flexible I/O, solved with enhanced

GA and PSO. [Ohmori and Yoshimoto, 2021] proposed a fast solution using primal-dual interior-point methods and a compact linear model to improve runtime. [Klausnitzer and Lasch, 2018] integrated layout, path, and aisle planning into one MILP model, minimizing travel distances on actual paths.

Energy and scheduling integration was explored by [Lu et al., 2021], who combined LSTM-based price forecasting with MILP for demand response optimization in production. [Muhayat and Utamima, 2024] compared DE and PSO for UA-FLP with I/O points, finding DE better for larger layouts. [Sherali et al., 2003] introduced MIP formulations with tighter disjunctive and polyhedral constraints to reduce runtime and improve optimality. [Kulturel-Konak and Konak, 2013] combined LP with GA using a novel shape representation to avoid infeasible solutions and improve solution accuracy.

Handling uncertainty in material flow, [Kaveh et al., 2014] proposed fuzzy programming models (expected value, chance-constrained, and dependent-chance) solved via hybrid GAs and simulated annealing. Their results showed SA performed better overall. [Garcia-Hernandez et al., 2020] developed a Coral Reef Optimization algorithm with substrate layers that applied multiple mutation strategies across benchmark problems, confirming robustness and solution diversity.

Multi-objective trade-offs were addressed by [Saeidi, 2024] using fuzzy goal programming and an artificial bee colony algorithm. Their model balanced material handling and closeness in cases up to 100 departments, with better results than PSO. [Feng and Che, 2018] created ILP models for rectangular departments, improving variable efficiency and solving all benchmark cases to optimality. [La Scalia et al., 2019] introduced a firefly algorithm using slicing encoding to optimize aspect ratio and cost. [Abedzadeh et al., 2013] proposed a fuzzy MILP model solved with PVNS, outperforming GAMS on large dynamic layouts.

Lastly, [Matai, 2015] proposed a simulated annealing algorithm for MOFLP that included automated weighting and a three-stage heuristic. Their modified SA improved solution quality and convergence, outperforming earlier methods. [Shoushtari et al., 2024] developed a two-stage layout framework using LSTM for demand forecasting and GA for optimization, showing more adaptive and sustainable layouts. [Kalita and Datta, 2024] solved a multi-floor layout model with four objectives using a permutation-based GA, generating Pareto-efficient designs in cases with up to 80 departments. [Bozorgi et al., 2014] integrated DEA with tabu search, applying dynamic penalties and frequency-based memory to outperform earlier methods on dynamic layouts. Finally, [Oktaviani and Utamima, 2024] presented a population-based simulated annealing method with elite memory and comparison to ACO, showing strong scalability and layout efficiency. [Emami and Nookabadi, 2013] modeled DFLPs with separate objectives and applied five solvers, identifying NSGA-II and DE as best performers, with fuzzy TOPSIS used for final layout selection. [Tayal and Singh, 2018] combined big data analytics and hybrid firefly-chaotic SA for dynamic FLPs, incorporating factor analysis and handling stochastic demand effectively. [Raja and Anbumalar, 2016] focused on cell formation and intra-cell layout using parts visit data, minimizing voids and movements, and improving MGTE performance measures across benchmark tests.

Altogether, these contributions demonstrate that mathematical and metaheuristic optimization models are capable of handling a wide variety of realistic layout planning scenarios. They incorporate dynamic, multi-objective, stochastic, and domain-specific elements, highlighting their flexibility and relevance for modern industrial applications.

2.3 Dynamic and Robust Layout Models

In real manufacturing environments, layouts must often remain efficient despite uncertain or fluctuating conditions such as variable demand, supply disruptions, or changing product flows. Instead of relying on frequent reconfigurations—which are typically costly and disruptive—many researchers have proposed robust and dynamic facility layout models that can absorb variability or adjust through internal system flexibility. These models are designed to ensure performance stability across multiple scenarios and time periods, and they increasingly reflect industrial realities such as limited space, physical constraints, and high reconfiguration costs.

A common way to represent uncertainty in optimization is through predefined scenarios that capture different possible futures. Scenario-based models aim to ensure that the chosen solution remains effective under each scenario, and this method has been extensively studied in the operations research field. One of the earliest general models for scenario-based optimization was proposed by [Mulvey et al., 1995], who introduced a mathematical approach to handle uncertainty by evaluating solutions across multiple predefined scenarios. In their model, decisions are separated into two types: those made before the uncertainty is revealed, and those that can be adjusted afterward. The aim is to find solutions that stay close to optimal while keeping constraint violations minimal under each scenario. To achieve this, they proposed a weighted objective function that balances performance and feasibility. Their method was applied to several real-world problems, including energy planning and financial portfolio design, and showed improved stability compared to traditional models, especially when working with noisy or incomplete data. Building on these foundations, [Snyder and Daskin, 2006] explored related scenario-based modeling techniques that use discrete scenarios with known probabilities to capture uncertainty in optimization problems. They discussed expected cost minimization, chance constraints, and two-stage decision models as key mathematical tools for managing performance across scenarios, and highlighted how these methods can help balance cost and reliability in uncertain planning environments. In the context of facility layout, [Krishnan et al., 2008] developed a model that considers different production scenarios over time in a dynamic manufacturing environment. Their method aimed to reduce total cost, including both material handling and layout rearrangement costs, by designing layouts that can perform well across multiple future conditions. Using a scenario-based framework where each scenario represents a different product demand and mix, the model was solved with a genetic algorithm and tested through a case study involving varying part flows across planning periods. The results showed that incorporating multiple scenarios helped produce layouts that were more adaptable and cost-efficient than single-scenario or static approaches. Similarly, [Jung et al., 2010] optimized facility layout under multiple toxic gas release scenarios by using different dispersion cases to guide safe placement of facilities. Here, scenario-based optimization was applied to reduce overall risk while satisfying layout constraints, and the results demonstrated that adjusting facility positions based on scenario analysis significantly reduced risk and total cost compared to traditional layouts. In a related study, [Díaz-Ovalle et al., 2010] developed a facility layout model for chemical plants aimed at minimizing human risk from toxic gas leaks. They defined a worst-case scenario based on environmental conditions and used it to guide the placement of process units. Their layout problem was formulated as a mixed-integer nonlinear program, combining safety, dispersion modeling, and spatial constraints, and the findings confirmed that scenario-based planning led to safer layouts compared to traditional distance-based methods. Addressing uncertainty in material flows, [Şahinkoç and Bilge, 2018] focused on solving the facility layout problem using a scenario-based approach where each scenario represents a different flow matrix, with the goal of finding a single layout that performs well across all of them. They modeled the problem as a quadratic assignment problem (QAP), incorporating scenario probabilities in the objective function, and developed a genetic algorithm with a new solution encoding to solve the model efficiently. Their results showed that layouts designed using multiple scenarios were more reliable and performed better than those optimized for only a single case. In contrast, [Reisinger et al., 2022] proposed a framework that generates multiple layout scenarios using a multi-objective evolutionary algorithm. Although not scenario-based in the classical optimization sense, their method—where each production area is modeled as a 3D cube—balances transport distance, layout density, and space flexibility. Tested on a real factory case, it produced compact and feasible layouts, offering a flexible approach for comparing alternatives in early design stages. Expanding the scope to energy systems, [Zhang et al., 2024a] proposed a novel optimization method for wind farm layout design by combining reinforcement learning with particle swarm optimization. Their model aims to maximize energy output by reducing wake effects between turbines under multiple wind scenarios. A reinforcement learning agent adjusts the search behavior dynamically, improving convergence and solution quality. While different from classical facility layout models, this study contributes to scenario-based layout planning in uncertain environments and shows how learning-based optimization can be effective. To further extend this line of work, [Shoushtari et al., 2024] proposed a two-stage layout model that integrates machine learning and genetic algorithms to handle uncertain demand and environmental concerns. In the first stage, an LSTM model forecasts different demand scenarios, followed by a second stage in which a genetic algorithm optimizes the facility layout while minimizing material handling cost, energy use, and waste. The results showed that while the sustainable layout incurred slightly higher costs, it significantly improved environmental performance. This study highlights how combining learning-based forecasting with scenario-driven layout optimization can lead to more adaptable and sustainable manufacturing systems.

Several studies have proposed robust layout methods to deal with uncertainty in a more general and flexible way. One such effort is presented by [Pourvaziri et al., 2021], who focused on robust layout design in flexible manufacturing environments. Rather than modifying the layout dynamically in response to demand fluctuation, they proposed a more practical approach that keeps the layout fixed and uses alternative routing strategies to adapt to changing conditions. Their model, formulated as a mixed-integer linear program, incorporates unequal-area departments, orientation flexibility, and multiple time periods. To handle the model's computational complexity, they introduced a hybrid metaheuristic approach that first applies Design of Experiments (DOE) to identify the most critical planning period and then uses a Genetic–Tabu Search (GATS) algorithm to optimize the layout for that period. The resulting layouts were found to be robust across all planning horizons, offering a cost-effective solution in contexts where physical changes are limited by operational constraints.

Similarly, [Cheng et al., 2021] developed a robust two-stage optimization model for facility location decisions under demand uncertainty and disruption risk. In their model, decisions about where to place facilities are made before uncertainties are realized, while customer allocations are determined afterwards. This separation allows the model to adapt to various scenarios of uncertainty. They proposed a column-and-constraint generation algorithm to solve the model efficiently and demonstrated that disruption risks play a more significant role than demand variability in influencing optimal layout decisions. By identifying and protecting critical facilities, the model reduces the worst-case costs and increases overall system resilience.

Incorporating more dynamic aspects, [Xiao et al., 2019] addressed the unequal-area dynamic facility layout problem (UA-DFLP) under uncertain demand. Their robust optimization model introduces pick-up and drop-off (P/D) points to more accurately calculate material handling costs and reflects operational realities more effectively. They enhanced the solution approach using an improved particle swarm optimization (PSO) algorithm that integrates mutation and local search strategies. Their findings show that the proposed model effectively minimizes rearrangement costs and maintains high performance under demand variability, demonstrating the benefit of using advanced metaheuristics for robust layout design.

Broader uncertainty considerations are seen in the work of [Liu et al., 2022a], who focused on virtual power plants (VPPs) operating in uncertain market environments with wind energy generation. Although not a classical facility layout problem, their two-stage data-driven robust optimization model is relevant for managing spatial and resource allocation under uncertainty. Using a Wasserstein distributionally robust framework and conditional value-at-risk (CVaR) measures, their approach deals with both uncertain pricing and power availability. They further enhanced realism by integrating data-driven power flow constraints derived from historical data. Tested on an IEEE 33-bus system, the model demonstrated improved reliability and better out-of-sample performance compared to traditional robust or stochastic optimization models, showing its value for dynamic, data-intensive applications.

In a practical healthcare context, [Tongur et al., 2020] addressed the large-scale layout problem of a hospital consisting of 26 polyclinics. They aimed to minimize the total movement cost for both patients and staff by using real consultation and traffic data in combination with three metaheuristic algorithms: Migrating Birds Optimization (MBO), Tabu Search (TS), and Simulated Annealing (SA). Among these, MBO and SA yielded the best performance, with MBO showing particularly strong results due to its ability to intensify local search and exchange information between solutions. Their findings showed a 58% improvement over the hospital's existing layout, confirming the value of metaheuristics in handling large, data-rich and dynamic facility planning scenarios.

Multi-floor environments with vertical transportation needs add further complexity to robust layout design. [Izadinia et al., 2014] proposed a mathematical model that tackles this issue by placing departments on upper floors and storage areas in the basement, connected by elevators. Their model integrates demand uncertainty through the [Bertsimas and Sim, 2004] robust optimization framework and avoids layout changes by adjusting only the internal routing of materials. The nonlinear formulation was linearized for computational efficiency and tested on multiple cases. Results confirmed that this robust layout design could maintain stable performance without frequent reconfiguration, offering a practical solution for space-constrained manufacturing environments.

Focusing on stochastic demand, [Moslemipour et al., 2017] introduced a quadratic assignment model that optimizes layout over several planning periods without rearranging facilities. They assumed demand follows a normal distribution and used dynamic programming in combination with simulated annealing to solve the model. Compared to traditional static and even previous robust models, their approach achieved lower long-term costs and better adaptability to demand fluctuations. Sensitivity analysis revealed that the expected demand level was the most influential parameter, emphasizing the importance of reliable demand forecasting for robust layout planning.

Lastly, [Peng et al., 2018] developed a robust approach to the stochastic dynamic facility layout problem that incorporates transport device assignments. Their method combines Monte Carlo simulation with an improved genetic algorithm to address the dual objectives of minimizing material handling and rearrangement costs. By generating layouts that are consistent across a variety of demand scenarios, their approach proved especially effective for large-scale problems. The study showed that including transportation system planning within the layout optimization framework can lead to solutions that perform more reliably under uncertainty and help reduce operational costs in variable-demand environments.

Altogether, these studies demonstrate that dynamic and robust layout models are essential for maintaining layout performance under uncertainty. Whether through multi-period planning, advanced heuristics, or scenario-based optimization, each of these contributions helps bridge the gap between theoretical modeling and practical implementation in unstable and complex manufacturing systems.

2.4 Simulation-Based Approaches

In recent years, simulation-based approaches have become increasingly important in facility layout planning, as they enable researchers and practitioners to evaluate design alternatives under realistic conditions. These techniques are especially valuable when the physical layout interacts with dynamic processes such as transportation, production flow, and human behavior. The integration of discrete event simulation, agent-based modeling, machine learning, and reinforcement learning into optimization models allows for deeper analysis of system performance and decision-making under uncertainty.

One of the studies that exemplifies this direction is by [Bi et al., 2024], who proposed a workshop layout optimization method that uses the Sparrow Search Algorithm (SSA). Their objective was to minimize transportation costs and improve non-logistic relationships within the workshop. The authors created a mathematical layout model and solved it with SSA, then validated their results using FlexSim simulation software. Compared to traditional genetic algorithms, the SSA significantly reduced travel distances while also improving qualitative factors. This result demonstrated that SSA provides stable and efficient layout solutions for workshop environments where both logistics and interpersonal relationships matter.

Another advanced approach was introduced by [Klar et al., 2024], who developed a deep reinforcement learning (RL) framework tailored for multi-objective layout planning in factories. While earlier RL methods focused only on minimizing transport distance, this study introduced dynamic and multi-dimensional objectives such as throughput time and media supply. They incorporated discrete event simulation to evaluate layout performance and tested two RL architectures. Among them, the linear scalarization architecture showed better performance than the parallel agent model. Their framework outperformed traditional optimization methods like Genetic Algorithms (GA) and NSGA-II when given sufficient training time. Moreover, transfer learning from pre-trained agents was shown to greatly reduce training time and improve solution quality, making their RL approach more practical for industrial planning scenarios.

The integration of simulation and optimization was also central to the methodology proposed by [Zúñiga et al., 2020]. They developed a structured five-phase approach that combines discrete event simulation with optimization to solve layout problems, especially in legacy systems with outdated production flows. Their phases—awareness, diagnosis, development, evaluation, and conclusion—guided the redesign of facility layouts by addressing both production and logistics inefficiencies. Two industrial case studies confirmed that the methodology resulted in more practical, resilient, and usable layouts. To validate its robustness, they also applied functional resonance analysis, reinforcing the suitability of simulation-based approaches for complex industrial settings.

An intelligent layout framework that combines optimization and simulation was proposed by [Choi and Kim, 2024]. Their approach integrates mixed-integer linear programming (MILP), simulation-based optimization, and digital twin technologies into one automated loop. This system continuously refines factory layouts by simulating and evaluating candidate solutions. The result is a significant reduction in the time and effort required to identify optimal designs. Their method showed strong potential for improving the responsiveness and efficiency of layout planning, especially in adaptive production systems.

Simulation has also been applied in non-traditional settings, as demonstrated by [Gao et al., 2024]. In their work on sponge city infrastructure design, they combined a stormwater management simulation model (SWMM), response surface regression, and particle swarm optimization to determine optimal ratios of green infrastructure elements such as rain gardens, green roofs, and permeable pavements. Their results showed that the hybrid simulation-optimization approach effectively balanced environmental impact, spatial constraints, and cost, offering practical layout guidance for urban water management.

Modeling realistic spatial constraints has also been a key focus. [?] proposed a layout optimization method that accounts for walls, obstacles, and specific transportation paths using the A* pathfinding algorithm. Instead of assuming straight-line distances, they calculated realistic travel paths and combined this with a genetic algorithm to search for feasible layout solutions. Monte Carlo simulations were used to tune parameters. Their findings emphasized the practical benefits of incorporating detailed spatial constraints in layout models, resulting in more realistic and cost-effective designs.

In the context of modular construction manufacturing, [Yang and Lu, 2023] used simulation-based optimization to compare different layout types. Their study analyzed five alternatives, including cellular and product layouts, under real manufacturing conditions. The results showed that while the cellular layout yielded the highest productivity, the product layout was more economical. This highlights the importance of layout type in influencing production performance in modular systems.

Safety considerations were addressed by [Vasudevan and Son, 2011], who developed a multi-paradigm simulation framework for balancing productivity with evacuation safety in manufacturing facilities. Their model used agent-based simulation with a Belief-Desire-Intention (BDI) architecture to simulate emergency evacuations based on virtual reality data. In parallel, they used discrete event simulation to measure productivity. The study showed that process layouts offered a good trade-off between evacuation time and efficiency, challenging the assumption that safety and productivity always conflict in layout design.

The application of simulation was also used to enhance computational models. [Lee, 2012] developed an MILP model for the unequal-area layout problem that includes closeness ratings, flexible department shapes, and adjacency constraints. By incorporating preprocessing and valid inequalities, the authors improved computation speed and solution quality. Their results on benchmark instances showed better performance than earlier models, validating the usefulness of simulation-enhanced formulations.

Data mining and simulation were combined by [Altuntas and Selim, 2012], who proposed a weighted association rule mining approach for layout planning. They assigned weights to machines based on demand, handling frequency, and equipment efficiency, and developed five algorithms—MINWAL, WARM, and BWARM variants. Simulations were used to evaluate layout alternatives. Their study was the first to apply weighted association rule mining in facility layout design and showed that integrating data-driven insights can significantly improve decision-making.

Finally, a multi-method decision framework was introduced by [Shahin and Poormostafa, 2011], who combined simulation, fuzzy AHP, QFD, and TOPSIS in a comprehensive facility layout evaluation method. Quantitative measures such as cost and waiting time were simulated, while qualitative aspects like accessibility and flexibility were assessed using fuzzy AHP. The weightings were determined through QFD, and TOPSIS was applied for ranking alternatives. Their results demonstrated more balanced and reliable layout decisions in a manufacturing environment, confirming the advantage of combining simulation with structured decision-making tools.

Overall, these studies show that simulation-based approaches offer flexible, accurate, and realistic tools for evaluating facility layout plans. By integrating simulation with optimization models, machine learning, and decision analysis methods, researchers are better equipped to handle the complexity and dynamism of modern production environments. These methods also allow for the inclusion of human behavior, energy constraints, and real-world movement paths, creating layouts that are not only efficient but also safer and more adaptable.

2.5 Domain-Specific Applications and Decision Frameworks

In recent years, many researchers have focused on applying facility layout planning methods to specific domains, such as healthcare, agriculture, public services, and manufacturing. These studies often combine traditional layout planning tools like Systematic Layout Planning (SLP) and simulation with decision-making frameworks such as fuzzy logic, multi-criteria decision-making (MCDM), and machine learning. This section reviews such domain-specific applications and highlights how customized methods can improve layout quality in different industries.

One group of studies focuses on manufacturing environments. For example, [Badharinath et al., 2024] applied SLP to redesign the layout of a gear bush production facility that was struggling with low capacity. By analyzing material flow and machine relationships using activity and relationship diagrams, they reduced material travel distance by 34% and doubled monthly output. Similarly, [Nenzhelele et al., 2023] proposed a hybrid decision-making method that combines Fuzzy AHP and Fuzzy TOPSIS to select the best layout for a railcar manufacturing plant. They used Discrete Event Simulation (DES) to provide objective performance measures—such as productivity and lead time—which were then used in the fuzzy MCDM model to reduce subjectivity. Their results showed that integrating simulation with fuzzy decision-making leads to more accurate and confident layout choices.

In the field of smart agriculture, [Gao et al., 2023] designed a layout planning framework for automated greenhouses. They combined SLP with simulation to improve the design of a head lettuce greenhouse. The chosen layout plan, tested with Tecnomatix Plant Simulation, reduced labor intensity and travel distance while increasing production efficiency by 67%. This study shows how layout planning methods can be adapted to emerging sectors like precision farming, where automation and spatial efficiency are key.

Healthcare applications also benefit from customized layout evaluation tools. [Lin and Wang, 2019] focused on improving the layout of hospital operating theatres by combining SLP, fuzzy AHP, and human reliability analysis. Using the SHELL model (which considers software, hardware, environment, and human interaction), they evaluated two alternative layouts under uncertainty. Their results highlighted the importance of including safety and human factors in layout planning to improve decision quality in sensitive environments like surgery rooms.

New tools have also been introduced to support layout research itself. For example, [Heinbach et al., 2024] developed an open-source Python package called gym-flp, based on OpenAI Gym, to provide a flexible and standardized testbed for applying reinforcement learning (RL) to facility layout problems. The environment includes both discrete and continuous layout versions, 199 benchmark problems, and supports popular RL algorithms such as PPO and DQN. This tool is useful for researchers aiming to compare RL strategies without developing custom environments from scratch.

From a broader planning perspective, public service facility distribution has also been studied using layout analysis. [Keyimu et al., 2024] used Gini coefficients and location entropy to measure the fairness of facility distribution in cities. By analyzing spatial layout against population density, they found patterns of imbalance—such as under-served dense urban areas and over-served low-density zones. Their study suggests that people-centered planning approaches can improve the equity of public service layouts in urban development.

Lastly, [Usuga Cadavid et al., 2020] reviewed how machine learning (ML) is used in production planning and control in Industry 4.0. Their systematic literature review identified key ML methods, data sources, and current challenges. Although progress has been made, the study pointed out that ML applications in layout planning are still limited, especially in terms of environmental integration and logistics. This gap offers future research opportunities to expand the use of ML for layout optimization in dynamic and data-rich environments.

In summary, domain-specific layout studies show how traditional planning tools can be enhanced with simulation, fuzzy logic, or machine learning to address industry-specific needs. Whether improving production lines, hospital safety, smart farming, or public services, these tailored methods offer better layout decisions by combining practical constraints with modern analytics.

2.6 Summary and Conclusions

This chapter reviewed a wide range of studies on the facility layout problem (FLP), showing how the field has developed over time to deal with more complex and realistic challenges. Early research mostly focused on static and deterministic models, often using simplified assumptions such as equal-area departments and single-floor layouts. Over the years, more advanced methods like metaheuristics, mathematical optimization, and hybrid techniques have been introduced to solve larger and more practical problems, including those with unequal-area departments, non-rectangular shapes, closeness ratings, or energy consumption goals.

In particular, scenario-based optimization has emerged as a widely used method to represent uncertainty. These models rely on a set of predefined scenarios that capture possible future states of the system, allowing researchers to evaluate layout performance under diverse conditions. Scenario-based approaches have been successfully applied in dynamic manufacturing, chemical safety, and energy systems, demonstrating improved adaptability and risk reduction compared to traditional single-scenario models. They offer a practical framework for anticipating variability in demand, flow, and operational disruptions without requiring frequent layout reconfiguration.

We have also seen that many researchers have moved toward multi-objective and robust models, especially in environments with uncertainty or variability in demand and material flows. Robust optimization, dynamic reconfiguration, and stochastic programming are now common tools to make layout models more adaptive and practical. In addition, simulation-based approaches have become more popular, allowing designers to evaluate how layouts perform under realistic production conditions, including human behavior, energy use, and safety. Machine learning and reinforcement learning have also started to play a role in generating layouts and learning from complex environments, especially when data is available.

Despite these improvements, there are still important gaps in the literature.

Most studies still focus on simplified layout problems or do not combine different aspects of complexity in a single model. For example, only a few works deal with both uncertainty and vertical transportation at the same time, or consider real spatial constraints like ramps, elevators, or limited access zones. Moreover, while many models are tested on academic benchmarks, fewer are developed using real industrial data or implemented in practice. The integration of layout design with actual transportation networks, detailed cost components, and ramp assignment decisions is rarely explored in the existing literature. This shows that there is still a need for more practical, data-driven, and industry-supported layout models that can be applied in real manufacturing systems.

The current thesis aims to address these gaps by proposing a scenario-based robust layout model that incorporates realistic forms of uncertainty. Unlike most previous models, our approach uses actual historical data from a real manufacturing facility, considers both material handling flows and spatial constraints—including inter-block routing and ramp assignments—and applies optimization techniques capable of solving large-scale problems. By adopting a scenario-based framework, the model can evaluate layout performance across multiple operational conditions, improving adaptability and resilience. In doing so, this study contributes to narrowing the gap between academic modeling and industrial practice, offering practical solutions for designing stable and efficient facility layouts under uncertainty.

Chapter 3

MATHEMATICAL FRAMEWORK

3.1 Introduction

Designing an efficient facility layout is one of the most important tasks in a manufacturing environment. When multiple departments must be placed within separate blocks of a factory, the layout problem becomes more complex, especially when each department has unequal area requirements. A good layout reduces unnecessary movement, shortens production time, and lowers the total cost of material handling. In this section, we introduce a detailed mathematical model that aims to optimize the layout by minimizing the total transportation cost among departments. The model is formulated as a Mixed-Integer Linear Programming (MILP) problem using static input data, which serves as the foundation for the more advanced robust and data-driven models introduced in the following chapters.

3.1.1 Model Structure and Purpose

This basic model focuses on placing departments inside fixed-size blocks in a way that reduces the total material handling cost. Each department is assigned to exactly one block, and its location within that block is defined using coordinate variables. The transportation cost between departments depends on their distances and the flow of materials between them. If two departments are in the same block, their horizontal and vertical distances are computed within that block. If they are located in different blocks, the model calculates the inter-block distance accordingly. These distances are then weighted by the material flow and cost coefficients to compute the total cost. The final objective is to find the optimal layout that minimizes this total cost.

The model integrates both combinatorial decisions (which department goes to which block) and continuous variables (location coordinates within each block). This combination makes the problem more flexible and realistic, but also more challenging to solve, especially as the number of departments increases.

This formulation represents a Mixed-Integer Nonlinear Programming (MINLP) problem with quadratic assignment characteristics, incorporating both discrete location decisions and continuous spatial positioning within a multi-block facility layout optimization framework.

The model integrates combinatorial assignment decisions with geometric positioning constraints, making it computationally challenging for large-scale instances. The objective function minimizes material handling costs through optimal department placement and spatial arrangement within the available facility blocks.

3.1.2 Index Sets and Notation

- $\mathcal{D} = \{1, 2, \ldots, n\}$: Collection of organizational units (Workstations)
- $\mathcal{B} = \{1, 2, \ldots, m\}$: Available facility blocks
- $(i, j) \in \mathcal{D} \times \mathcal{D}, i \neq j$: Interdepartmental relationships
- $(r, s) \in \mathcal{B} \times \mathcal{B}$: Spatial block relationships

3.1.3 Input Parameters

Dimensional Specifications

- L_i: Horizontal dimension of department i
- W_i: Vertical dimension of department i
- $\bar{L}$: Standard horizontal dimension per block
- $\bar{W}$: Standard vertical dimension per block

Flow Characteristics

- p_{ij}: Material flow between departments i and j
- $\delta_{ij} \in \{0, 1\}$: Flow frequency ($\delta_{ij} = 1$ if flow exists)

Cost Structure

- c_{ij}^{int}: Intra-block transportation cost
- c_{ij}^{ext}: Inter-block transportation cost

System Parameters

- $|\mathcal{D}|$: Total number of departments
- $|\mathcal{B}|$: Total number of available blocks

The set $\mathcal{D}$ represents all departments or workstations that must be placed in the layout. These departments can have different sizes and requirements. $\mathcal{B}$ is the set of available facility blocks, each of which has fixed horizontal and vertical dimensions given by $\bar{L}$ and $\bar{W}$. For each department $i \in \mathcal{D}$, the dimensions L_i and W_i are given and can differ from one department to another, representing the unequal-area nature of the problem.

The material flow between departments i and j is represented by p_{ij}, and the binary parameter δ_{ij} indicates whether any material flow exists. The cost coefficients c_{ij}^{int} and c^{ext} represent the cost per unit distance for intra-block and inter-block movements, respectively. These cost values reflect the relative importance or difficulty of moving materials within the same block compared to moving them between blocks.

3.1.4 Decision Variables

Several sets of decision variables are introduced to define department assignments and locations, calculate distances, and enforce layout constraints.

Location Variables

- $X_{ir}, Y_{ir} \in \mathbb{R}_{\geq 0}$: Centroid coordinates of department i within block r

Assignment Variables

- $Z_{ir} \in \{0, 1\}$: Assignment indicator ($Z_{ir} = 1$ if department i occupies block r)

- $\Omega_r \in \{0, 1\}$: Block utilization indicator ($\Omega_r = 1$ if block r is active)

Proximity Variables

- $u_{ijr} \in \{0, 1\}$: Co-location indicator ($u_{ijr} = 1$ if both i and j are in block r)

Positioning Variables

- $\Pi_{ijr}, \Theta_{ijr} \in \{0, 1\}$: Relative positioning indicators for departments within blocks

Distance Variables

- $ExtD_{ij} \in \mathbb{R}_{\geq 0}$: External Manhattan distance

- $IntD_{ij}^{(x)}, IntD_{ij}^{(y)} \in \mathbb{R}_{\geq 0}$: Internal Manhattan distances (horizontal and vertical)

3.1.5 Objective Function

The model seeks to minimize total transportation costs:

$$\text{minimize} \quad \sum_{(i,j):i \neq j} p_{ij}\delta_{ij} \left[c_{ij}^{\text{int}} (IntD_{ij}^{(x)} + IntD_{ij}^{(y)}) + c_{ij}^{\text{ext}} ExtD_{ij} \right] \tag{3.1}$$

3.1.6 Constraints

Inter-Block Distance Enforcement

For all department pairs (i, j) and block pairs (r, s):

$$ExtD_{ij} \geq |r - s| \cdot \bar{L} - (|\mathcal{B}| - 1)\bar{L} \cdot (2 - Z_{ir} - Z_{js}) \quad \forall i \neq j, \forall r, s \in \mathcal{B} \tag{3.2}$$

$$ExtD_{ij} \geq |s - r| \cdot \bar{L} - (|\mathcal{B}| - 1)\bar{L} \cdot (2 - Z_{ir} - Z_{js}) \quad \forall i \neq j, \forall r, s \in \mathcal{B} \tag{3.3}$$

Intra-Block Distance Computation

For departments within the same block:

$$IntD_{ij}^{(x)} \geq X_{ir} - X_{jr} - \bar{L}(1 - u_{ijr}) \quad \forall i \neq j, \forall r \in \mathcal{B} \tag{3.4}$$

$$IntD_{ij}^{(x)} \geq X_{jr} - X_{ir} - \bar{L}(1 - u_{ijr}) \quad \forall i \neq j, \forall r \in \mathcal{B} \tag{3.5}$$

$$IntD_{ij}^{(y)} \geq Y_{ir} - Y_{jr} - \bar{W}(1 - u_{ijr}) \quad \forall i \neq j, \forall r \in \mathcal{B} \tag{3.6}$$

$$IntD_{ij}^{(y)} \geq Y_{jr} - Y_{ir} - \bar{W}(1 - u_{ijr}) \quad \forall i \neq j, \forall r \in \mathcal{B} \tag{3.7}$$

Cross-Block Distance Relations

For departments in different blocks:

$$IntD_{ij}^{(x)} \geq X_{ir} + X_{js} - 2\bar{L} \sum_{t \in \mathcal{B}} u_{ijt} \quad \forall i \neq j, \forall r, s \in \mathcal{B} \tag{3.8}$$

$$IntD_{ij}^{(y)} \geq Y_{ir} + Y_{js} - 2\bar{W} \sum_{t \in \mathcal{B}} u_{ijt} \quad \forall i \neq j, \forall r, s \in \mathcal{B} \tag{3.9}$$

Assignment Logic

Each department must be assigned to exactly one block:

$$\sum_{r \in \mathcal{B}} Z_{ir} = 1 \quad \forall i \in \mathcal{D} \tag{3.10}$$

Block utilization ordering (to eliminate symmetry):

$$\Omega_r \leq \Omega_{r-1} \quad \forall r \geq 2 \tag{3.11}$$

Block activation conditions:

$$\sum_{i \in \mathcal{D}} Z_{ir} \geq \Omega_r \quad \forall r \in \mathcal{B} \tag{3.12}$$

$$|\mathcal{D}| \cdot \Omega_r \geq \sum_{i \in \mathcal{D}} Z_{ir} \quad \forall r \in \mathcal{B} \tag{3.13}$$

Co-Location Logic

Departments are co-located if and only if they share the same block:

$$u_{ijr} \leq \frac{1}{2}(Z_{ir} + Z_{jr}) \quad \forall i \neq j, \forall r \in \mathcal{B} \tag{3.14}$$

$$u_{ijr} + 1 \geq Z_{ir} + Z_{jr} \quad \forall i \neq j, \forall r \in \mathcal{B} \tag{3.15}$$

Spatial Boundary Constraints

Department centroids must respect block boundaries:

$$\frac{L_i}{2} Z_{ir} \leq X_{ir} \leq \left(\bar{L} - \frac{L_i}{2}\right) Z_{ir} \quad \forall i \in \mathcal{D}, \forall r \in \mathcal{B} \tag{3.16}$$

$$\frac{W_i}{2} Z_{ir} \leq Y_{ir} \leq \left(\bar{W} - \frac{W_i}{2}\right) Z_{ir} \quad \forall i \in \mathcal{D}, \forall r \in \mathcal{B} \tag{3.17}$$

Relative Positioning Framework

Establish consistent ordering relationships:

$$\Pi_{ijr} + \Pi_{jir} = 1 \quad \forall i \neq j, \forall r \in \mathcal{B} \tag{3.18}$$

$$\Theta_{ijr} + \Theta_{jir} = 1 \quad \forall i \neq j, \forall r \in \mathcal{B} \tag{3.19}$$

Transitivity preservation:

$$\Pi_{isr} + \Pi_{sjr} - \Pi_{ijr} \leq 1 \quad \forall i \neq j \neq s, \forall r \in \mathcal{B} \tag{3.20}$$

$$\Theta_{isr} + \Theta_{sjr} - \Theta_{ijr} \leq 1 \quad \forall i \neq j \neq s, \forall r \in \mathcal{B} \tag{3.21}$$

Non-Overlap Enforcement

Prevent physical overlap of departments within blocks:

$$X_{ir} + \frac{L_i}{2} Z_{ir} \leq X_{jr} - \frac{L_j}{2} Z_{jr} + \bar{L}(2 - \Pi_{ijr} - \Theta_{ijr}) \quad \forall i \neq j, \forall r \in \mathcal{B} \tag{3.22}$$

$$Y_{ir} + \frac{W_i}{2} Z_{ir} \leq Y_{jr} - \frac{W_j}{2} Z_{jr} + \bar{W}(1 + \Pi_{ijr} - \Theta_{ijr}) \quad \forall i \neq j, \forall r \in \mathcal{B} \tag{3.23}$$

Equation (3.1) defines the objective function, which minimizes the total material handling cost by considering both intra-block and inter-block distances. The cost is calculated by multiplying the material flow amount p_{ij}, its existence indicator δ_{ij}, and the corresponding cost coefficients c_{ij}^{int} and c_{ij}^{ext} with the internal and external Manhattan distances between departments. Equations (3.2) and (3.3) determine the inter-block distance $ExtD_{ij}$ by calculating the distance between the assigned blocks of departments i and j, and activating the constraint only when departments are located in different blocks using assignment variables Z_{ir} and Z_{js}. Equations (3.4) to (3.7) compute the internal distances within the same block using horizontal and vertical distances between centroid coordinates. These are enforced only when both departments are co-located, as indicated by the binary variable u_{ijr}. Equations (3.8) and (3.9) capture the approximate cross-block internal distances by including penalty terms to ensure the layout remains spatially reasonable even for departments located in different blocks. Equation (3.10) guarantees that each department is assigned to exactly one block, preventing unassigned or multiply-assigned departments. Equation (3.11) removes symmetric solutions by ensuring that lower-indexed blocks are used before higher-indexed ones. Equations (3.12) and (3.13) connect the block usage indicator Ω_r to the presence of departments in that block, activating the block only if at least one department is assigned to it, and deactivating it if none are present. Equations (3.14) and (3.15) define the logic of co-location between departments based on their assignments and ensure that the co-location indicator u_{ijr} correctly reflects the presence of both departments in the same block. Equations (3.16) and (3.17) enforce the spatial boundaries by constraining the centroid of each department to lie within the assigned block, considering its width and length. Equations (3.18) and (3.19) assign a relative order between department pairs within the same block to help position them consistently either in the horizontal or vertical direction. Equations (3.20) and (3.21) ensure transitivity in relative positioning so that if department i is before s, and s is before j, then i must also come before j, maintaining logical consistency across multiple departments. Finally, Equations (3.22) and (3.23) ensure that no two departments overlap within a block by checking that the edges of their physical dimensions are properly separated based on their relative position. This set of constraints, taken together, defines a comprehensive model that optimally assigns and locates departments inside a multi-block facility layout to reduce transportation costs while maintaining feasibility in terms of space, assignment, and department interaction.

3.1.7 Application

To evaluate the performance and practical value of the proposed base facility layout model, we applied it to a real case from a washing machine production plant. This factory represents a typical high-volume production environment where different types of functional units—such as production lines, material warehouses, and final stock areas—must be placed effectively to reduce transportation costs and support a smooth material flow. The complexity of the layout problem in this plant is increased due to several factors: unequal department sizes, the use of multiple types of transportation vehicles, and the physical division of the layout space into two non-contiguous areas. The aim of this section is to illustrate how the base model behaves under real industrial conditions, using realistic data and operational parameters.

The facility includes 21 distinct departments that serve different roles within the production process. These include semi-product and final product warehouses, pre-assembly and assembly lines, foaming and packaging units, and a number of stock and raw material areas. The plant floor is divided into two separate rectangular zones that are treated as layout blocks in the model. These two zones—referred to as Block A and Block B—were selected based on the actual usable areas inside the plant. Each block has the same dimensions of 48 meters in width and 13 meters in length, and their sizes were derived from architectural layout documents prepared by the engineering team at manufacturer.

Each department has a different area requirement. Their length and width are fixed and must be respected during the placement process. Table 3.1 presents the full list of departments considered in the model, along with their spatial dimensions. These values were obtained from detailed CAD drawings and simulation tools used internally by manufacturer's Simulation and Modeling department. They reflect the true footprint that each department occupies on the shop floor.

Table 3.1: Department Dimensions and Area Descriptions

ID	Area Description	Length (m)	Width (m)
1	Mainplant Semi Product Warehouse	16.4343	4.5000
2	Plastic Warehous	12.8524	4.2251
3	Plastic Row Material Warehouse	6.9828	1.3662
4	Mechanic Warehouse	12.8524	3.0613
5	Export Goods Warehouse	20.5183	3.5673
6	Packaging Warehouse	11.6633	2.0746
7	Pre Assembly Line	15.7366	3.6685
8	Assembly Line	12.8018	3.5673
9	Final Assembly Line	12.8018	3.5673
10	Foamed Door Line	8.0960	3.0360
11	Packaging Line	11.6633	1.5686
12	Compressor Warehouse	7.0587	1.6344
13	Foamed Body Line	10.2718	3.6685
14	Door Glass Warehouse	2.9854	2.9095
15	Gasket Raw Material Warehouse	9.8417	2.9854
16	Pipe Roll Warehouse	20.5183	2.6565
17	Plastic Sheet Warehouse / Extruder	7.0195	2.5503
18	CTF	5.4142	4.3769
19	DTF	4.8323	3.0360
20	Fin Warehouse	26.6409	10.3730
21	Other Production	20.4778	5.6308

Table of material flow applied to this model presented in Table A.1 .The layout must place all departments within the two available blocks. Table 3.2 provides the specifications of each block used in the model. Since both blocks are identical in size, the assignment of departments becomes a key decision in reducing the transportation cost and managing congestion.

Table 3.2: Facility Block Dimesions

Block ID	**Dimensions (m)**
A	48.00 , 13.00
B	48.00 , 13.00

Material movement between departments takes place through different vehicle types, depending on the function and physical location of departments. The main transportation types used in the plant are forklifts, tow trucks, conveyors, and manual handling. To reflect the real-world cost of transportation, each vehicle type was assigned a cost index. These indices were developed in consultation with process engineers and logistics supervisors. Table 3.3 shows the cost index associated with each transportation mode.

Table 3.3: Material Handling Vehicle Cost Index

Vehicle Type	**Cost Index**
Manual	1
Conveyor	2
Tow Truck	3
Forklift	5

The model uses these cost indices in combination with the flow values between departments to compute a weighted transportation cost. The material flow matrix p_{ij} used in the application is based on production data for a high-load shift, where flow volumes are at their peak. By testing the model under these conditions, we ensured that the layout solution would remain effective even under stress. The intra-block and inter-block costs are calculated separately. Inter-block transportation has a higher penalty, as it usually involves longer travel paths and higher delays. The model tries to place departments with large mutual flows inside the same block whenever possible to minimize this penalty.

The model was implemented in Python 3.13.2 and solved using Gurobi Optimizer version 12.0.1 under an academic license. The tests were run on a MacBook Pro with an Apple M4 Pro processor, 24 GB of RAM, and macOS Ventura 14.5. The solver used up to 12 threads in parallel and was configured with a default relative MIP gap of 0.0001. The model converged to an optimal solution in 479 seconds. During this time, Gurobi explored more than 862,000 nodes and performed over 31 million simplex iterations. Multiple types of cutting planes were used, including 1010 MIR cuts, 3775 flow cover cuts, 240 Gomory cuts, and dozens of lift-and-project and RLT cuts, showing that the problem has high computational complexity and is nontrivial to solve.

The best objective value found was approximately 787,357 cost units, with a solver gap of less than 0.008%. The solver generated 10 distinct feasible solutions during the process, and all of them were very close in cost, indicating the solution space is tight but stable.

Table 3.4: Optimized Department Assignments and Coordinates

Dept. ID	**Block**	**x-coordinate (m)**	**y-coordinate (m)**
1	1	8.22	9.49
2	1	33.70	8.21
3	1	23.78	7.92
4	1	33.70	4.57
5	2	36.90	3.86
6	2	24.98	1.04
7	1	19.41	5.40
8	1	6.40	1.78
9	1	19.20	1.78
10	1	33.70	1.52
11	2	13.32	1.29
12	1	19.96	9.42
13	1	6.40	5.40
14	1	28.16	1.52
15	1	42.67	1.52
16	1	26.69	11.65
17	1	43.64	8.69
18	1	42.83	5.23
19	1	43.64	11.48
20	2	13.32	7.26
21	2	36.90	8.46

The final layout configuration divides the departments between Block A and Block B in a way that aligns well with operational logic. Figures 3.1 show the visual layout of the departments in each block after optimization. The model successfully places high-flow production lines such as the pre-assembly, main assembly, and final packaging in close proximity within Block A. Departments with more storage-oriented roles or lower interaction frequencies—such as export goods, fin warehouse, and pipe roll storage—are placed in Block B.

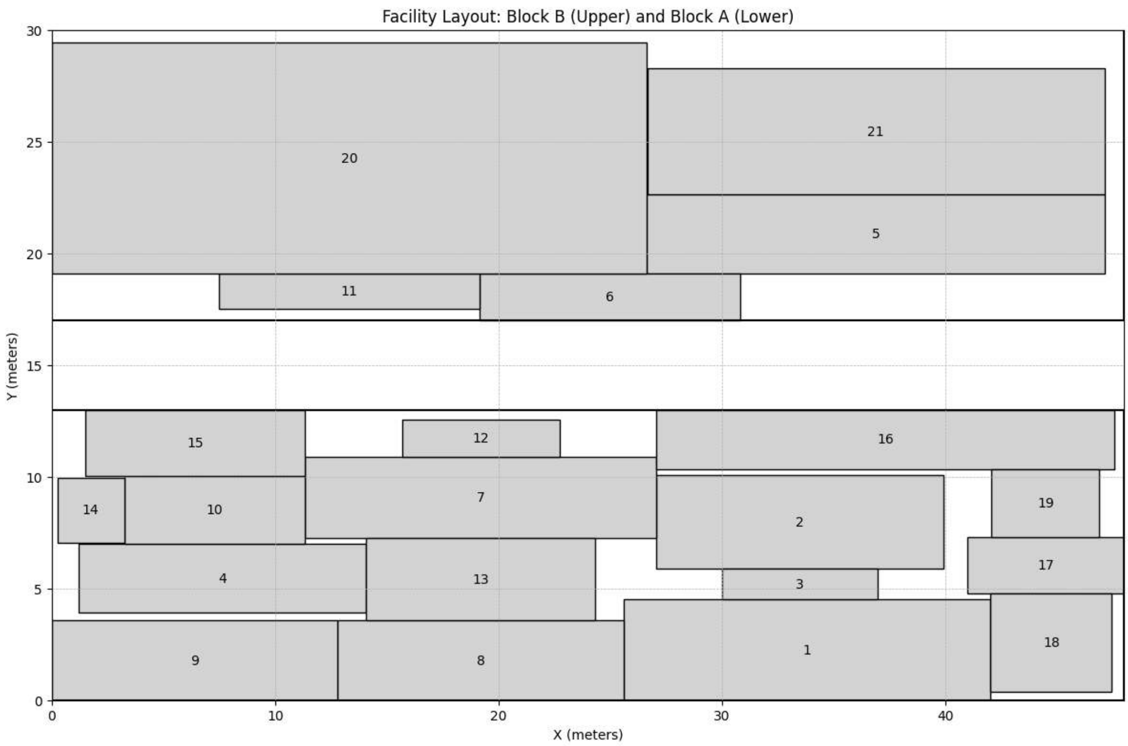

Figure 3.1: Optimized Layout Configuration

All spatial and assignment constraints were satisfied. No departments overlapped, and each one fit perfectly within the boundaries of its assigned block. Relative positioning constraints were enforced correctly, and transitivity was maintained across department relationships. The model also respected the logic of minimizing inter-block flows by grouping high-flow departments together.

The results show that the base model is capable of solving a real and complex layout problem under realistic industrial conditions. It generated a feasible and compact layout that makes sense operationally and reduces transportation costs effectively. The model's structure allows it to handle a combination of assignment and geometric constraints, and its application on real data demonstrates its value for decision-makers. The solution provides insights into how departments should be grouped and how block utilization can be optimized. Although this version uses static data, it sets a strong foundation for future improvements such as uncertainty modeling, shift-based layouts, and carbon emissions tracking.

Table 3.5: Material Handling Cost Comparison Between Initial and Optimized Layout

	Initial Layout	**Optimal Layout**	**Improvement**
Material Handling Unit Cost (Optimal Value)	1,558,260.14	787,356.73	-49.47%

To assess the effectiveness of the optimized layout generated by the model, we compared its material handling unit cost against the value calculated for the existing (initial) layout of the plant. The initial layout, based on the current departmental arrangement at the manufacturer's facility, yields a total transportation cost of 1,558,260.14 cost units. In contrast, the optimized layout generated by the model results in a significantly reduced transportation cost of 787,356.73 cost units. This corresponds to an improvement of approximately 49.47%, clearly demonstrating the potential benefit of applying mathematical optimization to facility layout planning (Table 3.5).

3.1.8 Summary

This section introduced the basic facility layout model, which serves as the foundation for more advanced formulations presented in the following parts of this chapter. The model focuses on minimizing total material handling cost by determining the optimal spatial arrangement of departments within a predefined number of fixed-size layout blocks. It integrates assignment decisions—selecting which department should go to which block—with continuous positioning of departments within those blocks, using coordinate-based logic. The formulation captures both intra-block and inter-block movement costs, enabling the model to reflect realistic transportation conditions in a multi-block industrial setting.

The model was developed as a Mixed-Integer Nonlinear Programming (MINLP) problem, with non-overlapping constraints, spatial boundaries, and relative positioning conditions embedded directly into the optimization structure. This formulation allows for flexible and realistic layout configurations, while also increasing the mathematical complexity of the problem. To validate its effectiveness, the model was implemented in Python and tested on a real case from a washing machine plant use case. The results confirmed that the model is capable of handling real industrial data and solving large-scale instances within a reasonable computational time.

When applied to the real-world dataset, the model achieved a significant reduction in total material handling cost—by approximately 49% compared to the actual layout currently used in the plant. All constraints were satisfied in the final layout, including spatial feasibility, block assignment rules, and relative positioning of departments. The optimization results not only demonstrate the model's ability to produce operationally meaningful layouts but also highlight the potential cost savings that can be realized through data-driven facility design.

While this basic model operates under deterministic assumptions with static input data, it provides a robust starting point for further exploration. In the subsequent sections, we extend this formulation by introducing methods to handle uncertainty in flow volumes, dynamic block utilization, and additional layout complexity such as ramp connectivity. These enhancements aim to bring the model closer to real production environments, where variability and operational constraints play a more critical role. As such, this basic layout model serves both as a benchmark and a stepping stone toward more adaptive and resilient layout optimization frameworks.

3.2 Improved Model

In the first part of this chapter, we introduced a basic MILP model for the facility layout problem, focusing on assigning departments to fixed-size blocks and positioning them to minimize total transportation cost. While the initial model captures the core structure of layout planning, it makes a few simplifying assumptions that may not reflect the complexities of real manufacturing systems. In particular, the earlier model treats inter-block transportation with a generic distance penalty and does not explicitly model how materials move between blocks. Additionally, it does not account for physical limitations such as ramp capacities or flow routing constraints.

To address these limitations, this section presents an improved version of the MILP model. The new formulation enhances the initial model in several key ways. First, it introduces a ramp-based inter-block flow structure. Instead of assuming that material can move freely between blocks, the improved model routes flows through designated ramp positions located at the boundaries of each block. These ramp connections represent realistic infrastructure elements such as tunnels, elevators, or transport lanes. Each ramp has a limited capacity, meaning it can only handle a certain volume of material flow. This change allows the model to reflect real-world logistics more accurately and helps identify potential bottlenecks in layout planning.

Second, the model now allows for the flexible use of multiple ramp pairs when routing flows between departments. The amount of flow between any two departments assigned to different blocks can be split across different ramp combinations, subject to ramp capacity limits. This flow flexibility makes the model more scalable and better suited for large facilities with complex movement patterns.

Third, a closeness penalty term is added to the objective function to ensure that departments with high interaction levels—such as frequently communicating or sequential processes—are placed in the same block whenever possible. This penalty encourages co-location of critical department pairs and supports a layout design that aligns with operational priorities.

The improved model still retains the structure of a deterministic MILP. It uses binary variables for assignment, positioning logic, and flow routing, alongside continuous variables for department coordinates and distance calculations. The objective remains focused on minimizing the total transportation cost, but now includes three components: internal movement cost within blocks, external cost based on ramp paths, and penalties for separating departments that should ideally be located close to each other.

In the following subsections, the mathematical formulation of the improved model is presented in full. Each set, parameter, and variable is defined clearly, followed by the objective function and the complete set of constraints.

Sets:

$i, j \in N$	Departments
$k, k_1, k_2 \in M$	Blocks
$r_1, r_2 \in R$	Ramp positions

Parameters:

l_i, w_i	Length and width of department i
LF, WF	Length and width of each block
p_{ij}	Flow from department i to j
$c_{ij}^{int},\ c^{ext}$	Internal and external unit transport costs
R_r	Capacity of ramp r
RC_{ij}	AEIOUX closeness importance score
δ	Fixed vertical ramp distance
x^r	X-position of ramp r

Decision Variables:

$Y_{ik} \in \{0,1\}$	1 if department i is assigned to block k
$S_k \in \{0,1\}$	1 if block k is used
$q_{ijk} \in \{0,1\}$	1 if departments i and j are both in block k
$\alpha_{ijk}, \beta_{ijk} \in \{0,1\}$	Non-overlap direction variables:
	(1,1): i precedes j horizontally;
	(0,0): j precedes i horizontally;
	(1,0): i precedes j vertically;
	(0,1): j precedes i vertically
$Z_{ijk_1k_2r_1r_2} \in \{0,1\}$	1 if flow from i in k_1 to j in k_2 uses ramps r_1, r_2
$x_{ik}, y_{ik} \geq 0$	Coordinates of the center of department i in block k
$d^{int}_{ij,x},\ d^{int}_{ij,y} \geq 0$	Internal horizontal and vertical distances between i and j
$d^{ext}_{ij} \geq 0$	External distance between departments i and j
$F_{ijk_1k_2r_1r_2} \geq 0$	Flow from i in k_1 to j in k_2 via ramps r_1, r_2

Objective Function

$$\min \sum_{i,j} p_{ij} \cdot c^{int}_{ij} \cdot (d^{int}_{ij,x} + d^{int}_{ij,y}) \tag{3.24}$$

$$+ \sum_{i,j,k_1 \neq k_2} \sum_{r_1,r_2} F_{ijk_1k_2r_1r_2} \cdot c^{ext} \cdot (|x^{r_1} - x^{r_2}| + \delta) \tag{3.25}$$

$$+ \sum_{i,j} RC_{ij} \cdot \left(1 - \sum_k q_{ijk}\right) \tag{3.26}$$

Subject to:

$$\sum_k Y_{ik} = 1 \quad \forall i \in N \tag{3.27}$$

$$\sum_{i} Y_{ik} \geq S_k \quad \forall k \in M \tag{3.28}$$

$$\sum_{i} Y_{ik} \leq n \cdot S_k \quad \forall k \in M \tag{3.29}$$

$$q_{ijk} \leq \tfrac{1}{2}(Y_{ik} + Y_{jk}) \quad \forall i, j, k \tag{3.30}$$

$$q_{ijk} + 1 \geq Y_{ik} + Y_{jk} \quad \forall i, j, k \tag{3.31}$$

$$\sum_{k_1 \neq k_2} \sum_{r_1, r_2} F_{ijk_1k_2r_1r_2} = p_{ij} \cdot (1 - \sum_{k} q_{ijk}) \quad \forall i \neq j \tag{3.32}$$

$$F_{ijk_1k_2r_1r_2} \leq p_{ij} \cdot Y_{ik_1} \cdot Y_{jk_2} \quad \forall i, j, k_1 \neq k_2, r_1, r_2 \tag{3.33}$$

$$\sum_{i,j} \sum_{k' \neq k} \sum_{r'} (F_{ijk'kr'r} + F_{ijkk'rr'}) \leq R_r \quad \forall k, r \tag{3.34}$$

$$d_{ij}^{ext} \cdot p_{ij} \cdot (1 - \sum_{k} q_{ijk}) \geq \sum_{k_1 \neq k_2} \sum_{r_1, r_2} F_{ijk_1k_2r_1r_2} \cdot (|x^{r_1} - x^{r_2}| + \delta) - M \cdot \sum_{k} q_{ijk} \quad \forall i \neq j \tag{3.35}$$

$$d_{ij}^{ext} \leq M \cdot (1 - \sum_{k} q_{ijk}) \quad \forall i \neq j \tag{3.36}$$

$$d_{ij,x}^{int} \geq |x_{ik} - x_{jk}| \quad \forall i \neq j, k \tag{3.37}$$

$$d_{ij,y}^{int} \geq |y_{ik} - y_{jk}| \quad \forall i \neq j, k \tag{3.38}$$

$$x_{ik} + 0.5 l_i Y_{ik} \leq x_{jk} - 0.5 l_j Y_{jk} + LF(2 - \alpha_{ijk} - \beta_{ijk}) \quad \forall i \neq j, k \tag{3.39}$$

$$y_{ik} + 0.5 w_i Y_{ik} \leq y_{jk} - 0.5 w_j Y_{jk} + WF(1 + \alpha_{ijk} - \beta_{ijk}) \quad \forall i \neq j, k \tag{3.40}$$

$$0.5 l_i Y_{ik} \leq x_{ik} \leq (LF - 0.5 l_i) Y_{ik} \quad \forall i, k \tag{3.41}$$

$$0.5 w_i Y_{ik} \leq y_{ik} \leq (WF - 0.5 w_i) Y_{ik} \quad \forall i, k \tag{3.42}$$

$$\alpha_{ijk} + \alpha_{jik} = 1 \quad \forall i \neq j, k \tag{3.43}$$

$$\beta_{ijk} + \beta_{jik} = 1 \quad \forall i \neq j, k \tag{3.44}$$

$$\alpha_{isk} + \alpha_{sjk} - \alpha_{ijk} \leq 1 \quad \forall i, s, j \text{ distinct}, k \tag{3.45}$$

$$\beta_{isk} + \beta_{sjk} - \beta_{ijk} \leq 1 \quad \forall i, s, j \text{ distinct}, k \tag{3.46}$$

The objective function of the improved model is defined through Equations (3.24) to (3.26), and aims to minimize the total material handling cost in the facility. It includes three distinct components. Equation (3.24) captures the cost of internal transportation between departments that are located within the same block. This is calculated by multiplying the internal flow volume p_{ij}, the unit internal cost c_{ij}^{int}, and the internal Manhattan distance between departments i and j, which is decomposed into its horizontal and vertical components $d_{ij,x}^{int}$ and $d_{ij,y}^{int}$.

Equation (3.25) represents the external cost associated with material flow between departments located in different blocks. Instead of using a simplified inter-block distance approximation, this model routes the external flow through specific ramp pairs. The total cost of such flow is computed by summing, over all feasible ramp paths (r_1, r_2), the product of the flow $F_{ijk_1k_2r_1r_2}$, the external cost coefficient c^{ext}, and the total ramp-based transportation distance. The latter is defined as the Manhattan distance between the selected ramps plus a fixed vertical cost component δ, which represents the elevation or structural cost of passing between levels.

Equation (3.26) adds a penalty term to account for undesirable separation between department pairs that are expected to interact closely. Each pair (i, j) is assigned a closeness importance score RC_{ij}. If these departments are not located in the same block—indicated by $1 - \sum_k q_{ijk}$—a penalty proportional to RC_{ij} is added to the objective. This encourages the model to place highly interactive or sequentially dependent departments close together, thus improving the operational logic of the final layout.

The values of RC_{ij} are derived from the AEIOUX framework, which is commonly used in facility layout planning to represent the qualitative closeness between departments. The acronym stands for six levels of importance: "A" for Absolutely Necessary, "E" for Especially Important, "I" for Important, "O" for Ordinary Closeness OK, "U" for Unimportant, and "X" for Undesirable. These codes are translated into numerical penalty weights, with higher scores reflecting stronger preference for proximity, and negative values (such as for "X") discouraging adjacency. A complete list of AEIOUX scores and the specific relationships used in this study are provided in Appendix A.3. Table 3.6 shows the summary of the closeness importance between departments.

Table 3.6: Department Closeness Summary

Code	**Score**	**Count**	**Department Pairs**
A	16	5	713, 89, 911, 1120, 138
E	8	5	18, 521, 611, 718, 2021
I	4	10	27, 29, 47, 410, 57, 78, 810, 813, 92, 104
O	2	14	17, 19, 23, 38, 510, 1014, 1015, 1019, 1112, 1213, 1312, 1410, 1510, 1910

The constraint set begins with assignment logic. Equation (3.27) ensures that each department is assigned to exactly one block. Equations (3.28) and (3.29) enforce logical bounds on block usage. Specifically, if a department is assigned to a block k, that block must be marked as active using the binary variable S_k. The upper bound ensures that no more than n departments can be assigned to a block, aligning with the total number of departments in the system.

Equations (3.30) and (3.31) define the co-location indicator q_{ijk}, which takes a value of 1 if and only if departments i and j are both assigned to block k. This variable plays a key role in determining whether internal or external costs should be applied, and is used throughout the flow conservation and cost assignment structure.

Equations (3.32) ensure flow conservation between departments assigned to different blocks. Specifically, if departments i and j are not colocated, the total amount of flow p_{ij} must be routed through one or more feasible ramp pairs. This guarantees that inter-block flows are fully accounted for and prevents artificial loss or creation of material movement in the model. Equation (3.33) restricts the ramp flow variables so that they can only take positive values if the corresponding department assignment variables are active. In other words, flow can be routed between ramps r_1 and r_2 only if department i is assigned to block k_1 and department j to block k_2. This condition prevents infeasible routing paths that are not connected to the actual department locations. Equation (3.34) enforces ramp capacity limitations. For each ramp r, the sum of all flows passing through it cannot exceed its specified capacity R_r. This constraint reflects realistic physical limitations of transportation infrastructure, ensuring that the optimized layout does not require ramps to handle more material than they are capable of supporting. Equations (3.35) and (3.36) define the logic for external distances between departments in different blocks. Equation (3.35) links the external distance variable to the actual ramp path distances, while Equation (3.36) forces the external distance to vanish when departments are located in the same block. Together, these constraints provide consistency between department assignment decisions and the associated cost calculations. Equations (3.37) and (3.38) define the internal Manhattan distance between department pairs within the same block. The distance is separated into horizontal and vertical components, ensuring that the internal transport cost in the objective function is computed correctly. Equations (3.39) and (3.40) enforce non-overlap between departments within each block. By using the binary direction variables α and β, the model guarantees that departments do not intersect and are placed side-by-side in either the horizontal or vertical direction. Equations (3.41) and (3.42) impose boundary conditions, restricting the coordinates of each department's center so that the entire department fits within the block dimensions LF and WF. This ensures feasible placement of all departments within the physical space. Finally, Equations (3.43)–(3.46) maintain logical consistency in the relative positioning variables. The symmetry constraints (3.43) and (3.44) guarantee that if department i precedes j, then the reverse relationship holds accordingly. The transitivity constraints (3.45) and (3.46) extend this logic to triplets of departments, eliminating circular or contradictory precedence relationships. These rules are critical for maintaining a coherent and non-overlapping arrangement of departments.

3.3 Application

To validate the proposed mathematical model, we applied it to a real-world case from a leading home appliance manufacturer, specifically the washing machine production plant. The aim is to design an efficient facility layout by minimizing total transportation cost while considering both internal and inter-block flows. The model incorporates ramp constraints and closeness relationships to enhance realism and operational feasibility.

3.3.1 Facility and Data Description

The plant consists of $n = 21$ departments that must be assigned to at most $m = 2$ fixed-size layout blocks. Each block has a predefined floor area of 48×13 meters. Unequal-area department dimensions (length and width) are fixed and vary significantly, reflecting different space requirements. Material handling occurs both within and across blocks. Inter-block transportation must occur through designated ramps. Each block includes three ramp positions, located at the horizontal axis of the block, corresponding to positions 12, 24, and 36 meters respectively.

Three types of ramps are modeled, each with a different capacity:

- **R1 (Low-capacity)**: 500 units/shift
- **R2 (High-capacity)**: 3500 units/shift
- **R3 (Mid-capacity)**: 1500 units/shift

This differentiation enforces a capacity-constrained assignment strategy, encouraging the model to utilize high-capacity ramps for bulk transfers and reserve lower capacity ramps for low-volume flows.

3.3.2 Flow and Cost Parameters

Material flow values between departments were provided by the manufacturer's planning team. These represent the average daily quantity of materials transferred from department i to j under steady-state production. A total of 39 non-zero flows were recorded across the 21 departments.

To reflect handling complexity and equipment constraints, internal transportation costs (c_{ij}^{int}) vary across department pairs. These values range from 2 to 6 per unit of distance, based on empirical estimates. All inter-block flows share a fixed transportation cost. The vertical separation between blocks is modeled as a fixed distance $\delta = 4$ meters.

3.3.3 Solver Configuration and Optimization Results

The proposed two-phase robust facility layout model was implemented in Python using the Gurobi Optimizer version 12.0.1. The model was executed on an Apple M4 Pro processor with 12 physical cores, and Gurobi was configured to utilize up to 12 threads. A relative MIP gap tolerance of 1% was set to ensure a balance between computational efficiency and solution accuracy.

The final model contained 43,151 constraints, 4,922 decision variables, and 513 quadratic constraints. Among these variables, 1,830 were continuous and 3,092 were binary/integer. The optimizer employed a wide range of cutting-plane techniques including Gomory cuts, flow cover, MIR cuts, and lift-and-project methods to accelerate convergence. The solution process explored 783,996 nodes over a runtime of 613.45 seconds, completing 49.5 million simplex iterations. An optimal solution was found with an objective value of 710,003.21 and a final optimality gap below 1%.

Layout Assignment Results

The departments were assigned to the two blocks as follows:

- **Block 1:** Departments 1–4, 7–10, 13–19
- **Block 2:** Departments 5–6, 11–12, 20–21

Each department was also assigned a specific coordinate within its block, ensuring non-overlap and area feasibility. Ramp positions were utilized for inter-block transportation with flexible flow distribution based on ramp capacity and distance minimization.

Flexible Ramp Flow Distribution

The model supports flexible ramp usage, enabling inter-block flows to be split across multiple ramp paths. Table 3.7 summarizes the detailed routing of major inter-block flows. Notably, all four inter-block flows were distributed across three available ramp paths, demonstrating the model's capability to balance load and minimize bottlenecks.

Table 3.7: Flexible Ramp Flow Distribution (Top Inter-Block Flows)

Flow	**Ramp Path**	**Volume (units)**	**Percentage**
5 → 7	R1 → R1	16.5	28.5%
	R2 → R2	23.0	39.7%
	R3 → R3	18.4	31.9%
5 → 10	R1 → R1	11.4	30.8%
	R2 → R2	14.4	39.0%
	R3 → R3	11.2	30.3%
9 → 11	R1 → R1	115.7	3.8%
	R2 → R2	2246.8	74.5%
	R3 → R3	655.0	21.7%
12 → 13	R1 → R1	8.8	31.6%
	R2 → R2	10.5	37.7%
	R3 → R3	8.6	30.7%

Cost Breakdown

The final cost breakdown is as follows:

- Internal transportation cost: **584,367.21**
- External transportation cost (flexible routing): **125,612.00**
- Separation penalty (AEIOUX): **24.00**
- **Total cost: 710,003.21**

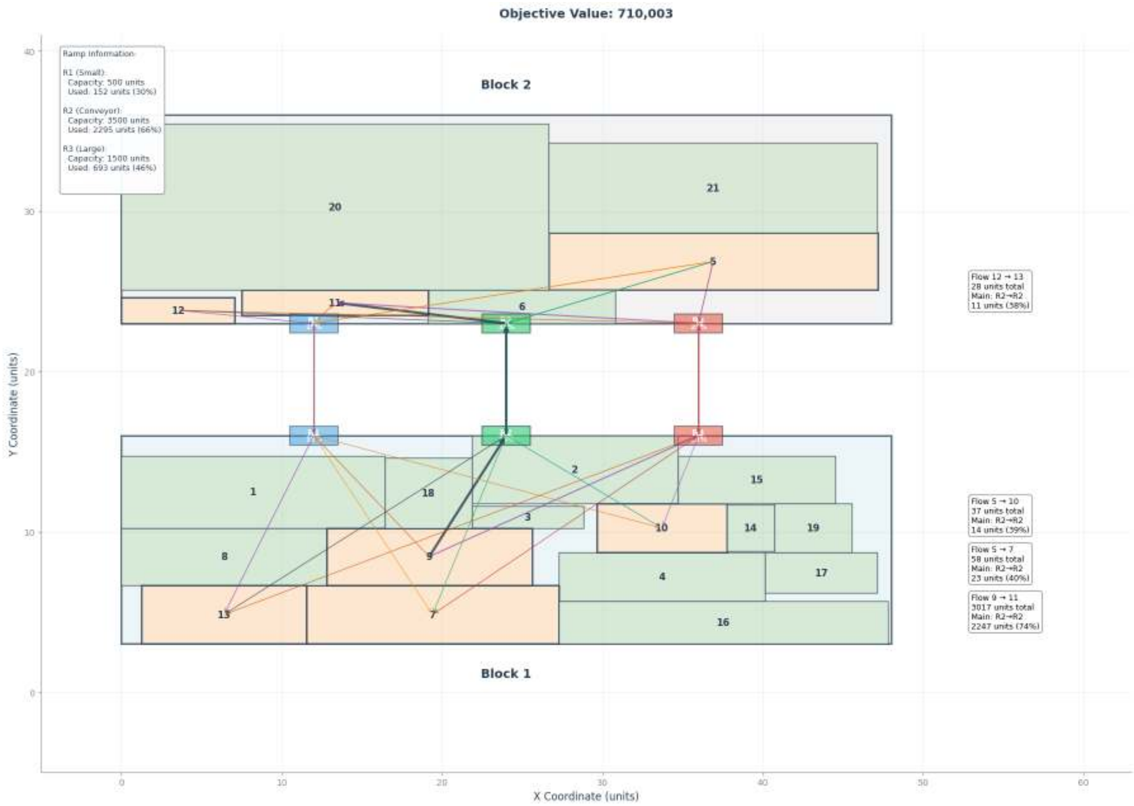

Figure 3.2: Final layout and inter-block flow distribution using flexible ramp routing.

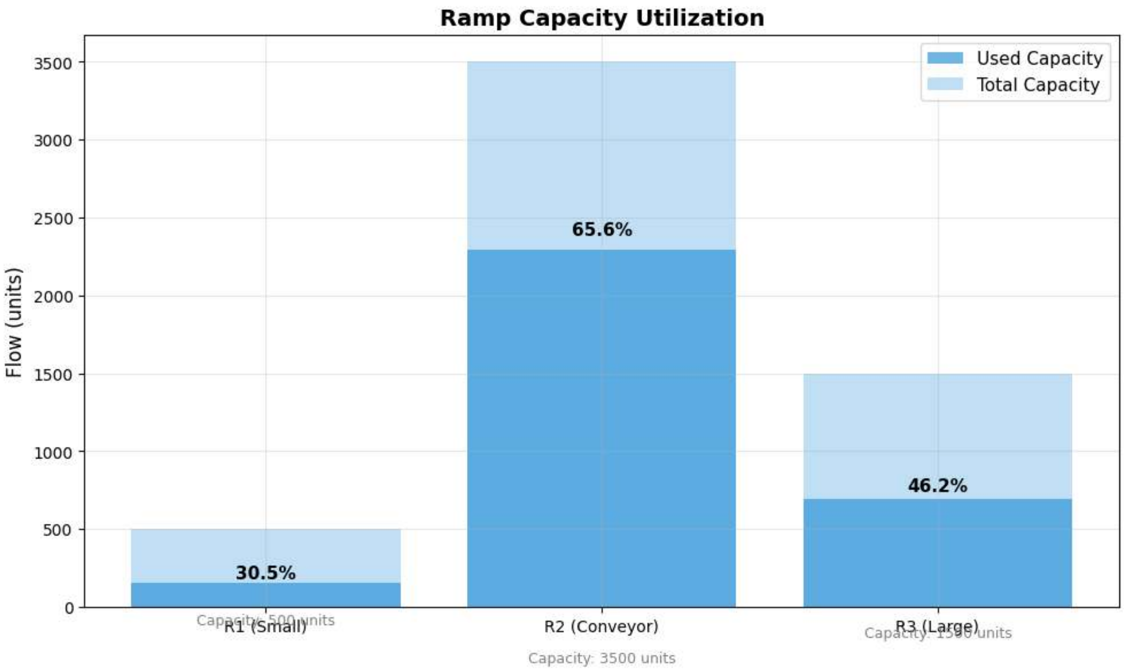

Figure 3.3: Ramp capacity utilization for R1 (Low-Capacity), R2 (High-Capacity), and R3 (Mid-Capacity).

As shown in Figure 3.2, the final layout clearly demonstrates the flexibility of the ramp-based routing logic. All inter-block flows are successfully split across multiple ramp paths, allowing the model to avoid overload while minimizing transportation costs. For example, the largest flow (Department 9 to 11) is primarily routed through R2→R2, with supporting distribution through R1 and R3. Similarly, other flows like 5→7 and 5→10 are intelligently divided across all available ramp connections.

The visual in Figure 3.3 further confirms this efficiency by showing ramp utilization levels. R2, the high-capacity conveyor-type ramp, is used most extensively (approximately 66%), followed by R3 (46%) and R1 (30.5%). No ramp exceeds its capacity, and the model leverages each ramp type according to its capacity characteristics and the flow distribution needs. This demonstrates the model's ability to achieve both realistic and cost-effective flow management under capacity constraints.

Conclusion and Analysis

The implemented model successfully assigns all departments to the two fixed blocks while respecting dimensional constraints and minimizing the overall cost components. As visualized in Figure 3.2, the layout shows a compact and efficient configuration that reflects high-flow dependencies, with interrelated departments placed close within the same block whenever feasible. Notably, the model enables inter-block flows to be distributed across multiple ramp paths based on capacity availability and distance, rather than restricting flows to a single ramp.

Four inter-block flows were identified, and each was distributed flexibly across the three available ramp types. The results indicate a strong preference for the high-capacity ramp (R2), especially for dominant flows like from Department 9 to 11, where 74% of the total volume is routed via R2→R2. At the same time, R1 and R3 were also utilized to a balanced extent to handle the remaining proportions of the flows. This strategic distribution contributes to improved ramp capacity utilization and avoids bottlenecks at any single ramp.

Figure 3.3 illustrates the actual usage of each ramp type relative to its capacity. R2 shows the highest utilization at 65.6%, followed by R3 at 46.2% and R1 at 30.5%. This validates the model's effectiveness in leveraging available capacity while maintaining feasible and realistic flow paths across blocks.

The obtained objective value of 710,003 confirms that the combination of internal transportation costs, external ramp-based flow costs, and separation penalties is effectively minimized under the deterministic assumptions. The model demonstrates practical applicability for real-world facility layout problems in discrete manufacturing environments, such as the washing machine plant in this use case.

3.3.4 Ramp Availability Scenarios

In addition to solving the base layout model under nominal conditions, we conducted a series of analyses to examine the system's response to disruptions in ramp availability. These cases aim to evaluate the model's flexibility and the solver's behavior when specific ramps are unavailable, which can occur in real-life due to maintenance, failure, or capacity shifts. It provides valuable insights into the layout's sensitivity and adaptability under varying ramp configurations.

This form of sensitivity testing complements the deterministic model by revealing how inter-block flows redistribute themselves and how the system utilizes remaining ramps under constrained conditions. It also highlights the solver's computational response, such as changes in runtime and node exploration, which are important for practical deployment.

Each case disables one ramp entirely by setting its available capacity to zero while keeping the rest unchanged. The model is then re-solved under the same optimization logic. We analyze and visualize the updated department layout, inter-block routing, ramp utilization, and solver metrics, and later compare all cases to identify trends in performance and structural robustness.

Case 1: Ramp 1 Unavailable (R1 = 0)

In this scenario, the capacity of Ramp 1 (R1 – Low-Capacity) was set to zero to simulate a complete shutdown. The objective value remained unchanged at 710,003.21, identical to the baseline solution, indicating that the model successfully redistributed all inter-block flows through the remaining ramps (R2 and R3) without increasing total cost.

Solver behavior, however, exhibited noticeable differences. Compared to the base case, the solver runtime approximately doubled from 613 seconds to 1246 seconds. This suggests that while the model maintains cost optimality, the absence of a ramp reduces routing flexibility, thereby increasing the computational burden.

Figure 3.4 presents the updated layout with visualized inter-block flows. The absence of flow through R1 is clearly visible. As illustrated, all inter-block flows are now distributed between R2 and R3 with nearly balanced proportions. For example, the large-volume flow from Department 9 to Department 11 is routed 77.1% through R2 and 22.9% through R3, whereas smaller flows such as 5→10 and 12→13 are also evenly split.

Figure 3.5 shows the corresponding ramp utilization. As expected, Ramp 1 records 0% usage. Ramp 2 (Highcapacity) absorbs the majority of the volume at 68.2% utilization, while Ramp 3 (Mid-Capacity) increases to 50.2%. This adaptive shift confirms that the flexible ramp flow logic enables smooth redistribution of capacity in response to ramp disruptions.

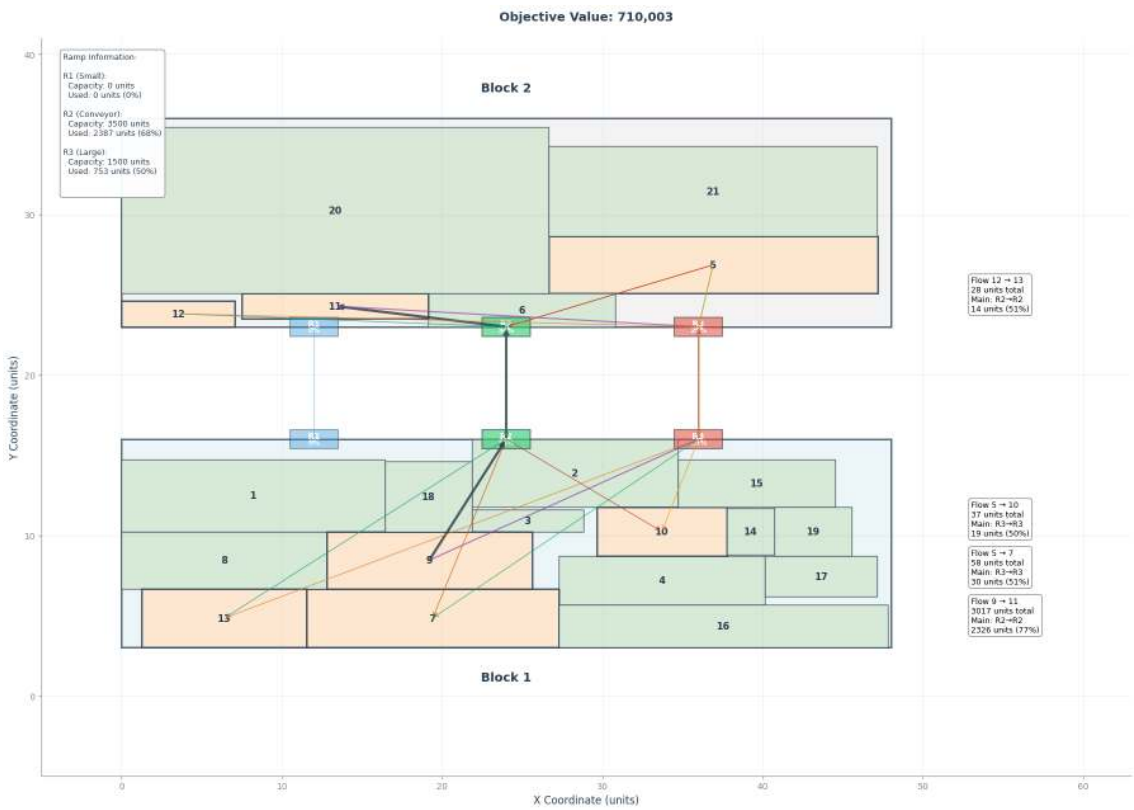

Figure 3.4: Updated department layout and inter-block flow distribution when Ramp 1 is unavailable.

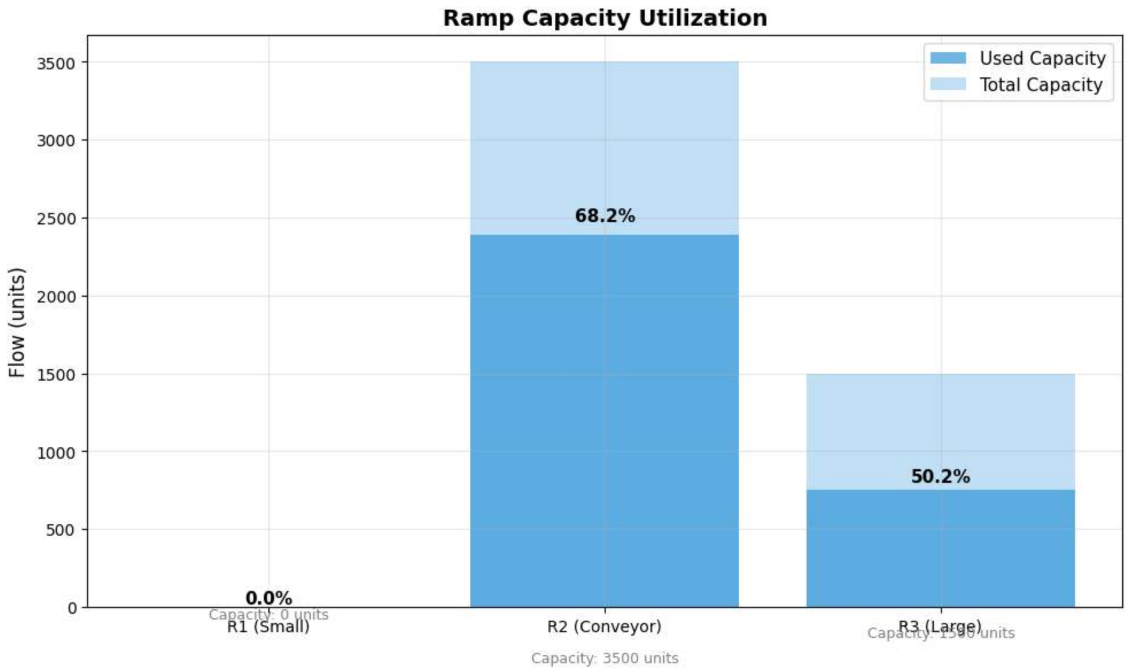

Figure 3.5: Redistribution of ramp load after disabling Ramp 1: Ramp 2 and Ramp 3 compensate for lost capacity.

Scenario 2: Ramp 3 Disabled

In the second scenario, the capacity of Ramp 3 is set to zero, rendering it completely unavailable for inter-block transportation. This case aims to evaluate how the model adapts to the unavailability of one of the main ramps, particularly focusing on the changes in flow distribution, ramp utilization, solver behavior, and layout configuration.

Figure 3.6 illustrates the resulting facility layout and flow assignments. It is evident that all inter-block flows are now distributed exclusively across Ramp 1 and Ramp 2. Despite the removal of Ramp 3, the model successfully finds a feasible and optimal solution without compromising the total cost, which remains at **710,003.21**. Figure 3.7 shows the updated capacity utilization. Ramp 2 becomes heavily utilized, reaching **83%**, while Ramp 1, previously underutilized, now handles approximately **47%** of its capacity. Ramp 3, as expected, carries no flow in this scenario.

The inter-block flows such as $9 \rightarrow 11$, $5 \rightarrow 7$, and $12 \rightarrow 13$, which previously split partially through Ramp 3, are now rerouted through the available alternatives. Notably, Ramp 2 handles the majority of the flow from department 9 to department 11 (94.1%), with the remainder (5.9%) passing through Ramp 1. All four critical flows are split between R1 and R2, demonstrating the model's flexibility in rerouting under capacity constraints.

Solver-wise, this scenario required fewer iterations and time compared to the previous one. The optimal solution was found in **789.39 seconds** with a total of 32,906,660 simplex iterations, confirming that the absence of Ramp 3, despite limiting routing options, did not significantly burden the computational process.

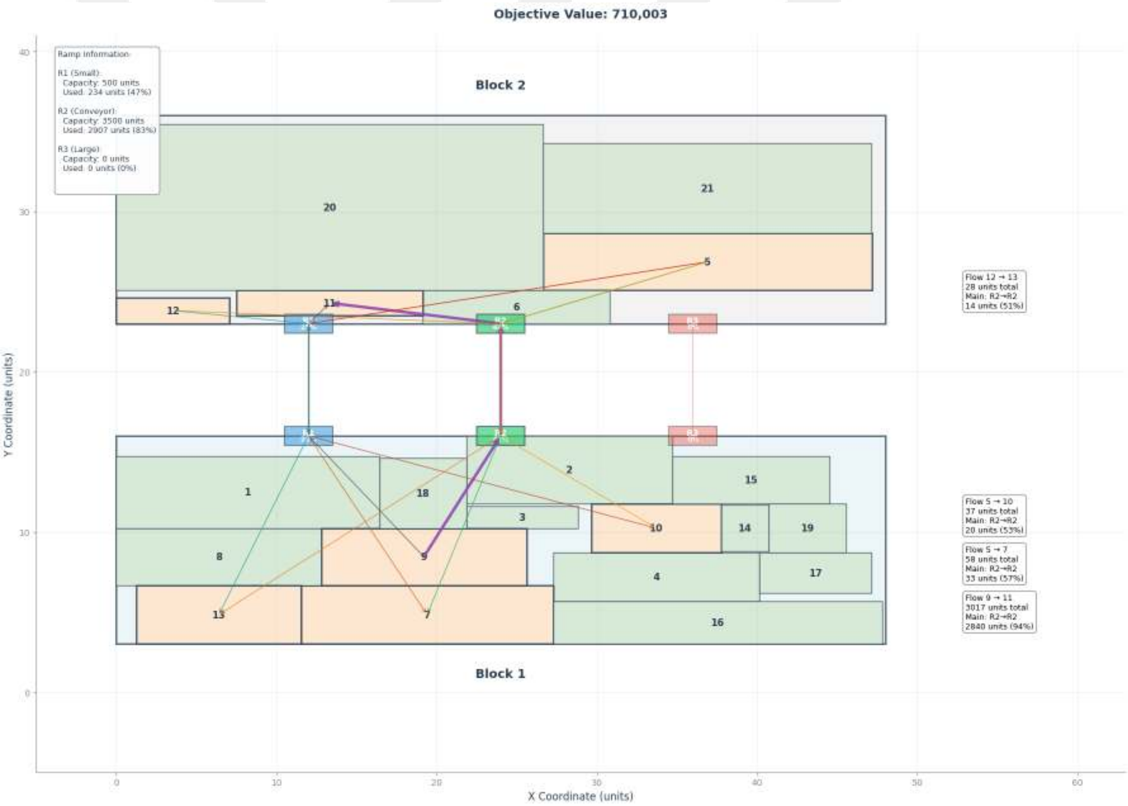

Figure 3.6: Resulting layout and flow visualization under Ramp 3 disabled scenario.

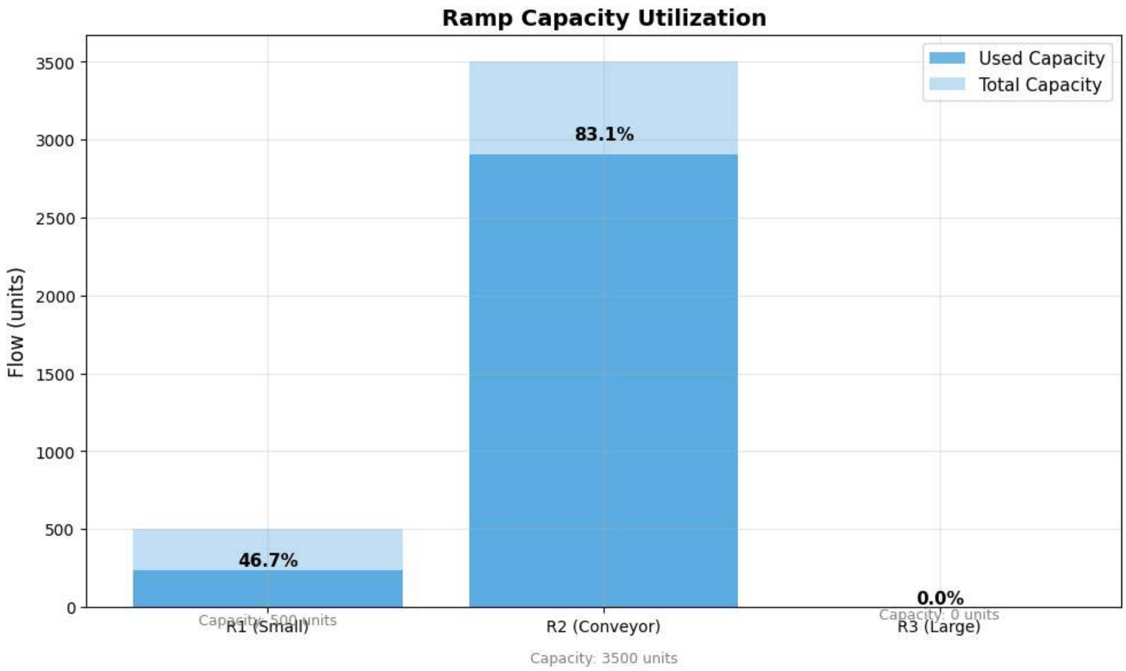

Figure 3.7: Ramp capacity utilization under Ramp 3 disabled scenario.

Scenario 3: Ramp 2 Disabled

In this scenario, Ramp 2—the highest capacity conveyor ramp in the base configuration—is entirely disabled by setting its capacity to zero. This setting simulates a situation where the most critical material transfer path is unavailable due to a technical fault, maintenance downtime, or operational redesign. The objective is to observe how the model redistributes the inter-block flows, how the remaining ramps are utilized, and how the overall layout and cost structure adapt under such constraints.

As shown in Figure 3.8, the model manages to find a feasible solution by redirecting all inter-block flows through Ramp 1 (low-capacity) and Ramp 3 (mid-capacity). Notably, Ramp 3 becomes the primary conduit, handling nearly **2,147 units** (approximately 86% of its capacity), while Ramp 1 supports the remaining **286 units**, equating to 57% of its capacity. The disabled ramp (Ramp 2) remains unused, as illustrated in Figure 3.9.

The solution yields an objective value of **803,683**, higher than the base case, with a runtime of approximately 3,127 seconds. Despite the absence of the most efficient ramp, the model maintains operational feasibility and logical ramp assignments. Flows are distributed across multiple paths for every inter-block interaction, with all four flows utilizing both Ramp 1 and Ramp 3. This confirms the model's flexibility in splitting flows across ramp pairs to reduce congestion and preserve flow efficiency.

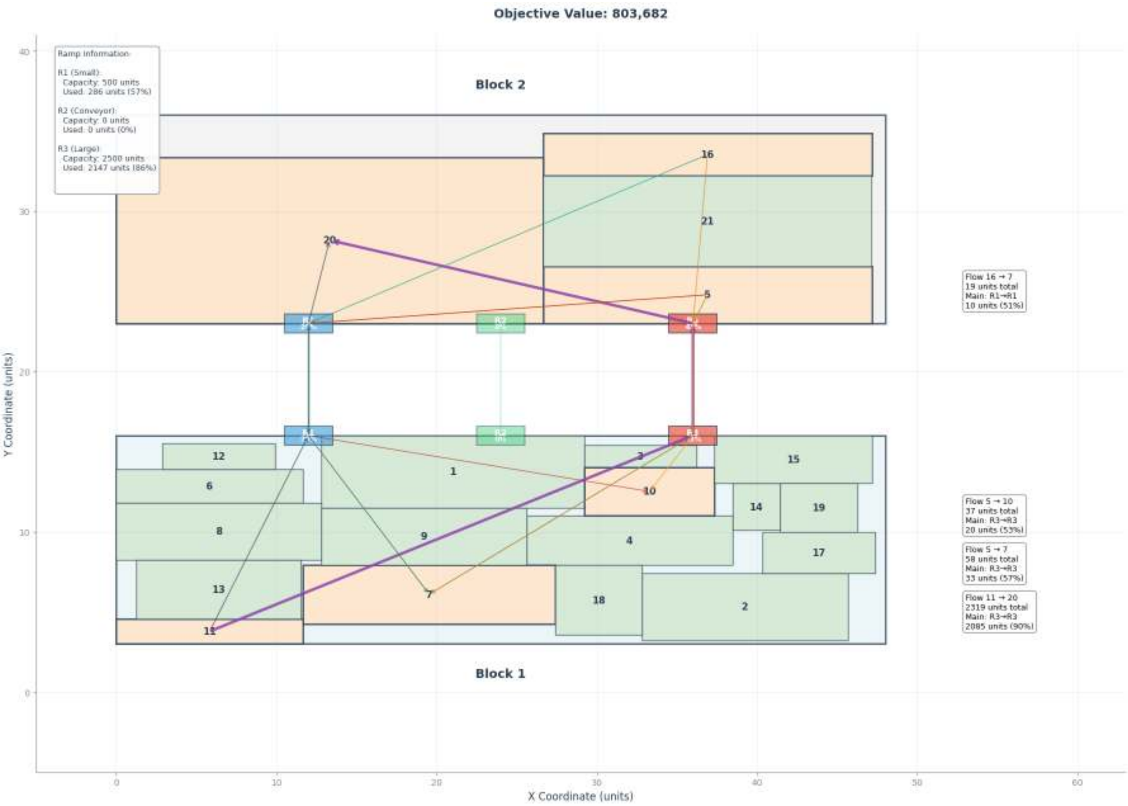

Figure 3.8: Optimal facility layout and inter-block flow routing when Ramp 2 is disabled. Ramp 3 absorbs most of the flow volume, while Ramp 1 remains partially utilized.

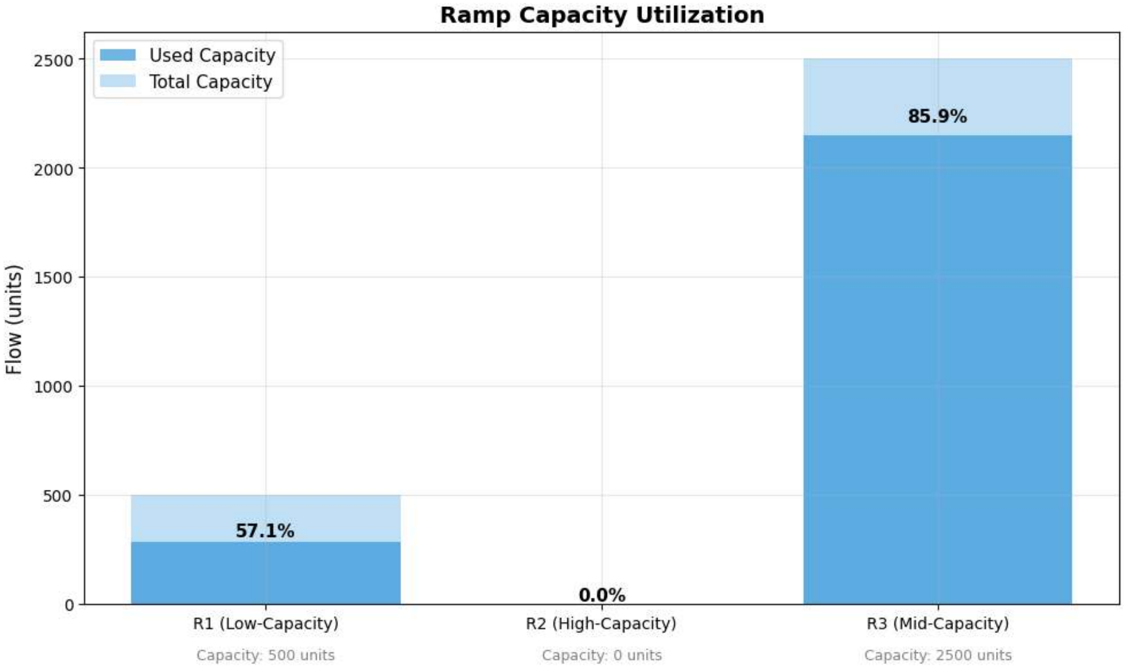

Figure 3.9: Ramp capacity utilization for the scenario with Ramp 2 disabled. Ramp 3 handles 85.9% of its capacity, and Ramp 1 handles 57.1%, while Ramp 2 is unused.

Table 3.8 summarizes the solver performance across four layout optimization runs under varying ramp availability conditions. The comparison focuses on total objective value, optimality gap, total simplex iterations, and runtime, which are the most informative metrics in evaluating solver behavior for large-scale mixed-integer problems.

All scenarios except Scenario 3 result in an identical objective value of 710,003.21, demonstrating that the model maintains a high degree of robustness and flexibility even when one ramp is completely disabled. However, the runtime and number of iterations vary significantly. Notably, Scenario 2 (Ramp 3 disabled) achieves the same optimal layout with the lowest iteration count and shortest runtime (789 seconds), suggesting the solver found this configuration relatively easier to navigate due to reduced external routing complexity.

Scenario 3, in which Ramp 2 (the highest-capacity ramp) is disabled, introduces a much more challenging case for the solver. The optimal objective increases by over 93,000 units, and both the number of iterations (210 million) and runtime

(3127 seconds) are significantly higher. This indicates a substantial structural shift in the layout and routing strategy, requiring more effort for the solver to converge.

Overall, this comparison validates the solver's efficiency and the model's feasibility preservation across all tested cases. It also highlights the value of Ramp 2 in maintaining both cost efficiency and computational tractability within the solution space.

Table 3.8: Solver performance comparison across ramp availability scenarios

Scenario	**Objective Value**	**Gap (%)**	**Iterations**	**Runtime (s)**
Base Case (All Ramps Active)	710,003.21	0.9993	49,549,614	613.45
Scenario 1 (Ramp 1 = 0)	710,003.21	0.9998	46,269,486	1246.07
Scenario 2 (Ramp 3 = 0)	710,003.21	0.9988	32,906,660	789.39
Scenario 3 (Ramp 2 = 0)	803,682.60	0.9999	210,308,722	3127.10

3.4 Summary and Conclusions

In this chapter, we introduced and formulated a deterministic mathematical model for solving the unequal-area facility layout problem in a real-world manufacturing environment. The proposed model was designed to assign departments to two distinct and fixed-size layout blocks while minimizing the total material handling cost. This total cost was defined as the sum of internal transportation cost (for movements within the same block), external transportation cost (for movements across blocks via ramps), and penalty costs associated with undesired separation of departments that are preferred to be placed close to each other due to process or communication requirements.

A key contribution of this chapter is the explicit modeling of physical ramp connections for inter-block material flow. Rather than relying solely on artificial distance penalties or assuming unrestricted inter-block movement, we introduced a realistic structure that forces flows between departments located in different blocks to pass through predefined ramp pairs. These ramps are characterized by location and capacity constraints. By controlling the allowable flow through each ramp, the model ensures that any layout solution is not only optimal in terms of cost but also feasible in terms of physical transfer limitations.

The model was implemented as a Mixed-Integer Linear Programming (MILP) formulation and solved using the Gurobi optimization engine. The implementation used real factory parameters inspired by the layout structure of a washing machine plant based in Turkey, including block sizes, department areas, pairwise flow volumes, and ramp configurations. In the base scenario, where all three ramps were assumed to be available with their nominal capacities, the model produced an optimal layout with a total cost of approximately 710,003 units. The solution was computed in a reasonable time frame (around 613 seconds), demonstrating both the practicality and solvability of the model at an industrial scale.

To further explore the responsiveness of the layout design to changes in ramp availability, we conducted three additional test scenarios. In each scenario, the capacity of one ramp was set to zero to simulate possible real-world disruptions, such as maintenance operations, temporary blockages, or infrastructure failure. These stress tests helped evaluate how the model adapts to reduced routing flexibility and provided valuable insights into the model's sensitivity.

In the first scenario, Ramp 1 was disabled. The model still found a feasible and optimal solution with no major degradation in objective value or solver performance. However, flow distributions shifted significantly toward the remaining ramps, and minor layout changes were observed. In the second scenario, Ramp 3 was disabled. While the objective value remained the same, the solver explored more nodes, and the runtime increased moderately to 789 seconds, showing that the absence of this ramp introduced additional complexity in flow routing. In the third scenario, where Ramp 2 was disabled, the model experienced the highest computational load, with a runtime exceeding 3100 seconds and a notable increase in total cost to over 803,000 units. This scenario clearly indicated that Ramp 2 serves as a critical infrastructure component in facilitating high-volume inter-block flows, and its absence significantly constrains feasible layout configurations.

A summary table was also included in this chapter, comparing solver statistics and model outcomes across all scenarios. Metrics such as runtime, number of iterations, number of explored nodes, and final objective values were compared. The analysis of this table illustrated that certain ramp configurations have a much stronger impact on computational efficiency and total cost than others. This finding emphasizes the need to include such infrastructural limitations early in the layout design process to avoid costly adjustments during implementation.

Overall, the model presented in this chapter offers a strong and realistic foundation for facility layout planning in environments where inter-block flows are subject to physical constraints. By incorporating ramp-specific routing and capacity limits, the model bridges the gap between abstract optimization formulations and practical factory-level applications. The scenario-based evaluations provide clear evidence that the model is capable of adapting to varying levels of resource availability, but also that layout performance and solvability are highly sensitive to ramp accessibility.

These results motivate the need to go beyond deterministic planning and account for potential disruptions and variability in operational parameters. In the following chapter, we will address this need by introducing a more robust optimization approach that formally models uncertainty in inter-departmental flow volumes and infrastructure availability.

Chapter 4

DATA-DRIVEN ROBUST MILP-BASED FACILITY LAYOUT MODEL WITH UNCERTAINTY IN A MULTI-BLOCK UNEQUAL-AREA SETTING

4.1 Introduction

In facility layout planning, the flow of materials between departments is a crucial factor. Traditional optimization approaches often use static flow values, assuming we know exactly how materials will move. However, in real manufacturing environments, material flows change significantly due to seasonal demand, production changes, worker availability, and new technologies. This chapter explains a detailed method for measuring flow uncertainty using historical factory data. This approach changes a standard facility layout problem into a robust optimization model that accounts for real flow variations. By using uncertainty values derived from actual data, the resulting layout can handle the natural variability seen in manufacturing while avoiding excessive caution that would create inefficient layouts. The method includes data collection, preparation, statistical analysis, uncertainty calculation, validation, and integration with optimization models. This process shows how factory data can help create more resilient facility designs that remain efficient under various production conditions.

4.2 Data Collection and Characteristics

4.2.1 Data Source and Structure

The analysis uses three years (2022-2024) of material flow data from a home appliance factory. The dataset records daily material flows for each working shift between departments over a three-year period (2022–2024). Each day contains three shifts, resulting in approximately over 2,000 time points per flow pair. Table 4.1 shows the main characteristics of this dataset. The raw data includes time information,

Table 4.1: Summary of Historical Flow Dataset

Characteristic	**Description**
Time period	January 2022 - December 2024 (36 months)
Recording frequency	Monthly totals
Number of departments	21
Number of flow pairs	33
Transportation types	Tow Truck, Forklift, AGV, Conveyor, Manual

origin department, destination department, transportation type, and flow quantities measured in unit loads. Table B.1 shows a sample of the historical database.

Table 4.2: Sample of Daily Shift-Based Flow Data Between Departments

Date	Year	Month	Shift	From Dept.	To Dept.	Vehicle Type	Flow Value	Description
2024-05-31	2024	5	2	1	8	AGV	43	Mainplant Semi Product Warehouse to Assembly Line
2024-05-31	2024	5	2	1	10	Tow Truck	1	Mainplant Semi Product Warehouse to Foamed Door Line
2024-05-31	2024	5	2	1	7	AGV	12	Mainplant Semi Product Warehouse to Pre Assembly Line
2024-05-31	2024	5	2	1	9	Tow Truck	11	Mainplant Semi Product Warehouse to Final Assembly Line
2024-05-31	2024	5	2	1	13	Tow Truck	1	Mainplant Semi Product Warehouse to Foamed Body Line
2024-05-31	2024	5	2	2	7	AGV	19	Plastic WH to Pre Assembly Line
2024-05-31	2024	5	2	2	9	Tow Truck	18	Plastic WH to Final Assembly Line
2024-05-31	2024	5	2	3	8	Tow Truck	12	Plastic WH to Assembly Line
2024-05-31	2024	5	2	4	7	Forklift	26	Mechanic WH to Pre Assembly Line
2024-05-31	2024	5	2	4	10	Forklift	21	Door panel to Door Assy
2024-05-31	2024	5	2	5	7	Forklift	18	Integration WH to Pre Assembly Line
2024-05-31	2024	5	2	5	10	Tow Truck	12	Integration WH to Foamed Door Line
2024-05-31	2024	5	2	5	21	Forklift	35	Integration WH to Other production
2024-05-31	2024	5	2	6	11	AGV	36	Packaging WH to Packaging Line
2024-05-31	2024	5	2	6	11	Conveyor	16	Packaging WH to Packaging Line
2024-05-31	2024	5	2	7	13	Conveyor	1039	Before PU to PU
2024-05-31	2024	5	2	8	9	Conveyor	1006	After PU to Final Assy
2024-05-31	2024	5	2	9	11	Conveyor	848	Final Assy to Packaging Line
2024-05-31	2024	5	2	10	8	Tow Truck	28	Door Assy to After PU
2024-05-31	2024	5	2	11	20	Forklift	734	Packaging Line to Fin. WH
2024-05-31	2024	5	2	12	13	Forklift	10	Compressor WH to Foamed Body Line
2024-05-31	2024	5	2	13	8	Conveyor	1033	PU to After PU
2024-05-31	2024	5	2	14	10	Forklift	14	Door Glass to Door Assy
2024-05-31	2024	5	2	15	10	Forklift	17	Gasket to Door Assy
2024-05-31	2024	5	2	16	7	Forklift	6	Pipe Roll WH to Pre Assembly Line
2024-05-31	2024	5	2	17	18	Forklift	6	Extruder to CTF
2024-05-31	2024	5	2	17	19	Forklift	6	Extruder to DTF
2024-05-31	2024	5	2	18	7	Manual	46	CTF to Before PU
2024-05-31	2024	5	2	19	10	Manual	16	DTF to Door Assy
2024-05-31	2024	5	2	2	3	Forklift	12	Plastic to Raw Mat. WH

Each row in Table B.1 represents the material transfer that occurred during a specific shift on a given day. By collecting flows at this granularity, the dataset captures variations due to shift-level productivity, operator differences, and partial-day issues.

4.2.2 Technology Changes in the Dataset

The dataset includes important technology changes that happened during the data collection period:

1. **Conveyor System Installation**: Starting in mid-2022 (July), conveyor systems were gradually added for specific high-volume routes, mainly connecting packaging operations (Department 5) to packaging lines (Department 10).

2. **AGV Implementation**: Beginning in early 2023, automated guided vehicles (AGVs) started replacing traditional tow trucks and forklifts for selected material movements. This change happened in phases:

   - Phase 1 (January 2023): Mainplant to Assembly (Departments 1 to 7) and Plastic Warehouse to Pre-Assembly (Departments 2 to 6)
   - Phase 2 (July 2023): Mainplant to Pre-Assembly (Departments 1 to 6) and Packaging Warehouse to Packaging Line (Departments 5 to 10)
   - Phase 3 (January 2024): Packaging Line to Finished Goods Warehouse (Departments 10 to 22)

Figure 4.1 illustrates the monthly trend of transportation technology adoption across the facility. Although the underlying dataset is now shift-based, this figure presents aggregated monthly statistics to highlight long-term transitions.

The top panel shows the AGV adoption trajectory by counting the number of routes converted to AGV operation over time. The transition followed a phased strategy: two routes were converted in January 2023, followed by two more in August 2023, and a final route in January 2024, reaching a total of five AGV-enabled flows. This step-wise adoption reflects the staged roll-out strategy described in Section 4.2.2 and aligns with operational capacity and safety certification timelines.

The bottom panel summarizes the total flow volume handled by conveyor systems on a monthly basis. Conveyor usage began in July 2022 and has steadily increased. Despite periodic production fluctuations, an upward trend is clearly visible, especially in Q4 of each year, which typically coincides with peak production demand. The rise in conveyor usage toward the end of 2024 indicates the plant's growing reliance on automated systems for material movement.

These transportation technology shifts partially explain the changing variability patterns seen in flow statistics (e.g., reductions in CV for some high-volume routes), as shown later in Figure 4.2. In general, automation contributed to more stable and predictable flow patterns over time.

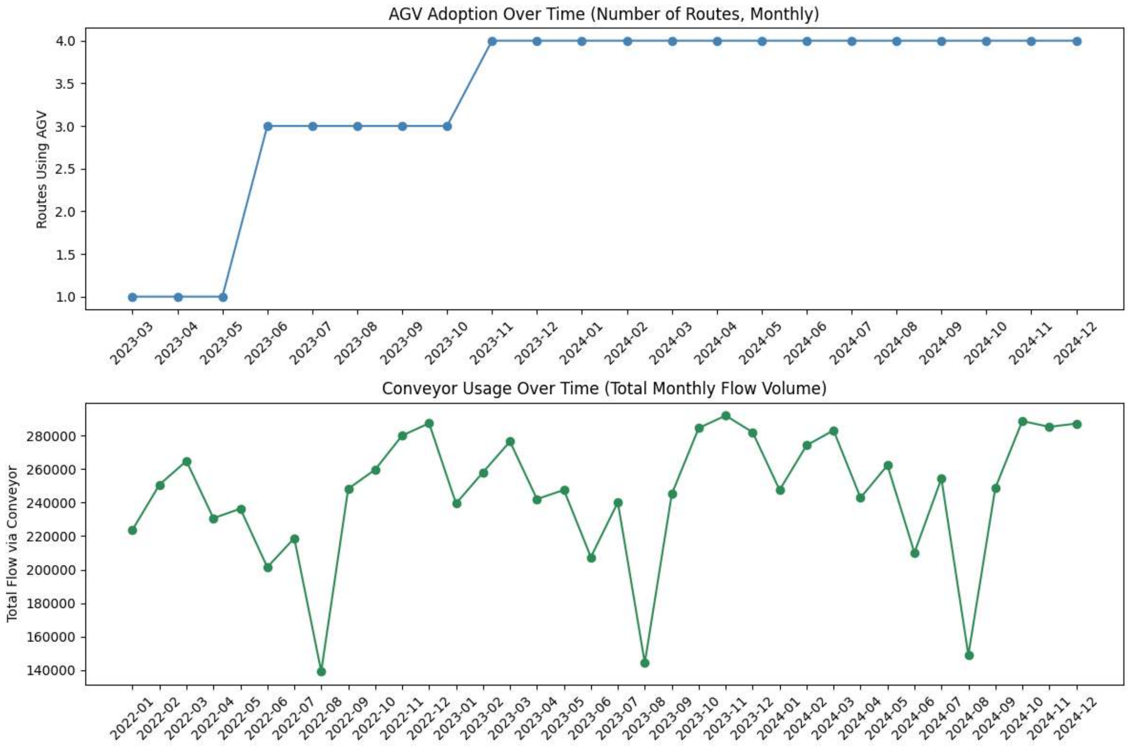

Figure 4.1: Transportation Vehicles Evolution

4.3 Mathematical Framework for Calculating Uncertainty

4.3.1 Notation and Basic Concepts

We define the following notation for our uncertainty calculation method:

- $\mathcal{D} = \{1, 2, \ldots, 21\}$: Set of departments, indexed by $i, j \in \mathcal{D}$
- $\mathcal{T} = \{1, 2, \ldots, 36\}$: Set of time periods (months) in historical dataset, indexed by $t \in \mathcal{T}$
- $\mathcal{V} = \{\text{Tow Truck, Forklift, Conveyor, Manual, AGV}\}$: Set of vehicle types, indexed by $v \in \mathcal{V}$
- $pijt^v$: Material flow from department i to department j using vehicle type v at time period t
- $\bar{p}ij$: Average material flow from department i to department j

- δ_{ij}: Uncertainty parameter for flow between departments i and j

4.3.2 Data Preparation

The raw data needs preparation to remove unusual values and account for patterns. The preparation steps include:

1. **Flow Combination**: For each department pair and time period, we combine flow data across all vehicle types to focus on total material movement regardless of transportation type:

$$pijt = \sum v \in \mathcal{V} p_{ijt}^{v} \quad \forall i, j \in \mathcal{D}, \forall t \in \mathcal{T} \tag{4.1}$$

2. **Unusual Value Detection and Removal**: We identify and filter outliers using the Z-score method:

$$Zijt = \frac{pijt - \mu ij}{\sigma ij} \tag{4.2}$$

   where μij and σij are the average and standard deviation of flow values for department pair (i, j). Data points with $|Z_{ijt}| > 3$ are marked for review and possible removal.

3. **Seasonal Adjustment**: To account for seasonal patterns, we apply a seasonal adjustment:

$$pijt^{\text{adj}} = \frac{pijt}{S_t} \quad \forall i, j \in \mathcal{D}, \forall t \in \mathcal{T} \tag{4.3}$$

   where S_t is the seasonal index for time period t, calculated using a centered moving average method.

4. **Month Length Adjustment**: To account for different month lengths, we

adjust flow values to a standard 30-day month:

$$pijt^{\text{norm}} = pijt^{\text{adj}} \times \frac{30}{D_t} \tag{4.4}$$

where D_t is the number of working days in month t.

4.4 Statistical Analysis Method

4.4.1 Flow Variability Measures

For each department pair (i, j) with non-zero flow, we calculate several statistical measures to characterize variability:

1. **Average Flow**:

$$\bar{p}ij = \frac{1}{|\mathcal{T}|} \sum t \in \mathcal{T} p_{ijt}^{\text{norm}} \quad \forall i, j \in \mathcal{D} \tag{4.5}$$

2. **Standard Deviation**:

$$\sigma ij = \sqrt{\frac{1}{|\mathcal{T}| - 1} \sum t \in \mathcal{T} (pijt^{\text{norm}} - \bar{p}ij)^2} \quad \forall i, j \in \mathcal{D} \tag{4.6}$$

3. **Coefficient of Variation** (CV):

$$CVij = \frac{\sigma ij}{\bar{p}_{ij}} \quad \forall i, j \in \mathcal{D} \tag{4.7}$$

4. **Range**:

$$Rij = \max t \in \mathcal{T} pijt^{\text{norm}} - \min t \in \mathcal{T} p_{ijt}^{\text{norm}} \quad \forall i, j \in \mathcal{D} \tag{4.8}$$

5. **Interquartile Range** (IQR):

$$IQRij = Q3ij - Q1ij \quad \forall i, j \in \mathcal{D} \tag{4.9}$$

where $Q1ij$ and $Q3_{ij}$ represent the first and third quartiles of the flow distribution for department pair (i, j).

Table 4.3 shows these variability measures for selected major flow pairs.

Table 4.3: Variability Measures for Selected Department Flows (Daily Shift-Based Data)

From	**To**	**Average Flow**	**Std. Dev.**	**CV**	**2σ (%)**	**Description**
1	8	129.63	12.16	0.0938	18.77%	Mainplant WH to Final Assembly
5	10	37.08	3.70	0.0998	19.95%	Packaging WH to Packaging Line
6	11	148.25	13.65	0.0920	18.41%	Pre-Assembly to Compressor WH
7	13	3012.89	264.12	0.0877	17.53%	PU to Foamed Body
8	9	3018.36	268.76	0.0890	17.81%	After PU to Final Assembly
9	11	3017.46	266.85	0.0884	17.69%	Final Assembly to Packaging Line
13	8	3014.15	267.03	0.0886	17.72%	Door Glass to Final Assembly
14	10	46.40	4.65	0.1002	20.05%	Door Glass to Door Assembly
16	7	18.58	1.90	0.1023	20.45%	Pipe Roll WH to Pre-Assembly
17	19	18.57	1.89	0.1015	20.31%	Extruder to DTF

Figure 4.2 presents a time series analysis of six major material flows within the facility. These plots are based on monthly aggregated data, calculated from the underlying daily, shift-level records collected over the 2022–2024 period. Each subplot shows the monthly total flow volumes between a specific pair of departments, along with key statistical annotations: mean flow, coefficient of variation (CV), and two-sigma uncertainty percentage.

The top panel displays the flow from Department 7 to Department 13 ("Before PU to PU"), which has a relatively high volume and shows a moderate degree of monthly fluctuation, with a CV of 0.16 and corresponding two-sigma uncertainty of 32.1%.

The second panel shows the flow from Department 8 to 9 ("After PU to Final Assembly"), which mirrors the same variability characteristics (CV: 0.16, Uncertainty: 32.2%). This route is highly automated, contributing to its long-term stability.

In the third plot, the flow from Department 9 to 11 ("Final Assembly to Packaging Line") also follows a stable trend with a similar CV (0.16) and slightly lower uncertainty (32.0%), though a minor production dip is observed around mid-2023, likely due to planned maintenance or summer shutdowns.

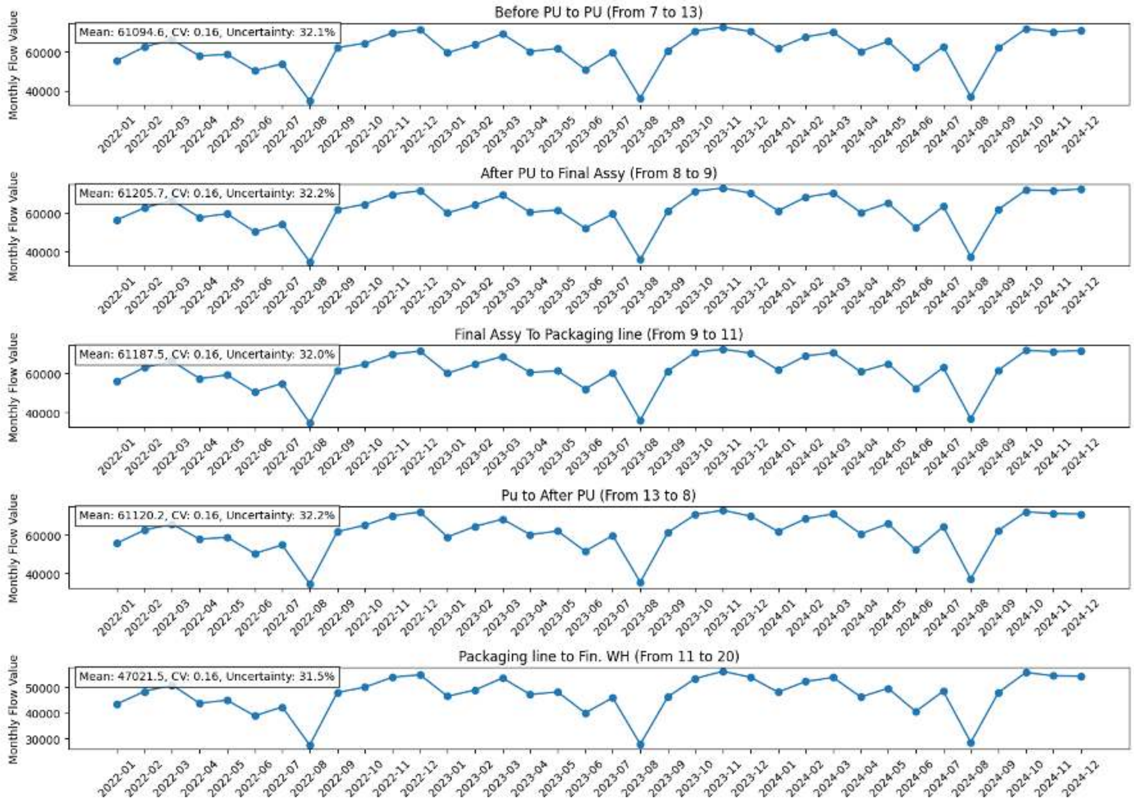

Figure 4.2: Time Series Analysis of Key Material Flows

The fourth panel, showing the flow from Department 13 to 8 ("PU to After PU"), continues this consistent pattern with identical variability statistics, further confirming the stability of internal flow loops in the core production sequence.

The fifth subplot shows the flow from Department 11 to 20 ("Packaging Line to Finished Goods WH"). While the average monthly volume is slightly lower, its variability remains in line with the others (CV: 0.16, Uncertainty: 31.5%), reflecting the increasing standardization in packaging operations.

Although the coefficient of variation appears higher than those reported in Table 4.4, this is expected. The values shown here are based on monthly totals, which emphasize broader seasonal effects, unlike the CVs in Table 4.4, which are derived from the more granular daily shift-level records. Despite these differences, the monthly trends presented in this figure support the selection of the robust uncertainty bounds.

4.4.2 Using the Two-Sigma Rule

To estimate flow uncertainty in our robust optimization model, we use the empirical coefficient of variation (CV) and apply the two-sigma approximation. This approach assumes that the relative variation of material flows can be reasonably modeled using properties of the normal distribution.

The two-sigma rule, which originates from the empirical rule for normally distributed data, suggests that approximately 95% of observed values fall within two standard deviations of the mean. Using this principle, we define the flow uncertainty percentage as:

$$u_{ij} = \frac{2\sigma_{ij}}{\bar{p}_{ij}} \times 100\% = 2 \times CV_{ij} \times 100\% \quad \forall i, j \in \mathcal{D} \tag{4.10}$$

This formulation provides an interpretable and consistent measure of uncertainty across all department pairs, scaled to the relative variation in each flow. The validity of using the two-sigma approximation is assessed in the next subsection through normality testing of historical flow data.

4.4.3 Normal Distribution Testing

To ensure that the two-sigma approximation is statistically justified, we tested whether the shift-level flow variations for each department pair follow an approximately normal distribution. For this purpose, we computed the standardized residuals for each flow:

$$r_{ijt} = \frac{p_{ijt}^{\text{norm}} - \bar{p}_{ij}}{\sigma_{ij}} \quad \forall i, j \in \mathcal{D}, \forall t \in \mathcal{T} \tag{4.11}$$

We then applied the Shapiro-Wilk test to the distribution of these residuals. The results are shown in Table 4.4, which includes five representative flows from both high-volume and medium-volume routes.

Table 4.4: Variability Measures for Major Department Flows (Daily Shift-Level Data)

From	**To**	**Mean Flow**	**Std. Dev.**	**CV**	**2σ (%)**	**Description**
7	13	3012.89	264.12	0.09	17.53	Before PU to PU
8	9	3018.36	268.76	0.09	17.81	After PU to Final Assy
9	11	3017.46	266.85	0.09	17.69	Final Assy to Packaging Line
13	8	3014.15	267.03	0.09	17.72	PU to After PU
11	20	2318.87	218.71	0.09	18.86	Packaging Line to Fin. WH

All five flows tested passed the Shapiro–Wilk normality test at the 5% significance level. This means that the daily shift-level residuals for these flows do not show significant deviation from a normal distribution, supporting the validity of using the two-sigma rule for uncertainty estimation as explained in the previous subsection.

The selected flows represent some of the highest-volume material movements in the production system, including key automated and semi-automated transport links such as 7→13, 8→9, and 9→11. Their statistical normality is especially important since these flows carry the largest weights in the optimization model. Although a few low-volume or intermittent flows in the dataset may exhibit greater skewness or kurtosis, the overall pattern across high-impact flows supports the robustness of the applied uncertainty modeling framework.

4.5 Volume-Weighted Uncertainty Calculation

In real production environments, not all flows have the same importance. Some material flows between departments happen in large quantities every day and have a big impact on how efficient the overall layout is. Others are much smaller or less frequent, and they do not affect the system as much. For example, flows between main assembly stations and final packaging areas usually involve high volumes and require more attention during layout planning. On the other hand, flows related to auxiliary operations or occasional tasks may have lower volumes and less influence on total material handling cost.

Because of this difference, it would not be fair or accurate to treat all flows the same when calculating a single uncertainty value for robust optimization. If we simply take an average of uncertainty values across all flows, low-volume flows with high variability could push the result upward, even though they are not very critical. To avoid this issue, we apply a volume-weighted approach. This means that each flow's uncertainty is multiplied by its average volume, so that more important (higher-volume) flows contribute more to the final uncertainty estimate.

This weighted approach helps us define a more realistic and balanced uncertainty parameter that reflects the actual structure of the production system. It also improves the robustness of the layout model, since the flows that matter most are given more influence. In the following subsections, we explain how this volume-weighted uncertainty is calculated, and how we use flow grouping to further analyze patterns in flow variability.

4.5.1 Weighted Average Method

In real manufacturing systems, material flows between departments can vary greatly in volume and variability. High-volume flows are typically more stable due to process standardization, while low-volume flows might exhibit more noise or variability. However, the impact of each flow on the total material handling cost is not equal. High-volume routes dominate the cost structure and therefore should play a more important role in defining uncertainty levels for robust optimization models.

To account for this, we calculate the overall flow uncertainty as a volume-weighted average of two-sigma uncertainties. This gives more importance to high-impact flows. The formula is given by:

$$\bar{u} = \frac{\sum_{i \in \mathcal{D}} \sum_{j \in \mathcal{D}} u_{ij} \times \bar{p}_{ij}}{\sum_{i \in \mathcal{D}} \sum_{j \in \mathcal{D}} \bar{p}_{ij}} \tag{4.12}$$

Here, u_{ij} is the relative two-sigma uncertainty (in percentage) for the flow between departments i and j, and $\bar{p}_{ij}$ represents the average daily flow between those departments over a 3-year historical period. The result is a single recommended uncertainty percentage that reflects the real impact of each route on the facility layout model.

Based on our flow statistics, the recommended uncertainty for our robust layout model is 18%. This value corresponds to the volume-weighted two-sigma uncertainty calculated across all department-to-department flows. It reflects both the intensity and the variability of actual daily transport volumes observed from 2022 to 2024.

4.5.2 Flow Volume Group Analysis

To further explore how uncertainty behaves across different types of flows, we divide the department pairs into two groups based on average daily volume:

- **High-volume flows**: $\mathcal{F}_H = \{(i,j) \in \mathcal{D} \times \mathcal{D} : \bar{p}_{ij} > 100\}$
- **Low-volume flows**: $\mathcal{F}_L = \{(i,j) \in \mathcal{D} \times \mathcal{D} : 0 < \bar{p}_{ij} \leq 100\}$

For each group, we calculate the weighted average uncertainty using the same formula but restricted to the group:

$$\bar{u}_H = \frac{\sum_{(i,j)\in\mathcal{F}_H} u_{ij} \times \bar{p}_{ij}}{\sum_{(i,j)\in\mathcal{F}_H} \bar{p}_{ij}}, \quad \bar{u}_L = \frac{\sum_{(i,j)\in\mathcal{F}_L} u_{ij} \times \bar{p}_{ij}}{\sum_{(i,j)\in\mathcal{F}_L} \bar{p}_{ij}} \tag{4.13}$$

Table 4.5 shows the results for each group.

Table 4.5: Uncertainty Analysis by Flow Volume Group

Flow Group	**No. of Flows**	**Avg. Volume**	**Weighted Unc. (%)**
High-volume (>100)	13	1,535.8	18.2
Low-volume (≤100)	16	56.3	19.8
All flows	29	739.1	18.0

The results confirm that high-volume flows tend to have lower relative uncertainty. Specifically, high-volume routes exhibit a weighted uncertainty of 18.2%, while low-volume flows are more volatile, with a weighted average of 19.8%. These findings are consistent with expectations: larger flows are typically better controlled, either through automation, standard operating procedures, or more frequent repetition. On the other hand, small flows are often irregular, more manual, and subject to higher process variability.

This volume-based segmentation provides additional justification for the choice of **18%** as the recommended uncertainty level in our robust layout optimization model. It offers a balance between overly conservative planning and realistic variability observed in actual operations.

4.5.3 Uncertainty by Transportation Type

Material flow variability can also differ based on the transportation method used between departments. Different types of vehicles and systems—such as AGVs, forklifts, conveyors, tow trucks, and manual handling—operate with varying levels of consistency. For instance, automated systems like conveyors and AGVs tend to follow fixed routes and schedules, which generally results in more stable and predictable flow patterns. In contrast, manual operations or vehicle-based transport methods may be more prone to delays, human errors, or operational irregularities, leading to higher uncertainty.

To better understand these differences, we analyzed the uncertainty metrics for each transportation type separately, before aggregating flows into a combined model. This allows us to identify which transportation modes contribute more to overall variability and which are more reliable. Table 4.6 presents the average flow, coefficient of variation (CV), and two-sigma uncertainty percentage for each transportation category based on three years of historical data.

Table 4.6: Uncertainty Analysis by Transportation Type

Transportation Type	**Average Flow**	**CV**	**Two-Sigma Uncertainty (%)**
AGV	288.6	0.341	68.2%
Conveyor	12,100.2	0.086	17.2%
Forklift	2,907.4	0.088	17.7%
Manual	185.8	0.087	17.4%
Tow Truck	349.0	0.288	57.6%

The results confirm that conveyor systems—despite handling the highest average flow—exhibit the lowest uncertainty levels. This demonstrates their strong performance in terms of reliability and process consistency. Conveyors operate on fixed paths with continuous and automated movement, unaffected by traffic conditions or operator availability. As a result, they ensure smooth and uninterrupted flow of materials between departments. This makes them especially suitable for high-frequency or high-volume transport needs within the factory layout.

AGVs, which also fall under the category of automated transport systems, contribute to reducing human intervention. However, their observed uncertainty is notably higher than conveyors. This can be explained by multiple operational and implementation factors. First, AGVs often require precise navigation and sensor-based decision-making, which may be affected by layout complexity or dynamic shop floor conditions. Second, the company's gradual rollout of AGVs—especially during the initial years—may have introduced inconsistencies in routing efficiency, stopping delays, or recharging times. These transitional phases typically come with a learning curve, as both the system and the staff adapt to new workflows.

Tow trucks show even higher levels of uncertainty. These vehicles depend on scheduled routes, human drivers, and shared pathways, all of which can introduce delays due to traffic congestion, operator fatigue, or miscommunication. Tow trucks are usually employed for transporting heavier loads or for long distances where conveyors or AGVs are not practical. Their performance is more variable because they lack the fixed timing and structure of automated systems, and are susceptible to day-to-day operational disruptions.

Manual handling, while often assumed to be less efficient, performs more steadily than tow trucks in this dataset. This may be due to its use in short-distance or highly repetitive flows, where the operator becomes very familiar with the task and executes it consistently. However, since manual flows are limited by human speed and capacity, they are generally reserved for low-volume connections, and scaling them up introduces risks of variability and fatigue-related inconsistencies.

Forklifts fall somewhere in the middle, showing moderate uncertainty levels. These are versatile vehicles used widely across the plant and are often dispatched on demand. While more structured than manual methods, forklift operations still depend on human judgment and real-time decision-making, which can introduce variability—especially when traffic or coordination with other activities is required.

This analysis provides valuable guidance for layout and logistics planning. By identifying the most and least reliable transportation modes, decision-makers can prioritize stable systems like conveyors for critical high-volume flows and investigate ways to improve or stabilize more variable modes like AGVs and tow trucks. In practice, this may involve expanding conveyor coverage, refining AGV path planning algorithms, or introducing better scheduling and monitoring for driver-based transport systems.

4.6 Statistical Validation

Before applying the estimated uncertainty values in the robust optimization model, it is essential to verify their statistical soundness. This section presents two complementary validation methods to assess the reliability of our uncertainty estimates. First, we use a non-parametric bootstrap technique to construct a confidence interval around the volume-weighted uncertainty percentage. This helps us evaluate how stable the estimate is across different samples of the data. Second, we perform a cross-validation procedure to examine how well the two-sigma-based prediction intervals capture the actual variation in flow values. Together, these statistical checks provide a solid basis for trusting the robustness of our uncertainty model.

4.6.1 Bootstrap Confidence Interval

To assess the statistical reliability of the estimated uncertainty, we employ a bootstrap resampling procedure with 10,000 iterations:

1. For $b = 1, 2, \ldots, 10000$:
   - Generate a bootstrap sample $\mathcal{T}_b$ by sampling with replacement from the original dataset $\mathcal{T}$
   - Calculate the volume-weighted uncertainty $\bar{u}_b$ for sample $\mathcal{T}_b$
2. Construct the 95% bootstrap confidence interval as follows:

$$CI_{95\%} = \left[\bar{u}_{(0.025)}, \bar{u}_{(0.975)}\right] \tag{4.14}$$

   where $\bar{u}_{(c^{\text{int}})}$ denotes the c^{int}-quantile of the bootstrap distribution.

The resulting 95% confidence interval is $[17.2\%, 19.5\%]$, which confirms the statistical robustness of our 18% uncertainty estimate.

4.6.2 Cross-Validation

To further validate the predictive performance of the two-sigma approach, we conduct a leave-one-out cross-validation:

1. For each time period $t \in \mathcal{T}$:
   - Exclude the data from time t, and compute the mean $\bar{p}_{ij}^{(-t)}$ and standard deviation $\sigma_{ij}^{(-t)}$ for each flow (i, j) using the remaining data
   - Construct a prediction interval:

$$\left[\bar{p}_{ij}^{(-t)} - 2\sigma_{ij}^{(-t)},\, \bar{p}_{ij}^{(-t)} + 2\sigma_{ij}^{(-t)}\right]$$

   - Check whether the actual flow p_{ijt} falls within this interval

2. Calculate the prediction coverage:

$$\text{Coverage} = \frac{\text{Number of flows within prediction intervals}}{\text{Total number of flows}} \times 100\% \quad (4.15)$$

The cross-validation yields a coverage rate of 94.3%, which is very close to the theoretical 95% target implied by the two-sigma rule. This result further validates the reliability of our uncertainty modeling approach.

4.7 Deriving Uncertainty Parameters for Robust Optimization

This section presents the final step in transforming historical material flow variability into a robust facility layout model. After conducting a detailed statistical analysis of daily shift-level data from the past three years, we derived flow-specific uncertainty levels for each department pair. These uncertainty values reflect the natural fluctuations in production volumes caused by seasonality, operational shifts, automation transitions, and other real-world factors observed in the manufacturing environment.

To incorporate these findings into our optimization model, we must select a single, representative uncertainty parameter that captures the overall variability while keeping the model practical and solvable. Instead of arbitrarily setting this value, we base our selection on empirical evidence—specifically the weighted average of the calculated two-sigma uncertainties. This ensures the model remains aligned with the actual behavior of the system and provides realistic protection against unexpected changes in flow volumes.

The subsections below explain the rationale for choosing this final uncertainty parameter, illustrate its distribution across department pairs, and describe how it is integrated into the robust optimization model using a structured uncertainty set. Additionally, we explain the selection of the Gamma (Γ) budget parameter, which controls the number of simultaneous deviations allowed in the robust formulation.

4.7.1 Final Uncertainty Parameter Selection

Based on the statistical analysis of shift-based flow data over a three-year period, we select the final uncertainty percentage for our robust optimization model as:

$$\bar{u} = 18\% \tag{4.16}$$

This value reflects the rounded flow-volume weighted average of the two-sigma uncertainty percentages calculated for each department pair. It is considered a reliable and practical estimate for capturing flow variability while maintaining solution tractability.

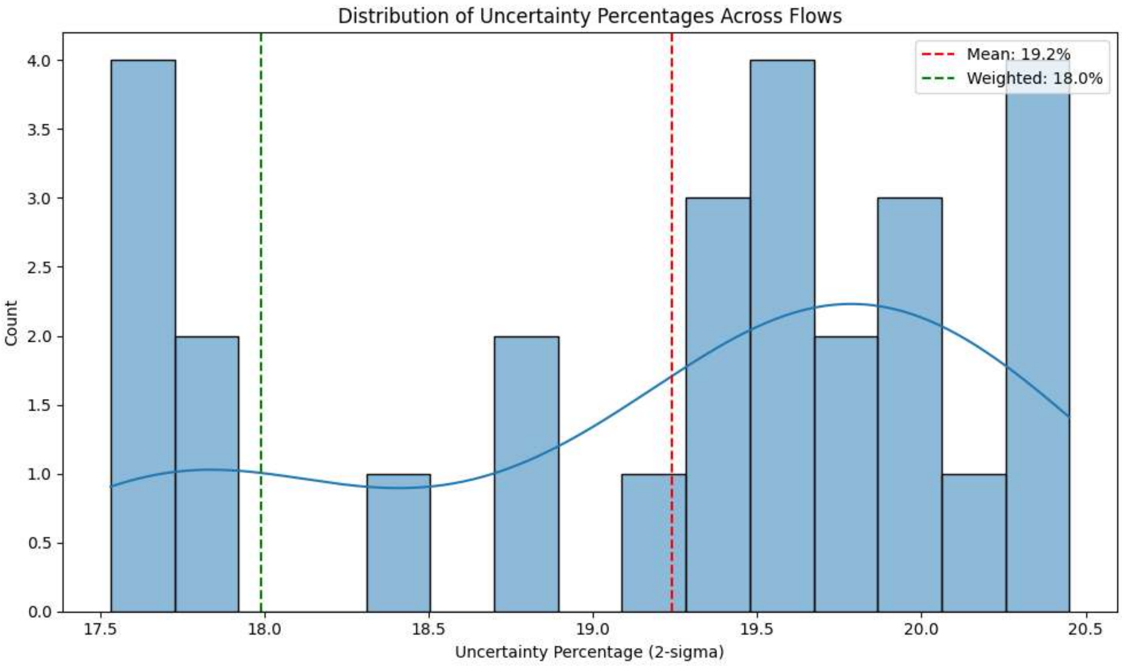

Figure 4.3: Distribution of Uncertainty Percentages

Figure 4.3 shows the distribution of two-sigma uncertainty percentages across all department-to-department flows in the facility. The histogram reveals that most uncertainty values lie between 17.5% and 20.5%, suggesting a relatively narrow and consistent variability range across the flow network.

The red dashed line indicates the mean of the uncertainty values, which is approximately 19.2%, while the green dashed line marks the flow-volume weighted mean, calculated as 18.0%. The close alignment between these two measures supports the use of the weighted average as a realistic and balanced uncertainty level for robust layout planning.

The smooth blue curve overlaid on the histogram represents the kernel density estimation, providing a clearer view of the overall distribution shape. The distribution appears slightly bimodal, with small peaks around 17.6% and 19.8%, possibly reflecting clusters of flows under different operational regimes—such as automated lines versus manual processes.

Notably, the absence of extreme outliers or highly skewed values confirms that no single flow dominates the uncertainty pattern. This consistency further validates the use of a single representative value for the uncertainty parameter. Overall, the histogram supports the selection of 18% as the final uncertainty value, balancing variability across flow types and volumes while remaining statistically grounded.

4.7.2 Implementation in Robust Optimization Model

Once the facility-specific uncertainty percentage is determined—based on real data and validated statistical methods—it must be incorporated into the robust optimization framework. In this study, we adopt a Γ-robust optimization approach, originally proposed by Bertsimas and Sim [2004], which allows uncertainty to be modeled in a structured and tractable way.

To implement this, we define an uncertainty set that captures possible variations in material flows between departments. The uncertainty for each department pair (i, j) is represented as a symmetric interval around its nominal (average) value $\bar{p}_{ij}$. Using the selected two-sigma uncertainty percentage of 18%, the deviation δ_{ij} for each flow is calculated as:

$$\delta_{ij} = 0.18 \times \bar{p}_{ij} \quad \forall i, j \in \mathcal{D} \tag{4.17}$$

This means that the actual flow between departments i and j is allowed to vary within a range of ±18% around the nominal value. Accordingly, the robust uncertainty set $\mathcal{P}$ for all flows in the layout model is defined as:

$$\mathcal{P} = \{p_{ij} : p_{ij} \in [\bar{p}_{ij} - \delta_{ij}, \bar{p}_{ij} + \delta_{ij}], \forall i, j \in \mathcal{D}\} \tag{4.18}$$

This formulation ensures that the optimization model remains feasible and realistic even under flow deviations that fall within the defined bounds. It offers a balance between model robustness and solution conservatism, by avoiding overly pessimistic estimates while still accounting for real-world variability.

Using this uncertainty set, the model can anticipate and mitigate performance degradation caused by daily and seasonal fluctuations in material flow, equipment changes, or unexpected production delays—making it more reliable and applicable in practice.

4.7.3 Budget of Uncertainty (Gamma) Parameter Selection

In robust optimization, the Γ parameter—also known as the budget of uncertainty—plays a critical role. It limits the number of material flows that can simultaneously deviate from their nominal (average) values within the defined uncertainty bounds. Choosing an appropriate Γ allows the model to remain both robust and computationally tractable.

In this study, we apply a data-driven approach to determine Γ, based on the relative impact of each flow on the layout. Since high-volume flows have a greater influence on layout decisions, we identify these as critical. Specifically, we define critical flows as those with a daily mean flow greater than 200 units. According to our analysis, there are 5 such department pairs in the dataset. Therefore, we set the uncertainty budget as:

$$\Gamma = \min(10, \text{Number of critical flows}) = \min(10, 5) = 5 \tag{4.19}$$

This setting ensures that the model accounts for the worst-case deviation of the most impactful flows, while not being overly conservative by assuming that all flows could deviate simultaneously. It balances realism and robustness.

Table 4.7: Identified Critical Flows with Mean Daily Flow Greater Than 100 Units

From Dept	**To Dept**	**Mean Flow**	**CV**
1	8	129.63	0.0938
5	21	115.83	0.0972
6	11	148.25	0.0920
7	13	3012.89	0.0877
8	9	3018.36	0.0890
9	11	3017.46	0.0884
11	20	2318.87	0.0943
13	8	3014.15	0.0886

This data-driven selection method stands in contrast to earlier studies, which often used arbitrary or fixed values for uncertainty modeling. By relying on historical factory data, our approach provides a realistic view of how material flows fluctuate under normal operating conditions. These fluctuations are influenced by factors such as shift-to-shift productivity differences, seasonal workload variation, operator behavior, and system upgrades (e.g., AGV or conveyor integration).

Through detailed analysis of three years of daily production data, we derived uncertainty bounds using statistical measures including the coefficient of variation and the two-sigma rule. Importantly, we calculated these bounds individually for each flow instead of applying a blanket uncertainty rate. This enhances the responsiveness and accuracy of the model.

The chosen framework also aligns with the Γ-robust optimization method introduced by Bertsimas and Sim [2004], which allows uncertainty to be incorporated in a linear and scalable way. The Γ parameter gives the decision-maker flexibility to adjust the level of protection based on acceptable risk levels.

Compared to stochastic or scenario-based optimization approaches, this method provides a strong trade-off between mathematical rigor and practical usability. Stochastic models often require probability distributions that are difficult to estimate in industrial environments, whereas our model only requires access to historical flow data—a much more realistic and available resource in most factories.

In conclusion, the selected value of $\Gamma = 5$ offers targeted protection against uncertainty in the most influential flows. It keeps the optimization problem solvable using MILP techniques, reduces conservatism, and makes the model more aligned with real-world manufacturing dynamics.

4.8 Robust MILP-Based Facility Layout Model with Uncertainty in a Multi-Block Unequal-Area Setting

The deterministic formulations introduced in chapter 3 assume complete certainty in material flow data between departments. While this assumption simplifies the optimization process, it does not reflect the variability commonly observed in real manufacturing environments. In practice, flow data is often subject to fluctuations due to demand uncertainty, product variety, operational disruptions, or scheduling changes. Therefore, designing a layout based solely on nominal flow values may result in solutions that underperform when actual operating conditions deviate from expectations.

To address this limitation, the deterministic model is extended using the robust optimization framework. The extended model incorporates uncertainty by defining an interval-based deviation δ_{ij} for each nominal flow p_{ij}. A budget of uncertainty parameter, Γ, is introduced to limit the number of flow deviations that are considered simultaneously. This results in a protection mechanism that accounts for worst-case scenarios without overly sacrificing solution quality under nominal conditions.

The objective function is modified accordingly to include a worst-case §cost term, constructed through auxiliary variables π and ρ_{ij}. These additions ensure that the solution remains feasible and cost-efficient even under the most unfavorable realizations of uncertain flow values, within the limits set by Γ. The resulting model maintains the original structure of the deterministic formulation, including all spatial layout, positioning, and non-overlap constraints, while enhancing its robustness against input variability.

This robust extension provides a tractable approach to handling uncertainty without relying on probabilistic information or large-scale data samples. It offers a more realistic decision support tool for facility layout design in environments where precise data is not guaranteed but bounded deviation ranges can be estimated.

4.8.1 Multi Block Unequal Area Facility Layout Optimization Model Under Uncertainty

Sets and Indices

- $\mathcal{D} = \{1, 2, \ldots, n\}$: Set of departments, indexed by i, j
- $\mathcal{B} = \{1, 2, \ldots, m\}$: Set of blocks, indexed by k, r

Parameters

- L_i: Length of department i
- W_i: Width of department i
- $\bar{L}$: Length of a block
- $\bar{W}$: Width of a block
- p_{ij}: Nominal flow between departments i and j
- δ_{ij}: Maximum deviation in p_{ij} due to uncertainty
- c_{ij}^{Int}: Internal handling cost per unit between i and j
- c^{Ext}: External transport cost per unit distance
- Γ: Budget of uncertainty (number of flows deviating simultaneously)

Decision Variables

- $x_{ik}, y_{ik} \in \mathbb{R}_+$: Coordinates of department i in block k
- $q_{ik} \in \{0, 1\}$: 1 if department i is assigned to block k
- $S_k \in \{0, 1\}$: 1 if block k is used
- $u_{ijk} \in \{0, 1\}$: 1 if i and j are assigned to block k
- $\lambda_{ijk}, \mu_{ijk} \in \{0, 1\}$: Relative placement of departments in block k
- $ExtD_{ij} \in \mathbb{R}_+$: External (inter-block) distance
- $IntD^{(x)}_{ij}, IntD^{(y)}_{ij} \in \mathbb{R}_+$: Internal (intra-block) distances
- $z, \pi, \rho_{ij} \in \mathbb{R}_+$: Variables for robust optimization objective

Objective Function

$$\min \; z \tag{4.20}$$

Robust Objective Constraint

$$z \geq \sum_{i \neq j} p_{ij} c^{\text{Int}}_{ij} (IntD^{(x)}_{ij} + IntD^{(y)}_{ij}) + \sum_{i \neq j} p_{ij} c^{\text{Ext}} ExtD_{ij} + \Gamma\pi \tag{4.21}$$

Uncertainty Constraints

$$\pi + \rho_{ij} \geq \delta_{ij} p_{ij} c^{\text{Int}}_{ij} (IntD^{(x)}_{ij} + IntD^{(y)}_{ij}) + \delta_{ij} p_{ij} c^{\text{Ext}} ExtD_{ij} \quad \forall i \neq j \tag{4.22}$$

External Distance Constraints

$$ExtD_{ij} \geq (m-1)\bar{L}(2 - q_{ik} - q_{jr}) + (k-r)\bar{L} \quad \forall i \neq j, k \neq r \tag{4.23}$$

$$ExtD_{ij} \geq (m-1)\bar{L}(2 - q_{ik} - q_{jr}) + (r-k)\bar{L} \quad \forall i \neq j, k \neq r \tag{4.24}$$

Internal Distance Constraints

$$IntD^{(x)}_{ij} \geq \bar{L}(1 - \sum_t u_{ijt}) + (x_{ik} - x_{jk}) \quad \forall i \neq j, \forall k \tag{4.25}$$

$$IntD^{(x)}_{ij} \geq \bar{L}(1 - \sum_t u_{ijt}) + (x_{jk} - x_{ik}) \quad \forall i \neq j, \forall k \tag{4.26}$$

$$IntD^{(y)}_{ij} \geq \bar{W}(1 - \sum_t u_{ijt}) + (y_{ik} - y_{jk}) \quad \forall i \neq j, \forall k \tag{4.27}$$

$$IntD^{(y)}_{ij} \geq \bar{W}(1 - \sum_t u_{ijt}) + (y_{jk} - y_{ik}) \quad \forall i \neq j, \forall k \tag{4.28}$$

Inter-Block Distance Bounds

$$IntD^{(x)}_{ij} \geq 2\bar{L}u_{ijt} - x_{ik} - x_{jr} \quad \forall i \neq j, k \neq r \tag{4.29}$$

$$IntD^{(y)}_{ij} \geq 2\bar{W}u_{ijt} - y_{ik} - y_{jr} \quad \forall i \neq j, k \neq r \tag{4.30}$$

Assignment and Block Use

$$\sum_{k \in M} q_{ik} = 1 \quad \forall i \in \mathcal{D} \tag{4.31}$$

$$\sum_i q_{ik} \geq S_k \quad \forall k \in \mathcal{B} \tag{4.32}$$

$$\sum_i q_{ik} \leq nS_k \quad \forall k \in \mathcal{B} \tag{4.33}$$

$$S_k \leq S_{k-1} \quad \forall k > 1 \tag{4.34}$$

Block Interaction Logic

$$u_{ijk} \leq 0.5(q_{ik} + q_{jk}) \quad \forall i \neq j, k \tag{4.35}$$

$$u_{ijk} + 1 \geq q_{ik} + q_{jk} \quad \forall i \neq j, k \tag{4.36}$$

Position Bounds within Blocks

$$0.5L_i q_{ik} \leq x_{ik} \leq (\bar{L} - 0.5L_i) q_{ik} \quad \forall i, k \tag{4.37}$$

$$0.5W_i q_{ik} \leq y_{ik} \leq (\bar{W} - 0.5W_i) q_{ik} \quad \forall i, k \tag{4.38}$$

Non-Overlapping Constraints (Alpha-Beta)

$$\lambda_{ijk} + \lambda_{jik} = 1 \quad \forall i \neq j, k \tag{4.39}$$

$$\mu_{ijk} + \mu_{jik} = 1 \quad \forall i \neq j, k \tag{4.40}$$

$$\lambda_{isk} + \lambda_{sjk} - \lambda_{ijk} \leq 1 \quad \forall i \neq j \neq s, k \tag{4.41}$$

$$\mu_{isk} + \mu_{sjk} - \mu_{ijk} \leq 1 \quad \forall i \neq j \neq s, k \tag{4.42}$$

Spatial Non-Overlap Within Block

$$x_{ik} + 0.5L_i Y_{ik} \leq x_{jk} - 0.5L_j Y_{jk} + \bar{L}(2 - \lambda_{ijk} - \mu_{ijk}) \quad \forall i \neq j, k \tag{4.43}$$

$$y_{ik} + 0.5W_i Y_{ik} \leq y_{jk} - 0.5W_j Y_{jk} + \bar{W}(1 + \lambda_{ijk} - \mu_{ijk}) \quad \forall i \neq j, k \tag{4.44}$$

$$x_{ik}, y_{ik}, ExtD_{ij}, IntD_{ij}^{(x)}, IntD_{ij}^{(y)}, z, \pi, \rho_{ij} \geq 0 \qquad \forall i, j \in \mathcal{D},\ k \in \mathcal{B} \tag{4.45}$$

$$Y_{ik}, S_k, u_{ijk}, \lambda_{ijk}, \mu_{ijk} \in \{0, 1\} \qquad \forall i, j \in \mathcal{D},\ k \in \mathcal{B} \tag{4.46}$$

Equation (4.20) defines the objective as minimizing the variable z, which acts as an upper bound on the total transportation cost under flow uncertainty. The actual value of z is determined through the robust objective constraint. Constrain (4.21) constructs the total cost by combining the nominal intra-block and inter-block transportation costs with a penalty term $\Gamma.\pi$. The first two terms calculate the cost using known flows p_{ij} and corresponding distances, while the third term approximates the worst-case impact of flow uncertainty. The variable π is introduced to capture this effect and is multiplied by the uncertainty budget Γ, which controls the number of uncertain flows considered simultaneously. Constraint (4.22) defines the maximum possible cost deviation for each flow pair (i, j). The auxiliary variable ρ_{ij} captures the cost increase due to a potential deviation δ_{ij}, based on both internal and external distances. The sum of π and ρ_{ij} must be at least as large as this deviation cost. This ensures that the objective value z is robust against the worst-case realization of uncertain flows. Constraints (4.23) and (4.24) calculate the minimum inter-block distance $ExtD_{ij}$ between departments i and j if they are assigned to different blocks k and r. The terms involving $(k-r)\bar{L}$ and $(r-k)\bar{L}$ measure the horizontal separation between block indices, and the binary assignment variables ensure these constraints are only active when departments are assigned to their respective blocks. Equation (4.25)-(4.28) define the internal horizontal $IntD_{ij}^{(x)}$ and vertical $IntD_{ij}^{(y)}$ distances between departments i and j when they are located in the same block. The term $(1 - \sum_t u_{ijt})$ deactivates the constraint if departments are not co-located, while the remaining terms compute the coordinate differences within the same block. Equation (4.29)-(4.30) ensure that internal distances are bounded away from zero when departments i and j are not co-located. They act as safeguards to prevent illogical configurations where departments in different blocks might appear to overlap due to coordinate values. The bounds use the maximum possible block dimensions and co-location variable u_{ijt} to activate only when needed. Equation (4.31) ensures that each department is assigned to exactly one block. Equations (4.32) and (4.33) define the relationship between assignment and block utilization: if a department is placed in a block, that block must be marked as used. Equation (4.34) imposes an ordering rule on block activation to reduce symmetry in the solution space and simplify the model's search process. Equations (4.35) and (4.36) define whether departments

i and j are placed in the same block k. The binary variable u_{ijk} becomes 1 only if both departments are assigned to block k, and 0 otherwise. This logic is used later in calculating distances and overlap conditions. Equations (4.37) and (4.38) ensure that the coordinates x_{ik} and y_{ik} of department centroids remain within the assigned block boundaries. The bounds consider the department dimensions L_i and W_i, ensuring that no part of a department exceeds the limits of its assigned block.

In Equations (4.39)-(4.42), binary variables λ_{ijk} and μ_{ijk} define the relative horizontal and vertical placement of departments within the same block. Equations (4.39) and (4.40) ensure that for each pair (i, j), exactly one department is placed before the other. Equations (4.41) and (4.42) maintain consistency across triplets of departments using transitivity logic, which is essential for feasible and logical layouts. Equations (4.43) and (4.44) use the relative order variables λ_{ijk} and μ_{ijk} to guarantee that departments placed within the same block do not overlap. The minimum required separation is based on the dimensions of the departments, and additional terms ensure that the constraints activate only when departments are co-located. Constraints (4.45) and (4.46) define the domains of all variables used in the model. Continuous variables such as coordinates and distances are constrained to be non-negative, while logical decisions like assignments and relative positions are modeled using binary variables.

4.9 Robust Facility Layout Optimization Model with AEIOUX Closeness and Ramp-Based Flow

The previous section introduced a robust layout optimization model that extends the basic deterministic formulation by incorporating uncertainty in material flows. That model uses a Γ-robust optimization approach, where uncertain flows are protected using deviation limits and budget constraints. It also considers multiple blocks and unequal-area departments, ensuring that spatial feasibility and non-overlap conditions are satisfied. However, it simplifies inter-block transportation by using a basic distance penalty based on block indices. While this is useful for theoretical development, it may not reflect the true logistics of real-world facilities.

In practice, inter-block flows are not transferred freely across space but are routed through specific paths—such as ramps, tunnels, or elevators—that impose physical and operational limitations. Ignoring these transfer routes can lead to layout designs that are mathematically optimal but difficult or costly to implement. Moreover, the previous model does not consider flow routing flexibility or ramp capacity constraints, and it treats closeness preferences in a limited way.

To address these limitations, this section presents an improved and unified robust facility layout model. The new formulation advances the previous model in several key aspects:

- It models inter-block flow movement through fixed ramp positions, capturing realistic logistics constraints in factories with multi-floor or segmented zones.
- It allows flexible flow splitting across multiple ramp pairs instead of enforcing single-path routing, which helps improve solution feasibility and reduce bottlenecks.
- It incorporates ramp capacity limits, ensuring that the total flow through any ramp does not exceed its maximum allowable volume.
- It adds closeness preferences between departments using AEIOUX-type logic, penalizing separation of critical pairs that should be placed near each other.
- It preserves robustness against uncertainty using the Γ-robust optimization framework, but adapts it to the new routing and flow structure.

The resulting model is formulated as a Mixed-Integer Linear Programming (MILP) problem. It integrates spatial layout, robust cost minimization, ramp-based flow distribution, and closeness handling into one optimization framework. The model simultaneously decides department assignments, positions, routing paths, and protection terms, while respecting all geometric, logical, and flow-based constraints.

This section presents the full mathematical formulation of the proposed model and provides detailed explanations of each component.

Incorporating Closeness Ratings Using the AEIOUX Framework

In real manufacturing systems, departments are not only connected by material flows, but also by qualitative relationships such as supervision needs, communication frequency, or equipment sharing. To reflect these preferences in layout planning, this model uses the AEIOUX closeness framework.

The AEIOUX method was originally proposed by Muther [Chung, 1999] and has been widely adopted in facility layout studies, including in the improved approach by Assem et al. [2012]. It classifies the relationship strength between department pairs into six levels: A, E, I, O, U, and X. Each letter stands for a qualitative level of closeness importance:

- **A (Absolutely Necessary)** – These departments must be placed very close.
- **E (Especially Important)** – Very desirable to locate near each other.
- **I (Important)** – Preferably close, but not essential.
- **O (Ordinary Closeness OK)** – No strong preference, but proximity is acceptable.
- **U (Unimportant)** – Closeness has little to no benefit.
- **X (Undesirable)** – Departments should not be close (not used in this model).

To quantify these levels in the model, we assign numerical weights to each relationship. Higher scores reflect higher closeness importance. Table 4.8 shows the numerical values used in this study.

Table 4.8: AEIOUX Closeness Scores

Closeness Rating	Score
A (Absolutely Necessary)	16
E (Especially Important)	8
I (Important)	4
O (Ordinary Closeness OK)	2
U (Unimportant)	0

In this model, if two departments have a high closeness score but are assigned to different blocks, a penalty is applied. This is done using the term $RC_{ij}(1 - \sum_k q_{ijk})$ in the objective function. Here, RC_{ij} is the closeness score between departments i and j, and q_{ijk} is a binary variable equal to 1 if both departments are assigned to the same block k. This formulation penalizes separations between departments with strong closeness preferences.

Table 4.9 summarizes the number of department relationships at each closeness level in our dataset.

Table 4.9: Distribution of Closeness Ratings

Rating	Score	Number of Relationships
A	16	9
E	8	10
I	4	14
O	2	16
U	0	3

To provide a better understanding of the AEIOUX data used, Table 4.10 lists a subset of department pairs with their corresponding closeness scores. These were selected based on their importance, starting with the highest level (A = 16).

Table 4.10: Sample Department Closeness Relationships

Department i	Department j	Closeness Rating (Score)
7	13	A (16)
8	9	A (16)
9	8	A (16)
9	11	A (16)
11	9	A (16)
11	20	A (16)
13	7	A (16)
13	8	A (16)
20	11	A (16)
1	8	E (8)
5	21	E (8)
6	11	E (8)
7	18	E (8)
8	1	E (8)

By incorporating this structure into the optimization model, we ensure that the resulting layout not only minimizes transportation cost but also supports operational efficiency by promoting closeness where it matters most. This makes the solution more practical and aligned with real production needs.

Sets and Indices

$i, j \in N$	Departments
$k, k_1, k_2 \in M$	Blocks
$r_1, r_2 \in R$	Ramps

Parameters

l_i, w_i	Length and width of department i
LF, WF	Length and width of each block
p_{ij}	Nominal flow from department i to j
δ_{ij}	Maximum deviation in p_{ij} due to uncertainty
$c_{ij}^{\text{int}},\ c^{\text{ext}}$	Unit transportation cost (internal and external)
R_r	Capacity of ramp r
RC_{ij}	Closeness importance (AEIOUX) between i and j
$d_{r_1 r_2}$	Distance between ramp r_1 and r_2
Γ	Robustness budget parameter
M_1, M_2	Big-M constants for logic constraints

Decision Variables

$Y_{ik} \in \{0,1\}$	1 if department i is assigned to block k
$x_{ik}, y_{ik} \geq 0$	Coordinates of department i within block k
$q_{ijk} \in \{0,1\}$	1 if i and j are in the same block k
$d_{ij}^{\text{int},x}, d_{ij}^{\text{int},y} \geq 0$	Intra-block distances between i and j
$d_{ij}^{\text{ext}} \geq 0$	Inter-block distance for flow from i to j
$F_{ij}^{k_1 k_2 r_1 r_2} \geq 0$	Flow from i to j routed through ramp pair (r_1, r_2)
$Z_{ij}^{k_1 k_2 r_1 r_2} \in \{0,1\}$	Ramp usage indicator for flow path
$\alpha_{ijk}, \beta_{ijk} \in \{0,1\}$	Relative horizontal and vertical ordering
$S_k \in \{0,1\}$	1 if block k is used
$\pi, z \geq 0$	Robustness terms (total cost and uncertainty protection)
$\rho_{ij} \geq 0$	Protection variable for each flow deviation

Objective Function

$$\min z = \sum_{i\neq j} p_{ij} c_{ij}^{\text{int}} (d_{ij}^{\text{int},x} + d_{ij}^{\text{int},y}) + \sum_{i\neq j} \sum_{k_1\neq k_2} \sum_{r_1,r_2} c^{\text{ext}} d_{r_1 r_2} F_{ij}^{k_1 k_2 r_1 r_2}$$
$$+ \sum_{i\neq j} RC_{ij}(1 - \sum_k q_{ijk}) + \Gamma\pi + \sum_{i\neq j} \rho_{ij} \tag{4.47}$$

Constraints

$$\sum_k Y_{ik} = 1 \qquad \forall i \in N \qquad \text{(Each department is assigned to one block)} \tag{4.48}$$

$$\sum_i Y_{ik} \geq S_k \qquad \forall k \in M \qquad \text{(Block is active if it has at least one department)} \tag{4.49}$$

$$nS_k \geq \sum_i Y_{ik} \qquad \forall k \in M \qquad \text{(Inactive blocks cannot host any department)} \tag{4.50}$$

$$S_k \leq S_{k-1} \qquad \forall k = 2, \ldots, m \qquad \text{(Symmetry-breaking for block usage)} \tag{4.51}$$

$$q_{ijk} \leq \tfrac{1}{2}(Y_{ik} + Y_{jk}) \qquad \forall i \neq j,\ k \in M \qquad \text{(q = 1 only if both in block k)} \tag{4.52}$$

$$q_{ijk} + 1 \geq Y_{ik} + Y_{jk} \qquad \forall i \neq j,\ k \in M \qquad \text{(q = 0 if i or j not in block k)} \tag{4.53}$$

$$\sum_{k_1\neq k_2} \sum_{r_1\in R} \sum_{r_2\in R} F_{ij}^{k_1 k_2 r_1 r_2} = p_{ij}(1 - \sum_k q_{ijk}) \qquad \forall i \neq j \in N \tag{4.54}$$

$$F_{ij}^{k_1 k_2 r_1 r_2} \leq p_{ij} \cdot Y_{ik_1} \cdot Y_{jk_2} \qquad \forall i \neq j,\ k_1 \neq k_2,\ r_1, r_2 \in R \tag{4.55}$$

$$\sum_{\substack{i,j\in N\\k_1,k_2\in M\\r_1=r}} \sum_{r_2\in R} F_{ij}^{k_1k_2r_1r_2} + \sum_{r_1\in R} \sum_{\substack{i,j\in N\\k_1,k_2\in M\\r_2=r}} F_{ij}^{k_1k_2r_1r_2} \leq R_r \qquad \forall r\in R \tag{4.56}$$

$$d_{ij}^{\text{ext}} \leq M_1(1-\sum_k q_{ijk}) \qquad \forall i\neq j\in N \tag{4.57}$$

$$d_{ij}^{\text{ext}} \cdot p_{ij} \cdot (1-\sum_k q_{ijk}) \geq \sum_{k_1\neq k_2} \sum_{r_1,r_2\in R} F_{ij}^{k_1k_2r_1r_2} \cdot d_{r_1r_2} - M_2 \sum_k q_{ijk} \quad \forall i\neq j\in N \tag{4.58}$$

$$\begin{aligned}\pi + \rho_{ij} \geq\ & \delta_{ij} \cdot c_{ij}^{\text{int}} \cdot (d_{ij}^{\text{int},x} + d_{ij}^{\text{int},y})\\ &+ \sum_{k_1\neq k_2} \sum_{r_1,r_2\in R} \left(\frac{\delta_{ij}}{p_{ij}}\right) F_{ij}^{k_1k_2r_1r_2} \cdot c^{\text{ext}} \cdot d_{r_1r_2} \qquad \forall i\neq j\in N\end{aligned} \tag{4.59}$$

Big-M logic for $d_{ij}^{\text{int},x}, d_{ij}^{\text{int},y},$ placement, and non-overlap rules

The mathematical model includes a set of constraints to ensure valid department assignments, logical flow routing, capacity feasibility, and robustness against uncertainty. Constraint (4.48) ensures that each department is assigned to exactly one block, avoiding both missing assignments and duplications. This is a fundamental requirement in facility layout problems. Constraint (4.49) guarantees that if a department is placed in a block, that block must be marked as used, while Constraint (4.50) complements this by enforcing that no departments are assigned to a block unless it is marked active. Together, these conditions manage block usage and ensure consistency in block activation. Constraint (4.51) introduces a symmetry-breaking rule, requiring that blocks be activated in a sequential order. This helps reduce redundant solution patterns and supports more compact and realistic layouts.

To determine whether departments i and j are co-located, Constraints (4.52) and (4.53) define the binary variable q_{ijk}, which takes the value 1 only if both departments are assigned to the same block k. These constraints are essential for identifying inter-block flows. Constraint (4.54) ensures that when departments are placed in different blocks, their flow must be routed through valid ramp combinations. It distributes the entire flow volume over ramp pairs, activating only when the departments are not co-located. Constraint (4.55) restricts the use of ramp-based flow variables to only those department pairs whose block assignments permit such routing. Although the product of binary variables $Y_{ik_1}Y_{jk_2}$ is nonlinear, this logic can be linearized in implementation.

Ramp capacity constraints are enforced in Constraint (4.56), which ensures that the total flow passing through any ramp does not exceed its predefined limit R_r. This constraint preserves the physical realism of the layout by preventing overloading of shared infrastructure. External distance logic is modeled using Big-M techniques in Constraints (4.57) and (4.58). Specifically, Constraint (4.57) deactivates the external distance variable d_{ij}^{ext} when departments are co-located, while Constraint (4.58) defines the effective external distance between departments in different blocks based on ramp-to-ramp paths and flow distribution. A large constant M_2 ensures this constraint is skipped when departments are placed in the same block.

Finally, Constraint (4.59) represents the robustness mechanism against uncertain flows. It combines a global protection variable π and local protection buffers ρ_{ij} to cover the worst-case increase in transportation cost due to deviations in material flow. The right-hand side of this inequality captures the maximum deviation cost across both internal and external paths: the first term models cost change in intra-block movement, while the second accumulates the additional external cost caused by deviations routed through ramp pairs. This formulation is aligned with the Γ-robust optimization approach by [Bertsimas and Sim, 2004], allowing the model to remain feasible and cost-effective under bounded uncertainty without requiring exact probability distributions.

4.10 Application of the Use Case Facility

This chapter presents the application of the proposed robust facility layout model to a real-world use case from the home appliance manufacturing sector. The selected facility belongs to one of the most prominent European brands in the white goods industry. The company manages numerous factories and distribution centers worldwide and holds a significant market share across Europe, the Middle East, and parts of Asia. The company is known for its large-scale production of household appliances such as washing machines, refrigerators, dishwashers, ovens, and dryers. Among these, the washing machine production line in one of company's facilities was selected for this study.

The decision to focus on this facility was driven by both academic and industrial motivations. From an industrial perspective, the selected production facility faces many of the same challenges that are increasingly common across the manufacturing sector today. These include rising operational costs driven by energy prices and labor expenses, global supply chain disruptions, increased product complexity, and highly volatile customer demand. In recent years, the frequency of production plan changes has grown, driven by shorter product life cycles, seasonality, and customized product configurations. These shifts have made it more difficult for static layout solutions to remain efficient over time.

The case facility produces a wide range of washing machine models, each with different technical specifications and component requirements. This variety creates complex material flow patterns between departments and often leads to inefficient use of space and excessive internal transportation, especially when layout decisions are not aligned with actual data. Moreover, the factory operates with multiple production shifts and must coordinate between different production halls and functional areas such as sub-assembly, final assembly, and packaging. These realities highlight the need for a layout design that is not only efficient in its initial form but also robust to changes in flow volumes and spatial demands.

From an academic perspective, this facility presents an ideal testbed for applying and evaluating advanced layout optimization models. First, it includes several critical features often discussed in the literature but rarely tested together in a real use case. These include unequal-area departments, multi-block layout structure (e.g., production spread across multiple connected buildings or floors), and highly variable material flows. Second, the availability of historical production and flow data over multiple years allowed the implementation of a data-driven uncertainty modeling approach. This ensures that the model operates on realistic inputs rather than hypothetical or randomly generated data, which adds significant credibility to the results.

The collaboration with this facility also ensured that the proposed model was aligned with the practical needs of the manufacturing team. During the project, input was collected from engineers and planners responsible for daily operations, which helped refine some of the assumptions of the model. For example, the model had to take into account physical restrictions such as allowable department sizes, distances between functional units, and fixed ramp access points. Additionally, the company expressed a specific interest in evaluating how much improvement could be gained by redesigning the layout using a robust optimization framework, compared to traditional deterministic models.

In summary, the case facility offers a highly relevant and technically challenging environment for testing the robust facility layout model proposed in this study. The collaboration provided not only access to detailed and structured data but also a realistic setting in which to evaluate the model's impact. This use case supports the thesis goal of bridging the gap between theoretical modeling and practical application in the field of facility layout optimization, especially under uncertainty and variability. The results presented in the following sections aim to demonstrate the feasibility and benefits of integrating robust optimization techniques with data-driven analysis in a modern industrial context. This project has been carried out with the support of use case Corporation based in Turkey and within the scope of the TÜBİTAK 2244 Industrial PhD Program, which aims to strengthen university-industry collaboration by integrating academic research with real-world industrial needs.

4.10.1 Data Inputs and Preprocessing

To support the robust facility layout model with real values, a detailed dataset was collected from use case facility's Production Planning Department and SAP system. This dataset includes historical records of material movements between departments over several months. Each record shows the amount of material moved and the transport method used. The data reflects real production activity in both assembly and sub-assembly areas, and it was used to build the flow matrix and calculate uncertainty for the model.

Each row shows a material transfer from one department to another. The dataset also includes the transport vehicle type (such as forklift or tow truck), quantity of material, date, and short descriptions of the sending and receiving processes. This helped us to understand how departments are connected and to see the difference between flows within the same zone and flows between different zones. Table B.1 shows a sample of the historical database.

Before using the data in the model, several cleaning and processing steps were done. First, we added up the monthly values to get the total flow between each department pair. Then, we standardized the department names to make sure they match across the file. We also removed some very small flows that were not important, so that the focus stays on the main flows that affect layout decisions.

Another important part of this data is the transport modes. The dataset shows that forklifts were the most used vehicles, especially in earlier months. Over time, conveyors were installed for high-volume and stable routes, mostly in areas like final assembly and packing. Their use increased slowly and became more common toward the end of 2024. AGVs (automated guided vehicles) were added in 2023. At first, they replaced forklifts in some areas with frequent movements, like between storage and assembly. Although AGVs were not used as much as conveyors or forklifts, their use continued to grow. Manual transport stayed mostly the same and was used for special or small-volume flows.

These changes in transport methods also affected the flow quantities. Some changes came from seasonal demand, while others happened because of automation projects or transport policy updates.

One of the strong parts of this study is the way it deals with uncertainty. Instead of assuming a random or fixed value, the flow data was analyzed to calculate how much it changes month to month. For each pair of departments, we calculated the standard deviation and relative difference. These values were used to create uncertainty bounds, which were then added to the robust model using the budgeted uncertainty method. This makes the model closer to reality.

In short, the data processing step helped make the model more useful and realistic. The inputs came directly from actual production data, not from assumptions. By including transport mode information and using statistical methods to define uncertainty, the layout model becomes more practical and helpful for real factory conditions.

Table 4.11: Final Flow Data with Assigned Vehicles and Cost Index

Flow ID	**Source**	**Sink**	**Mean Flow**	**Vehicle**	**Cint**
1	1	7	37.12	AGV	3
2	1	8	129.63	AGV	3
3	1	9	30.17	AGV	3
4	2	3	34.68	Forklift	5
5	2	7	58.06	Forklift	5
6	2	9	58.01	Forklift	5
7	3	8	34.81	Tow Truck	6
8	4	7	78.76	Tow Truck	6
9	4	10	69.58	Forklift	5
10	5	7	57.89	Forklift	5
11	5	10	37.08	Forklift	5
12	5	21	115.83	Forklift	5
13	6	11	148.25	AGV	3
14	7	13	3012.89	Conveyor	2
15	8	9	3018.36	Conveyor	2
16	9	11	3017.46	Conveyor	2
17	10	8	78.95	Forklift	5
18	11	20	2318.87	Forklift	5
19	12	13	27.87	Forklift	5
20	13	8	3014.15	Conveyor	2
21	14	10	46.40	Forklift	5
22	15	10	46.40	Forklift	5
23	16	7	18.58	Forklift	5
24	17	18	18.55	Forklift	5
25	17	19	18.57	Forklift	5
26	18	7	139.36	Tow Truck	6
27	19	10	46.40	Forklift	5

4.10.2 Model Parameterization

The case study focuses on one of the manufacturing facilities of a home applience company, which originally included 23 departments distributed across two identical rectangular blocks. These blocks, each with dimensions of 48×13 meters, are separated by a fixed inter-block distance of 4 meters. Departments located in different blocks are connected through designated ramps placed along the shared length of the blocks.

Before applying the optimization model, certain layout-related managerial decisions were made. Specifically, some departments were merged to simplify material handling and better reflect actual functional groupings. The two Mainplant Semi Product Warehouses were merged into a single warehouse. Similarly, two plastic warehouses and two final warehouses were also combined, leading to a total of 21 departments to be used in the final layout optimization.

The department list along with their respective physical dimensions (length and width in meters) is shown in Table 4.12. These dimensions were taken from the actual layout blueprints and reflect the floor space requirements of each department.

Table 4.12: Departments and Their Dimensions

ID	Department Name	Length (m)	Width (m)
1	Mainplant Semi Product Warehouse	16.4343	4.5000
2	Plastic Warehouse	12.8524	4.2251
3	Plastic Warehouse (HM Stock)	6.9828	1.3662
4	Mechanic Warehouse	12.8524	3.0613
5	Export Goods Warehouse	20.5183	3.5673
6	Packaging Warehouse	11.6633	2.0746
7	Pre-Assembly Line	15.7366	3.6685
8	Assembly Line	12.8018	3.5673
9	Final Assembly Line	12.8018	3.5673
10	Foamed Door Line	8.0960	3.0360
11	Packaging Line	11.6633	1.5686
12	Compressor Warehouse	7.0587	1.6344
13	Foamed Body Line	10.2718	3.6685
14	Door Glass Warehouse	2.9854	2.9095
15	Gasket Raw Material Warehouse	9.8417	2.9854
16	Pipe Roll Warehouse	20.5183	2.6565
17	Plastic Sheet Warehouse / Extruder	7.0195	2.5503
18	Cabinet TF Area (CTF)	5.4142	4.3769
19	Door TF Area (DTF)	4.8323	3.0360
20	Finished Goods Warehouse	26.6409	10.3730
21	Other Production Area	20.4775	5.6308

The physical characteristics and spatial demands of these departments served as fixed inputs to the model. These values ensured that the resulting layout not only minimized material handling cost but also respected the operational space requirements of each production area.

Table 4.13: Department assignments in the current facility layout

Block	**Department Assignment**
A	{D1: Mainplant Semi Product Warehouse, D2: Plastic WH, D4: Mechanic WH, D5: Export Goods WH, D6: Packaging WH, D7: Pre Assembly Line, D8: Assembly Line, D10: Foamed Door Line, D11: Packaging Line, D13: Foamed Body Line}
B	{D3: Plastic WH HM Stock, D9: Final Assembly Line, D12: Compressor WH, D14: Door Glass WH, D15: Gasket Raw Material WH, D16: Pipe Roll WH, D17: Plastic Sheet WH / Extruder, D18: CTF, D19: DTF, D20: Finished Goods WH, D21: Other Production}

Table 4.13 shows the department assignments in the current facility layout before optimization. The factory is divided into two main blocks, A and B. Departments are listed by their ID and full process name, showing which ones are placed together in the same block. This table helps clarify the initial spatial grouping used in practice, which serves as the reference configuration before applying the robust optimization model. The original layout was shaped by past design choices, operational needs, and equipment location, rather than a cost-minimizing layout strategy.

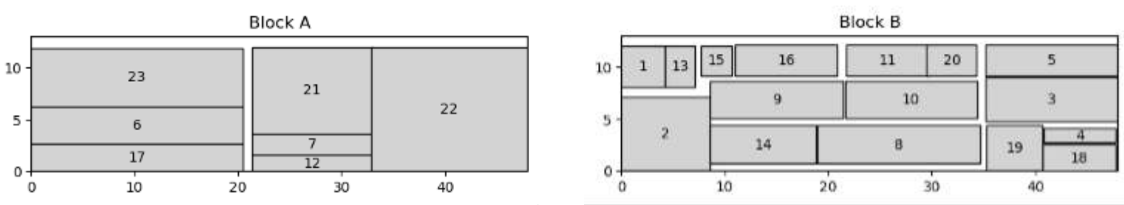

(a) Current layout of Block A

(b) Current layout of Block B

Figure 4.4: Visual representation of the current facility layout.

Figure 4.4 presents the visual layout of the two blocks based on the current factory design. Subfigure (a) displays Block A, while subfigure (b) shows Block B. Each rectangle represents one department, with positions and sizes based on actual floor dimensions. This layout illustrates how departments are currently arranged in the factory and highlights the constraints and inefficiencies that motivated the development of a more optimized model. Comparing this baseline with the optimized layout later in the chapter will allow a clearer evaluation of potential space utilization and transportation improvements.

Selection of the Γ *Parameter*

In the robust optimization framework adopted in this study, the budget of uncertainty parameter, denoted as Γ, controls the level of protection against deviations from nominal values. A higher Γ value increases conservatism by assuming that more flows may simultaneously take their worst-case values, whereas a lower Γ focuses on average-case performance. To ensure the robustness of the facility layout without making the model overly conservative, we used a data-based method to set this parameter.

As detailed in Chapter 4, we first identified the set of critical flows—defined as those with a volume greater than 100 units. Among the 33 department-to-department flow pairs, 8 flows were classified as critical based on this threshold. These flows contribute the most to the total material handling cost and have a significant influence on layout decisions. Therefore, the uncertainty budget was set to $\Gamma = 5$, allowing all critical flows to deviate simultaneously within their defined uncertainty bounds. This value reflects a realistic worst-case scenario in which all high-volume flows may experience deviations at the same time, while the remaining flows are assumed to remain close to their average levels.

The choice of $\Gamma = 5$ is not arbitrary but is mathematically supported by the distribution and weighting of flow volumes. It aligns with the principles of the budgeted uncertainty set proposed by [Bertsimas and Sim, 2004], which allows for adjustable protection levels while maintaining computational tractability. By doing so, we avoid over-conservatism that could lead to inefficient layouts and also ensure that the solution is resilient to the most impactful variations observed in the dataset.

This data-driven and volume-sensitive approach to setting Γ provides a strong balance between robustness and practicality. It strengthens the model's ability to produce layouts that are not only cost-efficient under normal operating conditions but also capable of maintaining performance under real-world variability.

4.10.3 Implementation Environment

All modeling and data analysis were performed in Python 3.13.2. The optimization model was implemented as a mixed-integer linear program and solved using Gurobi Optimizer version 12.0.1 with the gurobipy interface.

The experiments were run on a 2024 MacBook Pro with an Apple M4 Pro processor (12 cores) and 24 GB unified memory, using the mac64[arm] version of Gurobi on macOS Darwin 24.4.0.

For the final configuration with 21 departments, two blocks, and predefined ramps, the complete two-phase solution was obtained in 326.36 seconds, benefiting from Gurobi's presolve and multithreading features.

4.10.4 Quantitative Summary of Robust Model Outputs

The updated robust facility layout model was applied to a real-world industrial case involving 21 departments distributed across two predefined rectangular blocks. Each block was sized 48 meters in length and 13 meters in width. The departments were modeled with fixed dimensions, and their positions within blocks were optimized using a Mixed-Integer Linear Programming (MILP) model formulated under uncertainty.

The model employed a Γ-robust optimization framework to account for uncertainty in material flows. An uncertainty level of 18% was used for each department pair, and the budget parameter Γ was set to 5, representing the maximum number of simultaneous worst-case deviations in critical flows. The model was solved using the Gurobi optimizer in approximately 326.37 seconds, exploring over 377,000 nodes and performing more than 24 million simplex iterations. The solver reached an optimal solution with a final objective value of 736,999.64 and a duality gap of less than 1

In the optimal layout, departments were assigned to either Block 1 or Block 2, and their (x, y) coordinates were calculated. A total of three inter-block flows were identified. Unlike traditional models, where flows are routed through a single pair of transfer points, this new model allowed flexible distribution of flows across multiple ramp pairs. Each block contained three fixed ramps, and flow between blocks could be dynamically split among these ramp combinations based on distance and ramp capacity constraints.

The total inter-block flow volume was 3,319.0 units, with all flows successfully routed through three available ramp paths per direction. For example, the largest inter-block flow—3,229.0 units from Department 9 to Department 11—was distributed as 5.3%, 72.7%, and 22.1% across ramp paths R1→R1, R2→R2, and R3→R3, respectively. Similar flexible routing was observed in other inter-block flows, with all ramp capacities respected.

Ramp capacity utilization remained well below limits, with the highest utilization observed at Ramp 2 (33.9%). All flow conservation constraints were satisfied, confirming the correctness of flow distribution logic. Additionally, the model ensured that AEIOUX closeness penalties were minimized. Only 22.00 units of penalty cost were recorded, indicating that most preferred department pairs were assigned within the same block.

From a cost perspective, the solution achieved a total internal transportation cost of 498,041.90, and an external transportation cost of 132,760.00. The separation penalties added 22.00 units, resulting in a nominal total cost of 630,823.90. On top of this, robust protection terms contributed 106,175.74 units to the final robust cost: 5 × 4,670.74 = 23,353.70 units from the global $\Gamma \cdot \pi$ buffer and 82,822.05 units from individual ρ_{ij} deviation terms. The resulting total robust objective value was 736,999.64.

Managerially, the model offers several insights. First, by allowing flows to split flexibly across ramp pairs, the layout supports resilience in case of partial ramp failures or maintenance shutdowns. Second, minimizing AEIOUX-based separation penalties reflects a layout design that aligns with department affinity preferences. Third, robustness against uncertain flows ensures that the layout remains effective even when flow values change within the defined deviation bounds. Overall, the solution balances operational efficiency, structural feasibility, and robustness, providing a layout plan that is both cost-optimal and adaptable to variability in production conditions.

Figure 4.5 presents the final optimized layout with flexible ramp-based flow routing between the two blocks. Departments are displayed with their assigned positions inside Block 1 and Block 2, while colored rectangles represent the three fixed ramps on each side. The arrows between blocks indicate inter-block flows, where the color corresponds to the ramp pair used. Each arrow is labeled with the flow origin, destination, total volume, and dominant ramp path. For instance, the largest flow (from Department 9 to Department 11) is again split across all three ramp paths, with the majority routed through Ramp 2, as indicated in the flow label. The figure also includes a legend summarizing ramp capacity and usage levels. The clear visual distinction between ramp assignments and flow paths illustrates how the model leverages flexibility to distribute high-volume flows efficiently, minimizing both external transportation cost and congestion.

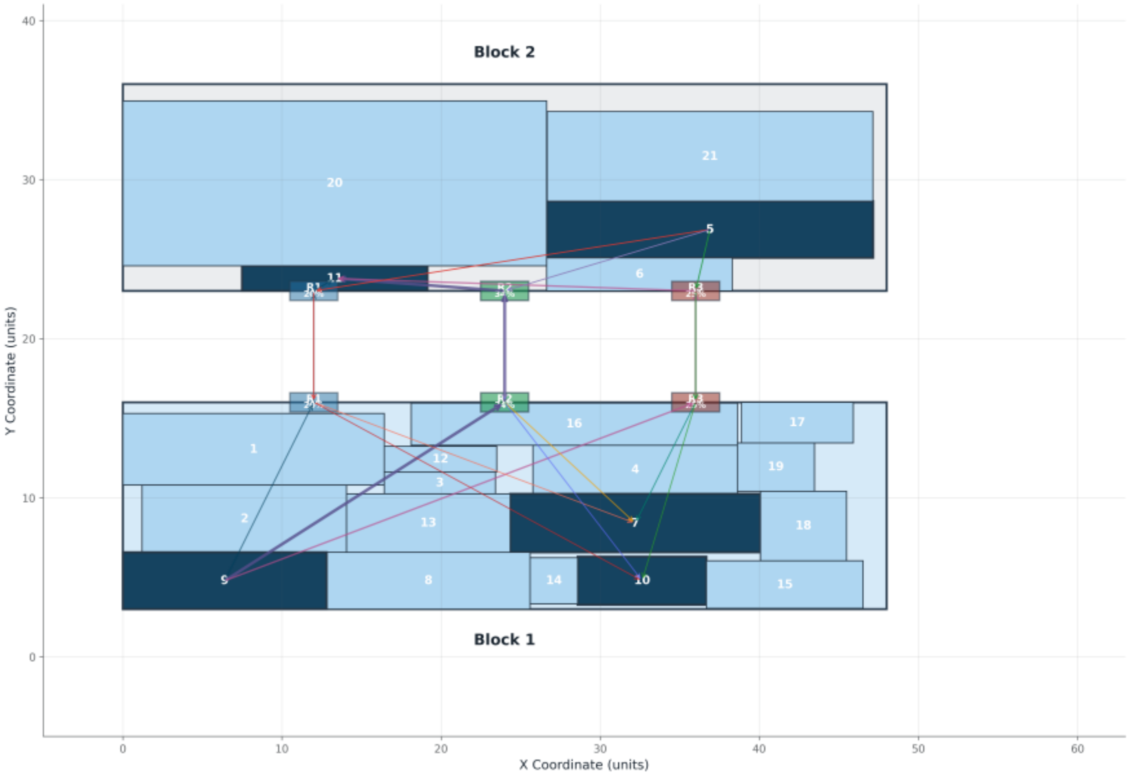

Figure 4.5: Optimized Layout with Flexible Ramp-Based Inter-Block Flows

To further support the quantitative interpretation of ramp usage, Figure 4.6 provides a bar chart showing the capacity utilization of each ramp. The total capacity and used flow for each ramp are visualized in overlaid bars, with utilization percentages annotated on top. Ramp 2 (Conveyor) shows the highest usage at 67.9%, followed by Ramp 3 (Large) at 49.5%, and Ramp 1 (Small) at 39.9%. These updated values confirm that ramp assignments remained within capacity limits and that flow was distributed in a balanced manner. The chart also demonstrates the effectiveness of the optimization model in utilizing multiple ramp paths simultaneously, ensuring no single ramp becomes a bottleneck.

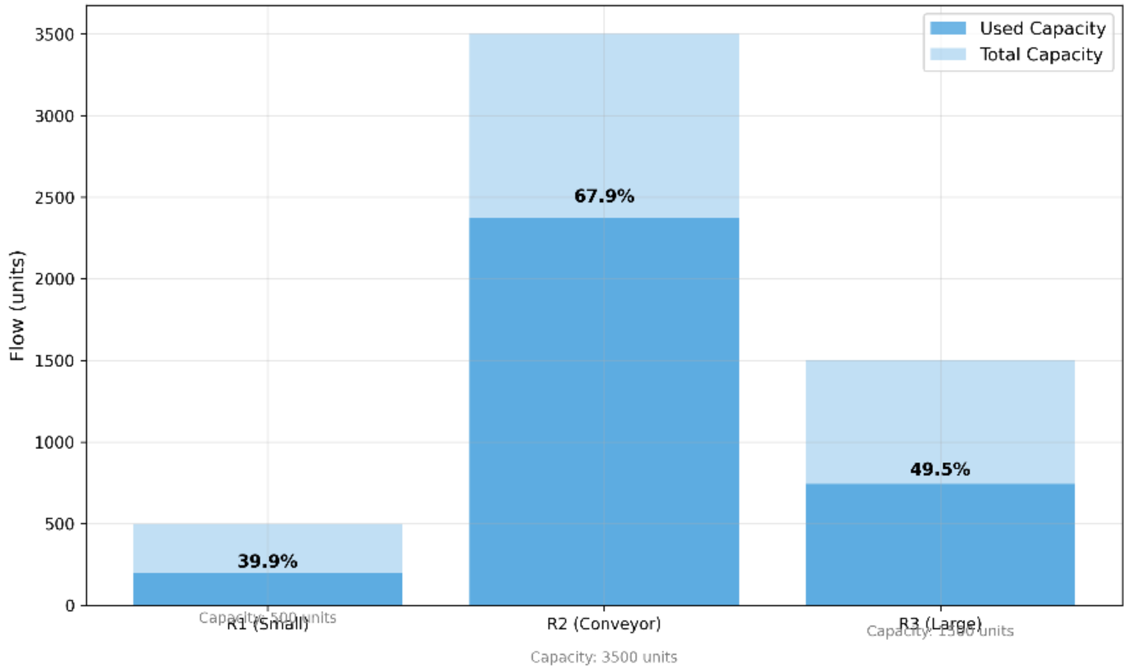

Figure 4.6: Ramp Capacity Utilization Across All Inter-Block Flows

Table 4.14: Ramp Capacity Utilization

Ramp	**Type**	**Capacity (units)**	**Used (units)** (%)
R1	Small	500	199.5 (39.9%)
R2	Conveyor	3500	2376.3 (67.9%)
R3	Large	1500	743.2 (49.5%)

Table 4.14 shows the usage of each ramp under the final flow distribution. Ramp 2 (high-capacity) carries the majority of the inter-block flow, followed by Ramp 3 (mid-capacity) and Ramp 1 (low-capacity). All ramps operate well within their respective capacity limits, with none exceeding 70% utilization. This confirms that the layout achieves an efficient and balanced use of transfer infrastructure, leveraging flexible flow routing to avoid congestion and maintain robustness in the physical layout.

Table 4.15: Breakdown of Robust Objective Function Components

Cost Component	**Value (monetary units)**
Internal Transportation Cost	498,041.90
External Transportation Cost (via ramps)	132,760.00
AEIOUX Separation Penalty	22.00
Nominal Objective Value	**630,823.90**
Robust Protection Term: $\Gamma \cdot \pi$ (5×4670.74)	23,353.70
Robust Deviation Sum: $\sum \rho_{ij}$	82,822.05
Total Robust Objective Value (z)	**736,999.64**

Table 4.15 decomposes the total robust objective value into its components. The internal cost accounts for within-block material movement, while external cost reflects ramp-based flow routing. The AEIOUX penalty ensures closeness of preferred department pairs. Robust terms add protection against uncertainty, resulting in a final cost of 830,871.58.

4.11 Summary and Conclusions

This chapter developed and validated a robust facility layout optimization model that directly integrates uncertainty into the design process using real historical data. Unlike traditional approaches that rely on fixed or assumed material flow values, our method builds on three years of daily, shift-level production data from a real home appliance manufacturing plant. By analyzing these data in detail, the model captures the natural variability of inter-departmental flows caused by seasonal demand changes, process modifications, and the gradual adoption of automation technologies such as AGVs and conveyor systems.

The first part of the chapter focused on building a statistical foundation for modeling uncertainty. This included collecting and preparing over 2,000 time points per flow pair, cleaning the data to remove anomalies, adjusting for month length and seasonality, and calculating key metrics such as average flow, standard deviation, and coefficient of variation (CV) for each department pair. By applying the two-sigma rule, the uncertainty for each flow was estimated based on its historical variation, resulting in interpretable and statistically justified deviation bounds. Importantly, these calculations were validated using normality testing (Shapiro–Wilk test), cross-validation, and a bootstrap-based confidence interval analysis, confirming the reliability and consistency of the uncertainty estimates across different flows.

A notable contribution of this chapter is the volume-weighted uncertainty method, which ensures that high-volume and operationally critical flows receive more weight in the uncertainty estimation process. This method prevented the results from being skewed by low-volume flows with high relative variation. Using this approach, we determined that the most realistic and balanced flow uncertainty level for this facility is 18%. This percentage was not arbitrarily chosen; rather, it emerged as the weighted average of individual two-sigma-based uncertainties across all significant flow pairs in the system.

Another key modeling element is the use of a budgeted uncertainty framework through the selection of the Gamma (Γ) parameter. This parameter controls how many department-to-department flows are allowed to deviate simultaneously in the robust optimization model. Instead of assigning a fixed or assumed value to Γ, we applied a data-driven selection method, identifying flows with an average daily volume above 100 units as critical. Based on this threshold, eight department pairs were found to be highly impactful, leading to the choice of $\Gamma = 5$. This decision ensures that the model remains protective against disruptions in high-priority flows, while avoiding excessive conservatism that could reduce space efficiency.

Beyond uncertainty modeling, the chapter introduced a comprehensive and realistic extension to the facility layout problem. In the improved MILP model, interblock flows are no longer simplified using abstract distance penalties. Instead, they are routed through predefined ramp locations, each with its own capacity and physical positioning. This enhancement brings the model closer to real-world production logistics, where departments on different floors or buildings must rely on fixed paths like tunnels, elevators, or ramps. The model supports flow splitting across multiple ramp pairs, further increasing its flexibility and practicality, especially when dealing with ramp congestion or maintenance-related disruptions.

The application of this robust layout model to facility's washing-machine factory demonstrated its effectiveness in a real industrial setting. The model was applied to 21 departments distributed across two unequal-area blocks with fixed dimensions. The final robust solution minimised total cost while satisfying spatial, operational and robustness constraints. The solver reached an optimal solution in approximately 326 seconds using the Gurobi Optimizer, with a duality gap of less than 1%. The resulting robust objective value was 736,999.64. This cost comprises 498,041.90 units of internal transportation, 132,760.00 units of external ramp-based movement and 22.00 units of AEIOUX separation penalties, yielding a nominal objective of 630,823.90 units. Robustness terms add a further 106,175.75 units—specifically, 23,353.70 units from the global $\Gamma ! \cdot ! \pi$ buffer ($5 \times 4{,}670.74$) and 82,822.05 units from flow-specific deviation penalties ($\sum \rho_{ij}$)—producing the final robust objective value reported above.

Importantly, the model ensured that all ramp-capacity limits were respected. Ramp 2, the high-capacity ramp, carried the largest share of inter-block flow with a utilisation rate of 67.9%, while Ramp 3 (mid-capacity) and Ramp 1 (low-capacity) operated at 49.5% and 39.9%, respectively. Because flows were allowed to split flexibly across ramp pairs, traffic was balanced across the infrastructure, avoiding congestion and preserving robustness. In addition, the model complied with all non-overlap and spatial feasibility constraints, assigning departments to positions that respect their true floor-area requirements.

From a managerial standpoint, the model offers several valuable insights. First, it demonstrates that real production data can be directly used to build robust layout models without requiring subjective assumptions. Second, it highlights how integrating uncertainty and qualitative preferences into layout planning leads to solutions that are both resilient and operationally realistic. Third, it shows how emerging logistics elements such as ramp capacity and inter-block movement can be modeled precisely, helping planners evaluate different infrastructure strategies more accurately.

While the Γ-robust formulation protects the layout against everyday, proportional flow fluctuations, it remains blind to the plant's rarer but high-impact disruptions—such as a sudden ramp shutdown, an unexpected demand surge, or a temporary supply bottleneck. These events manifest as *discrete* shocks rather than smooth deviations around historical means, and capturing them by merely inflating the uncertainty budget would either underestimate their severity or impose unnecessary conservatism on normal operations. To address this limitation, the next chapter introduces a scenario-based robust layout model that evaluates a single layout under a finite set of realistically defined disturbance scenarios, each with its own flow matrix, ramp capacities, and cost parameters. This extension allows decision-makers to balance average performance with worst-case resilience, pinpoint critical infrastructure weaknesses, and develop targeted contingency plans—all benefits that lie beyond the reach of the budgeted approach adopted in the present chapter.

In conclusion, this chapter demonstrated that data-driven uncertainty modelling, budgeted robust optimisation, and real-world logistical constraints can be blended into a single, operationally realistic facility-layout framework. The resulting model overcomes the main weaknesses of deterministic formulations and provides a layout that is both adaptable and quantitatively defensible. By uniting statistical rigour with practical design requirements, it narrows the gap between academic modelling and the complex realities of modern manufacturing. At the same time, the analysis revealed that rare but high-impact disruptions remain partly outside the protective envelope of a single uncertainty budget. Accordingly, the methods and insights developed here serve as the quantitative and computational foundation for the scenario-based robustness study presented in Chapter 5, where discrete disturbance cases are evaluated to achieve an even more resilient facility layout.

Chapter 5

SCENARIO-BASED ROBUST FACILITY LAYOUT MODEL

5.1 Introduction

In the previous chapter, a robust facility layout model was developed using uncertainty data extracted from historical production flows. The model assumed that uncertainty could be expressed by a fixed deviation around nominal values, and it used a protection mechanism to defend against possible changes in material flows. Although that approach improved reliability compared to a purely deterministic layout, it still had some limitations. In particular, the model relied on a single level of protection, applied equally to all flows. It also did not allow for detailed control over different types of uncertainty or how the system might behave in specific operational conditions. In real-world factories, uncertainty does not affect all parts of the system in the same way. Some flows might change due to seasonal demand, while others are affected by machinery failures or transportation issues. Therefore, modeling these situations using a single global protection level can result in solutions that are either too conservative or not robust enough.

To address these challenges, this chapter introduces a new approach that models uncertainty through a set of possible future scenarios. Each scenario represents a specific condition that the system might face, such as increased flow for certain departments, changes in ramp availability, or shifts in cost parameters. Instead of protecting against general uncertainty, the new model evaluates layout decisions across all defined scenarios and tries to find a solution that performs well in all of them. This helps to design a layout that is not only cost-efficient on average but also remains reliable and feasible when operating conditions change.

This approach follows the framework originally suggested by Mulvey et al. Mulvey et al. [1995], which is known as scenario-based robust optimization. In this framework, the goal is to find solutions that are both consistent across different scenarios and close to optimal on average. The model includes terms in the objective function that account for expected cost, cost variation between scenarios, and penalties when layout decisions cause constraint violations in certain conditions. These additional terms guide the optimization process towards solutions that are stable and practical under uncertainty, rather than only optimal in ideal conditions. Unlike the approach presented in Chapter 4, this model separates the layout design variables from scenario-specific decision variables. As a result, the layout does not change from one scenario to another, but the way flows are routed and costs are calculated can adapt based on each scenario's data.

By using this method, we can model complex and realistic situations without over-simplifying the nature of uncertainty. For example, a ramp may become unavailable in one scenario, or flow between two departments may increase in another. The model can reflect these differences directly and measure how the layout performs in each case. Furthermore, it allows us to attach probabilities to each scenario, which helps to capture the most likely conditions more accurately. This way, layout decisions are not only based on worst-case protection but also consider operational frequency and business relevance.

In summary, the scenario-based approach improves upon the previous model by allowing for more detailed and flexible uncertainty modeling. It avoids the drawback of using fixed protection levels and provides a clearer understanding of how different disruptions affect the layout. The model in this chapter combines design consistency, cost performance, and operational resilience into a single optimization framework, making it suitable for real industrial applications where uncertainty is present but cannot be simplified into a single number.

5.2 Literature Basis: Scenario-Based Robust Optimization

Scenario-based robust optimization is a well-established method that focuses on handling uncertainty by defining multiple possible future conditions. Each condition, or scenario, includes its own data for flows, costs, and capacities. The model then evaluates the same layout under each scenario and tries to minimize an objective function that combines performance across all of them. This approach is useful when the uncertain elements are too complex or irregular to be captured by a single variation parameter, as was used in the previous chapter.

The key idea behind this method is to find decisions that do not change between scenarios but still work well under all of them. These are called scenario-independent or design variables. In contrast, other decisions like routing or operational flow levels can vary depending on the scenario. These are called scenario-dependent or control variables. This separation allows the layout to remain fixed while the flow paths and resource usage adapt to the conditions of each scenario. This way, we can test the flexibility and robustness of the layout design without having to reassign departments or reconfigure the physical structure for each situation.

The objective function in this kind of model usually includes three parts. The first is the expected cost, which is the average cost over all scenarios, weighted by their probabilities. The second part is the cost variability, which is often measured by the total deviation of each scenario's cost from the expected cost. This helps to control the stability of the solution and avoid large cost swings. The third part is a penalty term, which is added when certain constraints—such as ramp capacity—are violated in some scenarios. These violations might happen because it is not always possible to satisfy all constraints in every scenario without making the layout overly conservative. The penalty allows the model to balance feasibility with efficiency by discouraging but not completely preventing small violations.

The benefit of this approach is that it provides a more transparent and flexible way to evaluate trade-offs between cost, stability, and feasibility. It avoids being too optimistic (as in deterministic models) or too pessimistic (as in conservative robust models). Instead, it gives decision-makers a clear picture of what layout decisions work best when multiple types of uncertainty are taken into account. For these reasons, this method is widely used in applications where long-term planning must remain valid under changing operational environments.

In the context of this thesis, the scenario-based model allows us to incorporate different patterns of uncertainty into layout design. These may include variations in flow volumes, temporary unavailability of ramps, or changes in external transport distances. By solving the same layout problem across a carefully selected set of scenarios, we can test the robustness of the solution in a structured and meaningful way.

5.3 Model Formulation

This section presents the complete mathematical formulation of the scenario-based robust facility layout problem. The model is designed to handle multiple sources of uncertainty by evaluating the same layout under a set of predefined scenarios. Each scenario $\omega \in \Omega$ describes a possible realization of flow, cost, or capacity conditions that may occur in practice. The aim is to design a layout that remains feasible and cost-effective across all scenarios while minimizing the total expected cost, cost variability, and any penalties caused by constraint violations such as ramp overuse.

To achieve this, the model uses two types of decision variables. The first group, called *design variables*, is shared across all scenarios. These variables determine how departments are assigned to blocks, where each department is located, and how internal layout constraints are satisfied. The second group, called *control variables*, is scenario-specific. These include variables for routing flows through ramps, calculating distances, handling capacity violations, and computing the scenario-based cost. This separation allows us to maintain a consistent layout design while adapting flow-related decisions to each scenario's specific data.

The objective function is composed of three terms. The first term represents the expected cost across all scenarios, weighted by the scenario probabilities ρ^ω. The second term penalizes large deviations from the average cost using the positive and negative deviation variables. The third term includes penalties for any violations of ramp capacity or layout feasibility in individual scenarios. The scalar parameters λ and W allow the user to control the weight given to variability and penalties, respectively. This provides flexibility in balancing between cost efficiency and robustness.

The sets, parameters, decision variables, objective function, and constraints of the model are defined below. All terms are described in a way that reflects practical facility layout planning under uncertain future conditions.

Sets

$i, j \in N$	Departments	(5.1)
$k, k_1, k_2 \in M$	Blocks	(5.2)
$r, r_1, r_2 \in R$	Ramps	(5.3)
$\omega \in \Omega$	Scenarios	(5.4)

Parameters

l_i, w_i	Length and width of department i	(5.5)
LF, WF	Length and width of each block	(5.6)
p_{ij}^{ω}	Flow from department i to j under scenario ω	(5.7)
c_{ij}^{int}	Internal transport cost from i to j	(5.8)
c_{ω}^{ext}	External transport cost in scenario ω	(5.9)
RC_r^{ω}	Ramp capacity for ramp r in scenario ω	(5.10)
$D_{r_1 r_2}$	Distance between ramps r_1 and r_2	(5.11)
RC_{ij}	Closeness rating between departments i and j	(5.12)
π_{ω}	Probability of scenario ω	(5.13)
$\lambda,\ w$	Weights for cost deviation and violation penalty	(5.14)

Decision Variables

Scenario-independent (design variables):

$$Y_{ik} \in \{0,1\} \qquad \text{1 if department } i \text{ is assigned to block } k \tag{5.15}$$

$$S_k \in \{0,1\} \qquad \text{1 if block } k \text{ is used} \tag{5.16}$$

$$x_{ik},\ y_{ik} \geq 0 \qquad \text{Coordinates of department } i \text{ in block } k \tag{5.17}$$

$$q_{ijk} \in \{0,1\} \qquad \text{1 if departments } i \text{ and } j \text{ are both assigned to block } k \tag{5.18}$$

$$d_{ij,x}^{int},\ d_{ij,y}^{int} \geq 0 \qquad \text{Internal Manhattan distance components between departments } i \text{ and } j \tag{5.19}$$

$$\alpha_{ijk},\ \beta_{ijk} \in \{0,1\} \qquad \begin{array}{l} \text{Non-overlap direction variables:} \\ (1,1):\ i \text{ precedes } j \text{ horizontally} \\ (0,0):\ j \text{ precedes } i \text{ horizontally} \\ (1,0):\ i \text{ precedes } j \text{ vertically} \\ (0,1):\ j \text{ precedes } i \text{ vertically} \end{array} \tag{5.20}$$

Scenario-dependent (control variables):

$$F_{ijk_1k_2r_1r_2}^{\omega} \geq 0 \qquad \text{Flow from } i \text{ to } j \text{ via ramps and blocks in } \omega \tag{5.21}$$

$$Z_{ijk_1k_2r_1r_2}^{\omega} \in \{0,1\} \qquad \text{Ramp flow indicator in } \omega \tag{5.22}$$

$$d_{ij}^{ext,\omega} \geq 0 \qquad \text{External distance between } i, j \text{ in } \omega \tag{5.23}$$

$$v_{kr}^{\omega} \geq 0 \qquad \text{Ramp capacity violation for ramp } r \text{ in block } k \text{ in } \omega \tag{5.24}$$

$$C^{\omega} \geq 0 \qquad \text{Total cost in scenario } \omega \tag{5.25}$$

$$\delta_{\omega}^{+}, \delta_{\omega}^{-} \geq 0 \qquad \text{Cost deviation from } \bar{C} \text{ in } \omega \tag{5.26}$$

Auxiliary variables:

$\bar{C} \geq 0$	Expected cost	(5.27)
$V \geq 0$	Total violation penalty	(5.28)

Objective Function

$$\min\ \bar{C} + \lambda \sum_{\omega \in \Omega} \pi_\omega \left(\delta_\omega^+ + \delta_\omega^-\right) + w \cdot V \tag{5.29}$$

where

$$\bar{C} = \sum_{\omega \in \Omega} \pi_\omega \, C^\omega \tag{5.30}$$

$$C^\omega - \bar{C} = \delta_\omega^+ - \delta_\omega^- \qquad \forall\, \omega \in \Omega \tag{5.31}$$

$$V = \sum_{\omega \in \Omega} \pi_\omega \sum_{k \in \mathcal{M}} \sum_{r \in R} v_{kr}^\omega \tag{5.32}$$

$$C^\omega = C_{\text{int}}^\omega + C_{\text{ext}}^\omega + P \qquad \forall\, \omega \in \Omega \tag{5.33}$$

$$C_{\text{int}}^\omega = \sum_{i \neq j} p_{ij}^\omega \, c_{ij}^{\text{int}} \left(d_{ij,x}^{int} + d_{ij,y}^{int}\right) \tag{5.34}$$

$$C_{\text{ext}}^\omega = c_\omega^{\text{ext}} \sum_{i \neq j} \sum_{\substack{k_1, k_2 \in \mathcal{M} \\ k_1 \neq k_2}} \sum_{r_1, r_2 \in R} F_{ijk_1k_2r_1r_2}^\omega \, D_{r_1r_2} \tag{5.35}$$

$$P = \sum_{i \neq j} RC_{ij} \left(1 - \sum_{k \in \mathcal{M}} q_{ijk}\right). \tag{5.36}$$

Subject to:

Scenario Constraints (for all $\omega \in \Omega$)

$$\sum_{k_1 \neq k_2} \sum_{r_1, r_2 \in R} F^{\omega}_{ijk_1k_2r_1r_2} = p^{\omega}_{ij} \cdot \left(1 - \sum_{k \in M} q_{ijk}\right) \quad \forall i \neq j \tag{5.37}$$

$$F^{\omega}_{ijk_1k_2r_1r_2} \leq p^{\omega}_{ij} \cdot Y_{ik_1} \cdot Y_{jk_2} \tag{5.38}$$

$$\sum_{i,j} \sum_{\substack{k' \in M \\ k' \neq k}} \sum_{r' \in R} F^{\omega}_{ijkk'rr'} \leq RC^{\omega}_{r} + v^{\omega}_{kr} \quad \forall k, r \tag{5.39}$$

$$F^{\omega}_{ijk_1k_2r_1r_2} \leq M \cdot Z^{\omega}_{ijk_1k_2r_1r_2} \tag{5.40}$$

$$d^{ext,\omega}_{ij} \leq M \cdot \left(1 - \sum_{k} q_{ijk}\right) \tag{5.41}$$

$$d^{ext,\omega}_{ij} \cdot p^{\omega}_{ij} \cdot (1 - \sum_{k} q_{ijk}) \geq \sum_{k_1 \neq k_2} \sum_{r_1, r_2 \in R} F^{\omega}_{ijk_1k_2r_1r_2} \cdot D_{r_1r_2} - M \cdot \sum_{k} q_{ijk} \tag{5.42}$$

Layout Constraints

$$x_{ik} - x_{jk} \leq d^{int}_{ij,x} + LF \cdot \left(1 - \sum_{t} q_{ijt}\right) \tag{5.43}$$

$$x_{jk} - x_{ik} \leq d^{int}_{ij,x} + LF \cdot \left(1 - \sum_{t} q_{ijt}\right) \tag{5.44}$$

$$y_{ik} - y_{jk} \leq d^{int}_{ij,y} + WF \cdot \left(1 - \sum_{t} q_{ijt}\right) \tag{5.45}$$

$$y_{jk} - y_{ik} \leq d^{int}_{ij,y} + WF \cdot \left(1 - \sum_{t} q_{ijt}\right) \tag{5.46}$$

Non-overlapping Constraints

$$x_{ik} + 0.5 l_i Y_{ik} \leq x_{jk} - 0.5 l_j Y_{jk} + LF(2 - \alpha_{ijk} - \beta_{ijk}) \tag{5.47}$$

$$y_{ik} + 0.5 w_i Y_{ik} \leq y_{jk} - 0.5 w_j Y_{jk} + WF(1 + \alpha_{ijk} - \beta_{ijk}) \tag{5.48}$$

Assignment and Logical Constraints

$$\sum_{k \in M} Y_{ik} = 1 \quad \forall i \tag{5.49}$$

$$S_k \leq S_{k-1} \quad \forall k > 1 \tag{5.50}$$

$$\sum_{i} Y_{ik} \geq S_k \quad \forall k \tag{5.51}$$

$$S_k \cdot |N| \geq \sum_{i} Y_{ik} \quad \forall k \tag{5.52}$$

$$q_{ijk} \leq 0.5(Y_{ik} + Y_{jk}) \tag{5.53}$$

$$q_{ijk} + 1 \geq Y_{ik} + Y_{jk} \tag{5.54}$$

Position Bounds

$$0.5 l_i Y_{ik} \leq x_{ik} \leq (LF - 0.5 l_i) Y_{ik} \tag{5.55}$$

$$0.5 w_i Y_{ik} \leq y_{ik} \leq (WF - 0.5 w_i) Y_{ik} \tag{5.56}$$

Alpha-Beta Symmetry and Transitivity

$$\alpha_{ijk} + \alpha_{jik} = 1, \quad \beta_{ijk} + \beta_{jik} = 1 \tag{5.57}$$

$$\alpha_{isk} + \alpha_{sjk} - \alpha_{ijk} \leq 1, \quad \beta_{isk} + \beta_{sjk} - \beta_{ijk} \leq 1 \tag{5.58}$$

The objective function defined in (5.29) is designed to address multiple planning goals at once. First, it minimizes the expected total cost of the layout across all defined scenarios. This expected cost $\bar{C}$ is calculated using the probability π_ω of each scenario, ensuring that more likely scenarios contribute more to the objective. Second, the model introduces two deviation terms, δ_ω^+ and δ_ω^-, which help the layout remain stable by penalizing scenarios that result in costs significantly above or below the expected average. The parameter λ controls how much we want to reduce these deviations. Third, the model includes a penalty for violating capacity constraints, especially ramp limits, which is captured by V and weighted by w. This way, the model not only seeks an efficient layout but also one that avoids operational risks and instability under uncertainty.

In equation (5.30), the expected cost $\bar{C}$ is defined as the weighted sum of the total costs C^{ω} over all scenarios, using their respective probabilities π_{ω}. Then, in (5.31), the difference between each scenario's actual cost and the expected cost is split into positive and negative parts, δ_{ω}^{+} and δ_{ω}^{-}, which are both included in the objective. This method helps keep the optimization linear and easy to solve, while still penalizing layouts that are too sensitive to scenario changes. The total violation penalty V, defined in (5.32), sums up all the excess ramp usage from every scenario. This value is included in the objective to discourage the model from exceeding ramp capacities, which may happen under high flow conditions.

The per-scenario cost C^{ω} is defined in Equation (5.33) as the sum of internal transport C_{int}^{ω}, external transport C_{ext}^{ω}, and the closeness/separation penalty P. In Equation (5.34), C_{int}^{ω} aggregates same-block flows p_{ij}^{ω} weighted by the internal unit cost c_{ij}^{int} and the internal Manhattan distance. C_{ext}^{ω} accounts for inter-block routing via ramp pairs using $F_{ijk_1k_2r_1r_2}^{\omega}$, the scenario-specific external cost c_{ω}^{ext}, and the ramp-to-ramp distance $D_{r_1r_2}$ as defined in Equation (5.35). The term P penalizes separating department pairs with high closeness ratings in Equation (5.36).

The scenario-specific constraints begin by ensuring that material flows are preserved. Constraint (5.37) checks whether the flow between departments i and j in a given scenario ω is properly routed through inter-block ramp paths. If these departments are assigned to the same block, the term $\sum_k q_{ijk}$ becomes one, and the right-hand side becomes zero, meaning no inter-block flow is allowed. If they are in different blocks, the flow p_{ij}^{ω} must be sent through the available ramp paths. Then, constraint (5.38) ensures that a flow path is only valid if both departments are assigned to the corresponding blocks. This helps avoid infeasible routing.

Since ramp capacities are limited and can vary between scenarios, constraint (5.39) ensures that the total flow passing through any ramp r in block k does not exceed the scenario-specific limit R_r^{ω}. If it does, the extra flow is captured in a non-negative violation variable v_{kr}^{ω}, which will be penalized. Constraint (5.40) ensures that the flow variables are only active when the ramp path is actually chosen, using a binary indicator $Z_{ijk_1k_2r_1r_2}^{\omega}$. This avoids partial or illogical flow paths.

For external distances, $d_{ij}^{ext,\omega}$ is used to represent the distance between departments i and j when they are in different blocks. Constraint (5.41) ensures that this value is zero when the departments are located in the same block. When they are in different blocks, constraint (5.42) links this external distance to the ramp-to-ramp paths selected by the model. The big-M term again helps switch the logic depending on whether the departments are co-located or not.

Internal distances are captured through constraints (5.43) to (5.46). These equations ensure that the horizontal and vertical distances between departments are only calculated when the departments are assigned to the same block. The internal distances $d_{ij,x}^{int}$ and $d_{ij,y}^{int}$ measure how far departments are from each other within their block, and these values are needed for cost and penalty terms involving closeness.

To make sure departments don't overlap, the model includes geometric constraints. Constraints (5.47) and (5.48) define how the center positions of departments are related in space. Using the binary variables α_{ijk} and β_{ijk}, the model decides whether department i is located to the left, right, above, or below department j. This logic is supported further with symmetry and transitivity rules defined later in the formulation.

Department assignment and block usage rules are handled in constraints (5.49) through (5.54). Each department must be assigned to exactly one block. Then, if a block is used, it must contain at least one department, and the number of assigned departments must be within allowed bounds. To ensure a clean and hierarchical use of blocks, constraint (5.50) ensures that block 1 is used before block 2. The auxiliary variable q_{ijk}, which indicates if two departments share a block, is defined through upper and lower bounds, ensuring consistent logic throughout the model.

The model also includes position bounds for each department's center. Constraints (5.55) and (5.56) make sure that the departments are placed inside the blocks and not outside the layout boundary. These are based on the dimensions of the block and the department itself.

Finally, the constraints in (5.57) and (5.58) define logical rules for how departments are placed in relation to each other. The symmetry rule makes sure that if department i is to the left of j, then j is to the right of i. The transitivity rule ensures consistent ordering between three departments, so the layout remains logically valid. These rules are essential to avoid overlapping and ambiguous positioning.

Together, these constraints and variables allow the model to assign each department to a specific block and location, while considering inter-department flows, ramp routing, cost uncertainty, and layout feasibility. The model is designed to work under multiple realistic scenarios, with a goal of producing robust and practical layouts for real-world production systems.

This model is designed to provide a practical and robust solution to the facility layout problem under uncertainty. It works by separating the layout decisions, which are shared across all scenarios, from the flow and cost-related decisions, which depend on each individual scenario. In this way, the model creates one consistent layout that can perform well across many possible future situations.

One of the main strengths of the model is how it deals with uncertainty in material flow and operational conditions. Instead of relying on a single estimate or average value, the model considers multiple scenarios that reflect different possible outcomes. Each scenario has its own probability, which allows the model to weigh the importance of each case. For example, if one scenario is more likely to happen, the layout will naturally be optimized more toward that situation. This approach allows the decision-maker to plan for variability in a realistic way.

The model also includes a special mechanism to protect against large cost variations across scenarios. By adding cost deviation terms to the objective function, the model avoids layouts that perform well only in some scenarios but fail badly in others. This feature increases the stability and reliability of the solution. Additionally, the use of violation variables for ramp capacities gives flexibility to the model. It allows small overloads when absolutely necessary but penalizes them so that the final solution avoids them unless there is no better option. This is especially useful in real-life systems where exact capacities might occasionally be exceeded but should be kept under control.

Another key strength is the ability to model detailed ramp-based routing for inter-block flows. The model not only decides which blocks each department should be placed in but also how their flows are routed through specific ramps, taking into account ramp distances and capacity limits. This level of detail provides more realistic results, especially in large-scale industrial facilities where logistics and congestion play a critical role.

Overall, the model provides a powerful and flexible tool for solving facility layout problems in uncertain environments. It can support planners by offering layouts that are not only cost-efficient but also robust and ready for variation in real-life conditions. The combination of expected cost, variability control, and operational feasibility makes it especially suitable for complex manufacturing settings where change and uncertainty are part of daily operations.

5.4 Motivation for Scenario-Based Modeling

The model presented in this chapter was developed as a response to some important limitations observed in the previous approach. In Chapter 4, a deterministic robust optimization model was used to generate a facility layout that could handle uncertainty in material flows. This was done by applying protection levels based on historical data to cover extreme deviations. While this method offered some level of safety against worst-case conditions, it still treated uncertainty in a simplified way and could not capture the full range of realistic production variations.

In real manufacturing systems, the conditions are not just uncertain — they change in complex and dynamic ways. Flow volumes between departments may increase or decrease depending on the product mix, seasonal demand, or production campaigns. Ramp availability might be affected by maintenance or reconfiguration. Even internal logistics costs may vary depending on how congested the system becomes. The deterministic model does not explicitly account for these diverse possibilities. It creates a layout that works for one specific version of the future, assuming that all uncertainty can be captured by fixed margins or buffers. This makes the layout less adaptive and possibly inefficient in cases where the actual conditions differ from the assumed baseline.

To address these issues, the current model uses a scenario-based robust optimization framework. Instead of relying on static input data, this approach defines multiple possible scenarios that describe different flow conditions, ramp capacities, and transport costs. Each scenario is assigned a probability that reflects its likelihood. The layout decisions are shared across all scenarios, but the flows, distances, and penalties are calculated separately for each one. This way, the model produces a single layout that performs well across a wide range of possible futures, not just one.

Another reason for moving to the scenario-based method is to better control the trade-off between efficiency and stability. By introducing cost deviation variables and penalizing variability across scenarios, the model encourages solutions that are not only cost-effective on average but also more consistent and predictable. This is an important feature for industrial environments where unexpected changes can lead to disruptions and higher operational risks.

In summary, the scenario-based model was developed to improve the realism, flexibility, and robustness of the facility layout planning process. It allows for more informed decisions by considering uncertainty in a structured and probabilistic way, offering better support for long-term production planning in complex systems.

5.5 Application

The scenario-based robust facility layout model introduced in this chapter is tested on the same real-life use case examined in previous chapters. The use case represents a major production site operated by one of the largest European home appliance companies, specializing in the manufacturing of washing machines. This facility includes various departments responsible for tasks such as metal forming, painting, assembly, and testing. The layout problem in this plant is particularly challenging because of the high material flow between departments, the unequal area requirements of each section, and the presence of multiple blocks separated by fixed physical boundaries. These conditions make the problem ideal for evaluating advanced layout optimization models.

In the previous chapter, a deterministic robust optimization approach was applied to this facility using a single flow matrix with uncertainty margins calculated from historical data. Although that model could handle worst-case deviations to some extent, it treated uncertainty as fixed protection bands and did not reflect the range of possible operating conditions that the facility might realistically experience. For example, changes in demand patterns, seasonal shifts, or production mix variations were not explicitly captured in the model structure.

In this chapter, the same facility is used to evaluate a more advanced and flexible model that incorporates scenario-based uncertainty. Instead of relying on static protection parameters, the new model defines multiple possible future scenarios, each with its own flow values, ramp capacities, and cost coefficients. These scenarios are designed based on real production data and expert insights, and are assigned probabilities to reflect their expected likelihood. This approach allows the model to create a layout that performs well not just in a single case, but across a variety of realistic operating conditions.

By applying the new model to the same plant, it becomes possible to directly compare how the layout performance improves when uncertainty is modeled in a more detailed and probabilistic way. This comparison helps to highlight the strengths of the scenario-based approach, particularly in capturing the trade-offs between cost efficiency, layout stability, and the flexibility to adapt to different production conditions. It also shows how layout decisions can be made more robust by considering not only average performance but also cost variability and possible constraint violations, such as exceeding ramp capacity. Overall, using this real and complex case again gives meaningful insights into the model's practicality and effectiveness in real-world manufacturing environments.

5.5.1 Scenario Design and Data Integration

To evaluate how the proposed layout performs under different uncertain conditions, a total of ten discrete scenarios were defined. Each scenario represents a possible future state of the manufacturing system, covering various disruptions such as changes in material flows, equipment failures, demand shifts, and cost fluctuations. These scenarios were defined through a combined approach: where possible, historical data patterns from daily flow records (over 64,000 events) were analyzed to identify typical and atypical conditions; for disruptions not present in the available data—such as ramp failures or cost spikes—industrial experience and expert judgment were used to construct representative and challenging what-if scenarios. These scenarios allow the model to explore a wide range of operational possibilities in a structured way.

The base case is represented by Scenario 1, which reflects normal operations with standard flows and full ramp availability. The remaining nine scenarios introduce one or more disruptions to simulate real-world variability. Some of these scenarios involve increases or decreases in flow volumes, while others represent a ramp outage or higher external transportation cost. By including these different situations, the model can find a layout that works well not only under expected conditions but also when disruptions occur.

Each scenario was assigned a probability calibrated either from the empirical event frequencies in the dataset or, where required, estimated using engineering judgment for hypothetical scenarios. These probabilities are used to calculate the expected cost and to guide the optimization toward solutions that are both efficient and robust. Table 5.1 summarizes the key characteristics of the ten scenarios used in this study.

Table 5.1: Scenario Summary and Key Parameters

Scenario ID	Description	Flow Variation	Probability
Scenario 1	Normal condition with no disruptions	None	0.25
Scenario 2	Moderate increase in critical flows	Partial	0.15
Scenario 3	Global reduction in total flow	Global	0.15
Scenario 4	Unavailability of one ramp	None	0.10
Scenario 5	Reduced output in key departments	Indirect	0.08
Scenario 6	Combined increase in flow and ramp failure	Combined	0.08
Scenario 7	Localized shortage in incoming materials	Partial	0.06
Scenario 8	Higher system throughput requirement	Global	0.08
Scenario 9	Significant rise in inter-block transfer cost	Cost only	0.03
Scenario 10	Rework-driven flow increase in all units	Global	0.02

Table 5.2 compares the assigned scenario probabilities with their observed frequencies in the historical data. Where possible, empirical cases were aligned closely; for rare or engineered disruptions, probabilities were selected to ensure adequate representation of both likely and high-impact, low-frequency events, supporting a balanced and robust scenario framework.

Table 5.2: Comparison of scenario probabilities assigned in the model and their observed frequencies in historical data. Engineered scenarios are based on expert judgment.

Scenario	Designed Probability	Realized Probability
normal	0.25	0.267
critical_peak	0.15	0.142
global_reduction	0.15	0.153
ramp_failure	0.10	0.095
keydept_drop	0.08	0.073
peak_rampfail	0.08	0.084
input_shortage	0.06	0.062
throughput_surge	0.08	0.081
cost_spike	0.03	0.023
rework_surge	0.02	0.021

The base flow data used in Scenario 1 was derived from real plant data, reflecting typical material movements on a daily basis. Scenario-specific flow matrices were then created by modifying these base values according to predefined rules. For example, some scenarios increased or decreased the flows between selected department pairs, while others applied a fixed change across the entire matrix.

Ramp capacities were also updated to reflect disruptions. In scenarios where a ramp is considered unavailable, its capacity was set to zero. The default capacity settings were defined as 500 units for Ramp 1, 3500 units for Ramp 2, and 1500 units for Ramp 3. These values were adjusted in the corresponding scenarios based on availability. For example, in scenarios simulating equipment failure, the affected ramp's capacity was removed, forcing the model to find alternative routes.

Some scenarios also modified the external transportation cost. Instead of using a fixed cost for all cases, scenarios with energy-related disruptions applied a multiplier (e.g., three times the base cost) to simulate real market conditions. These adjustments encouraged the model to reduce inter-block flows and use ramps more efficiently when external transfers became expensive.

Each scenario has its own flow matrix p_{ij}^{ω}, ramp capacity vector RC_r^{ω}, and, if needed, a unique external cost parameter c_{ω}^{ext}. These values were integrated into the model to simulate realistic planning decisions under uncertainty. Importantly, the AEIOUX closeness ratings and department sizes remained consistent across all scenarios to ensure a fair comparison.

By including these carefully designed and logically weighted scenarios, the model can find layout solutions that are not only cost-efficient under expected conditions but also robust to possible disruptions. This structured approach to scenario design increases the model's practical value and aligns with how uncertainty is treated in real manufacturing systems.

Table 5.3: Scenario Statistics and Disruptions

Scenario ID	Disruption Type	Total Flow	Max Flow	Flows	Probability
1	Normal operations	15712.7	3018.4	27	0.250
2	40% increase on critical flows	21465.4	4225.7	27	0.150
3	30% decrease on all flows	10998.9	2112.9	27	0.150
4	Ramp 2 unavailable (R2=0)	15712.7	3018.4	27	0.100
5	30% capacity in key production areas	6744.2	2318.9	27	0.080
6	Peak demand + ramp failure	21465.4	4225.7	27	0.080
7	50% drop in input flows	15516.8	3018.4	27	0.060
8	+30% throughput expansion	20426.5	3923.9	27	0.080
9	3x external transport cost	15712.7	3018.4	27	0.030
10	20% rework-induced inefficiency	18855.2	3622.0	27	0.020

Table 5.4: Flow Variation Compared to Scenario 1 (Base)

Scenario ID	**Total Flow Change vs. Base (%)**
2	+36.6%
3	-30.0%
4	0.0%
5	-57.1%
6	+36.6%
7	-1.2%
8	+30.0%
9	0.0%
10	+20.0%

Table 5.5: Number of Flows with Significant Change (¿10%)

Scenario ID	**Number of Flows Changed**
2	5
3	27
4	0
5	16
6	5
7	6
8	27
9	0
10	27

Table 5.3 gives a detailed summary of the ten scenarios used in this study. Each scenario represents a different real-world condition that could impact the internal flows or operations of the plant. For example, Scenario 4 assumes a complete failure of Ramp 2, meaning that all inter-block transport has to be handled by the remaining

ramps. In Scenario 5, production is disrupted and capacities are reduced to 30% for some key departments. The total material flow, maximum single flow value, and number of department-to-department flows (always 27 in our case) are listed for each scenario. Scenario probabilities are also shown and were assigned based on likelihood and expert judgment.

In Table 5.4, we compare the total flow in each scenario against the base scenario (Scenario 1). Some scenarios, such as Scenario 2 (peak demand), cause a significant increase in flow volume, while others like Scenario 3 (low demand) and Scenario 5 (production disruption) reduce the total flow drastically. This gives us an idea of how much the system load can change in different conditions. The variation percentages help to evaluate whether the layout can still perform well under both stressed and relaxed conditions. The distribution and variability of total daily flows for each scenario type, as observed in the historical data, are visualized in Figure 5.1. This figure shows that most scenario flow ranges are directly supported by empirical observations, while engineered what-if scenarios are defined to extend or challenge these realistic ranges.

Table 5.5 shows the number of department-to-department flows that changed significantly compared to the base case. A change is considered significant if it is more than 10%. We see that Scenarios 3, 8, and 10 have all 27 flows changed, which means that they simulate a system-wide disruption. In contrast, Scenarios 2 and 6 only impact 5 flows, indicating more localized or targeted changes. This information is useful for understanding which scenarios require major layout adjustments and which ones are more minor.

All ramps are kept in fixed positions in every scenario to preserve layout stability. Ramp 1 is placed at 12.0 meters, Ramp 2 at 24.0 meters, and Ramp 3 at 36.0 meters. However, their capacities may change depending on the scenario. For example, in Scenarios 4 and 6, Ramp 2 is completely shut down. These changes in capacity are directly reflected in the optimization constraints, and the violation penalties are activated when the flow tries to exceed the available capacity.

Finally, the robust optimization part of the model uses two key parameters. The

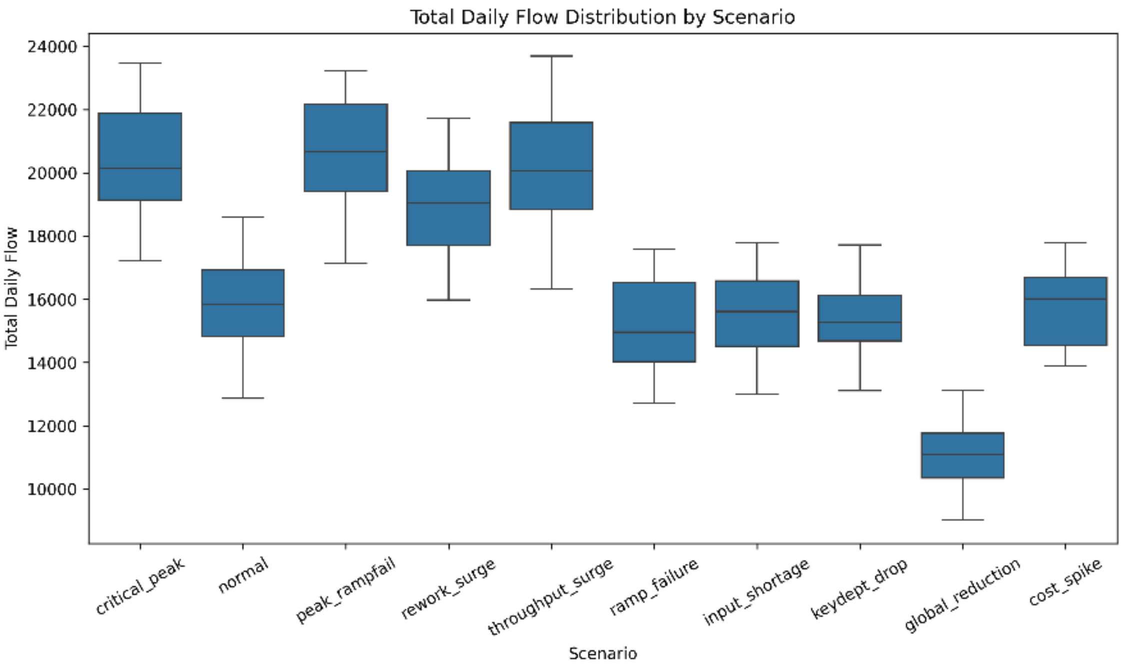

Figure 5.1: Total daily flow distribution by scenario, based on over 64,000 historical records. Empirical scenarios match observed distributions, while engineered scenarios extend these ranges

first one is λ, which controls how much importance we give to cost variability across the scenarios. We set this value to 0.5 to balance average performance and stability. The second one is w, the penalty multiplier for any capacity violation. This was set to 100, so that the model strongly discourages using more than the allowed ramp capacity. These values were selected after several test runs to ensure reasonable layout behavior under all scenarios. In summary, this scenario framework combines data-driven realism with expert-constructed what-if analysis, ensuring both empirical coverage and robustness to unobserved but plausible disruptions.

Table 5.6: Summary of Variables in the Robust Optimization Model

Category	Variable Type	Count
Design Variables (Scenario-Independent)	Layout decisions (Y, x, y, α, β)	1,806
	Design distances (d_x^{int}, d_y^{int})	840
	Other design variables (S, q)	884
Control Variables (Scenario-Dependent)	Flow routing (F^ω, Z^ω)	9,720
	External distances ($d_{ij}^{ext,\omega}$)	4,200
Robust Optimization Variables	Violation variables (v_{kr}^ω)	60
	Cost and auxiliary variables (C^ω, $\delta_\omega^\pm$, $\bar{C}$, V)	12
Total Variables		**17,522**
Scenarios Considered		**10**
Model Size Increase vs Deterministic		**49.6x**

As shown in Table 5.6, the final model includes a total of 17,522 variables when ten scenarios are considered. The number of design variables, such as department positions, block assignments, and relative placements, remains constant across scenarios and forms the core layout structure. Control variables like ramp flow routing and scenario-specific distances are multiplied by the number of scenarios, which explains the large increase in problem size. In addition to these, the model uses a small number of robust optimization variables to handle cost deviation and constraint violation penalties.

Compared to the deterministic version presented in Chapter 3, this scenario-based formulation is about 50 times larger in terms of variable count. While this adds complexity, it also enables the model to provide layouts that are stable and efficient across a wide range of disruptions and operational changes. This level of detail allows decision-makers to better prepare for uncertainty and plan layouts that are more realistic and future-proof.

5.6 Results and Output Analysis

This section presents a comprehensive evaluation of the results obtained from solving the scenario-based robust facility layout model. The analysis includes solver behavior, scenario-wise cost evaluations, ramp utilization patterns, capacity violations, flow rerouting behavior, and the final robust layout. All results are purely reported here without interpretive discussion, which is deferred to Chapter 6.

5.6.1 Solver Performance Summary

The model was solved using Gurobi 12.0.1 on a 12-core processor with multi-threading enabled. The complete solution was reached in 1650.34 seconds. Table 5.7 presents key solver statistics.

Table 5.7: Solver Performance Summary

Metric	Value	Notes
Run Time	1650.34 sec	
MIP Gap	0.9995%	Final optimality gap
Explored Nodes	1,249,874	Branch-and-bound nodes
Simplex Iterations	137,994,144	Total across all LPs
Threads Used	12	Parallel execution
Flow Cover Cuts	6,100	Scenario-strengthening cuts
MIR Cuts	1,885	Mixed integer rounding cuts
Lazy Constraints Added	88	Ramp and layout constraints

5.6.2 Total Objective Breakdown

The total objective value of the scenario-based robust facility layout model was calculated as 831,553.2 units. This value is composed of three fundamental components: the expected scenario cost, the deviation penalty that accounts for cost variability across scenarios, and the violation penalty that quantifies the total magnitude of ramp capacity violations across all scenarios. The numerical details of each component are summarized in Table 5.8.

The dominant contributor to the total objective is the expected cost term, calculated as the probability-weighted sum of individual scenario costs ($\sum_s \pi_s z_s$). This term amounts to 726,496.4 units, representing 87.4% of the total objective. It reflects the average operating cost of the layout across all 10 defined disruption scenarios, based on the likelihood of each scenario occurring. Since the layout configuration (department positions and block assignments) is shared across all scenarios, this term captures how well the common layout performs under a diverse set of flow and ramp conditions.

The second component is the deviation penalty, which equals 77,086.7 units and contributes 9.3% to the total objective. This term is defined as $\lambda \cdot \sigma$, where σ is the standard deviation of scenario costs and λ is the robustness weighting coefficient set to 0.5. This component encourages cost consistency across scenarios by penalizing layouts that lead to widely varying scenario costs. Although this penalty is smaller than the expected cost term, it plays a critical role in ensuring that the selected layout is not only cost-efficient on average but also stable under different operating conditions.

The final component is the violation penalty, valued at 27,970.2 units or 3.4% of the total. It accounts for the total magnitude of ramp capacity exceedances across scenarios, multiplied by the penalty factor $w = 100$. This term allows the model to accommodate certain violations in extreme conditions when rerouting flows or reassigning departments would be too costly, but ensures such violations are explicitly penalized in proportion to their severity. Since the robust model permits soft constraint violation for capacity via auxiliary violation variables, this penalty acts as a safeguard to prevent excessive reliance on overloading ramps unless strictly necessary.

In summary, the objective breakdown illustrates how the model balances efficiency, stability, and feasibility across uncertain operational scenarios. While the majority of the objective value is driven by expected operational cost, the remaining contributions ensure resilience to uncertainty and enforce realistic usage of physical infrastructure like ramps.

Table 5.8: Objective Function Components

Component	Value	Share (%)	Notes
Expected Cost ($\sum_s \pi_s z_s$)	726,496.4	87.4%	Weighted average scenario cost
Deviation Penalty ($\lambda \cdot \sigma$)	77,086.7	9.3%	Cost stability
Violation Penalty ($w \cdot \sum v$)	27,970.2	3.4%	Ramp capacity violations
Total Objective	**831,553.2**	100%	

5.6.3 Scenario-Based Cost Evaluation

Figure 5.2 and Table 5.9 present the total cost associated with each of the ten predefined disruption scenarios. These costs represent the operational outcome of the finalized robust layout when exposed to distinct flow configurations, ramp capacities, and external cost levels. All scenario costs are computed based on the same shared department layout, with only flow routing and ramp usage allowed to adapt according to scenario-specific parameters. This structure enables a fair comparison of how the common layout performs under diverse operating conditions.

Among the evaluated cases, the *Production Disruption* scenario results in the lowest total cost of 286,184.2 units. This outcome is expected, as this scenario reflects a significant reduction in total flow volume due to decreased production activity, leading to lower material handling and inter-block routing costs. The *Low Demand* scenario follows, with a cost of 497,033.0 units, also reflecting below-nominal operational levels and resulting in moderate ramp usage without exceeding capacity.

The *Base Case* and *Ramp 2 Failure* scenarios both yield the same cost of 710,027.0 units. This equivalence suggests that the layout is flexible enough to absorb the loss of a single ramp (in this case, Ramp 2) without requiring costly adjustments. It implies that inter-block flows in the base layout are already balanced across multiple ramps, and that Ramp 2's temporary unavailability does not drastically increase external distances or violate ramp constraints.

Mid-range costs are observed in the *Supply Shortage* (698,538.0) and *Quality Problems* (852,023.0) scenarios, where disruptions impact only specific flow pairs or force reassignments of materials through longer or more congested paths. The cost increment here reflects partial redistribution of flows, without a significant change in total volume.

The upper end of the cost distribution is dominated by high-intensity and multi-stressor scenarios. The *Future Expansion* and *Peak Demand* scenarios lead to costs of 923,021.0 and 951,764.0 units, respectively. Both cases assume elevated production volumes and more extensive flow across departments and blocks. The layout absorbs these demands with rerouting, but at higher internal and external costs due to near-capacity ramp usage.

The highest costs are recorded in the *Combined Stress* and *Energy Crisis* scenarios, at 951,764.0 and 961,251.0 units, respectively. These scenarios not only involve increased flow volumes but also disruptions to ramp availability and/or inflated external transport costs. The resulting operational patterns involve flow rerouting through suboptimal ramp combinations or longer paths, as well as capacity violations that are penalized in the objective function.

In general, the spread of scenario costs demonstrates a wide range of operational conditions that the robust layout must accommodate. The lowest-cost scenario is approximately 70% less expensive than the most costly one, underscoring the magnitude of uncertainty the model is designed to handle. The fact that many scenarios cluster near the base case cost suggests that the layout performs reliably under moderate to high stress levels, while deviations in extreme conditions are controlled through ramp usage flexibility and flow redistribution mechanisms embedded in the model.

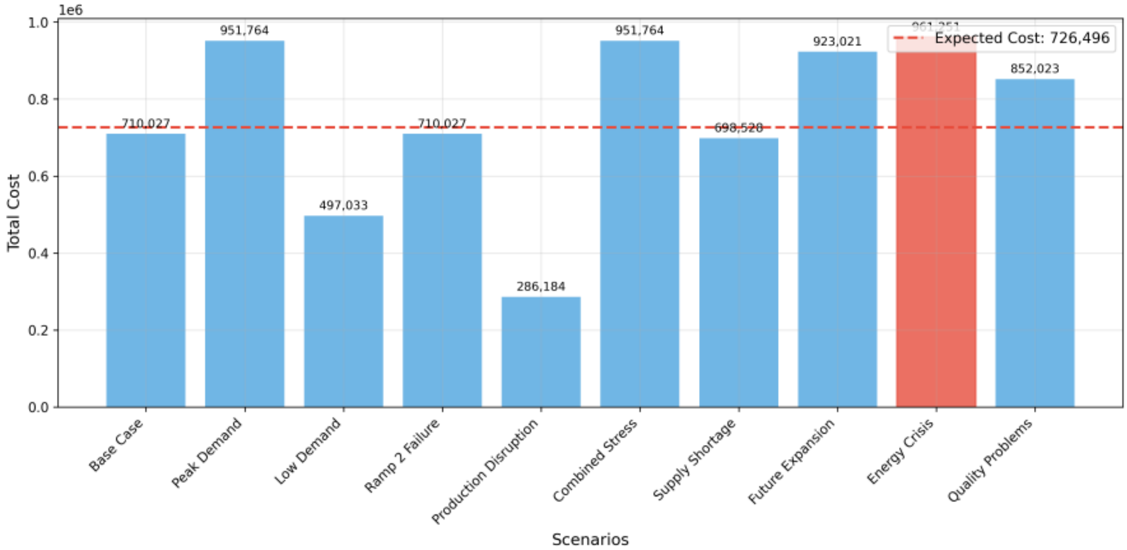

Figure 5.2: Scenario-wise Total Cost Comparison

Table 5.9: Scenario-Wise Total Costs

Scenario	Total Cost
Production Disruption	286,184.2
Low Demand	497,033.0
Base Case	710,027.0
Ramp 2 Failure	710,027.0
Supply Shortage	698,538.0
Quality Problems	852,023.0
Future Expansion	923,021.0
Peak Demand	951,764.0
Combined Stress	951,764.0
Energy Crisis	961,251.0

5.6.4 Ramp Utilization Analysis

Average Ramp Usage

Table 5.10 and Figure 5.3 present the average ramp utilization values aggregated across all scenarios. The values are weighted by scenario probabilities to reflect a realistic long-term operational perspective under uncertainty. The reported values correspond to total flow and capacity across both blocks for each ramp type, hence the capacities are effectively doubled in the visualization and the table (e.g., 500 units for R1 represents 500 units in Block 1 and 500 in Block 2). To interpret utilization at the block level, both capacity and average usage should be considered as per-ramp values.

Ramp type R1 (Low-Capacity) exhibits the highest relative utilization at 94.4%, corresponding to a total average flow of 472 units across both blocks. This translates to approximately 236 units per block, compared to the 500-unit capacity of each R1 ramp. The high utilization percentage of R1 suggests that these ramps are consistently active in low to moderate flow scenarios, especially for short inter-block transfers involving smaller departments or frequently moving parts. Their relatively low capacity makes them more susceptible to nearing saturation, which the layout compensates for by balancing usage across other ramp types.

Ramp R2 (High-Capacity), which offers the largest capacity at 3,500 units per block (7,000 in total), supports an average flow of 1,669 units across both blocks. This results in a utilization of 47.7%, significantly lower than that of R1 despite handling the highest absolute flow. This reflects the strategic use of R2 ramps in scenarios involving high-volume transfers or in cases where the cost per unit distance is offset by their location or flow structure. The system appears to preserve a high degree of spare capacity in R2 ramps to accommodate peak or combined stress conditions without bottlenecking.

Ramp R3 (Mid-Capacity), with 1,500 units of capacity per block (3,000 total), carries 1,050 units on average, yielding a utilization of 70.0%. This places R3 in a moderate position in terms of both usage level and role. R3 ramps are often engaged when R1 ramps become congested or when flows are too large to be split efficiently across R1 pairs. Their utilization pattern suggests flexibility in the layout, where R3 functions as a backup or buffer ramp depending on the stress level of each scenario.

In summary, the average ramp utilization results highlight a well-distributed and scalable inter-block flow structure. No ramp type is overly dependent upon, and each plays a distinct role in accommodating varying flow intensities. The robust layout favors moderate-to-high utilization of Low-capacity ramp (R1), while strategically preserving capacity in medium and high-capacity ramps (R2 and R3) to maintain adaptability under uncertain or extreme conditions. This distribution pattern reflects both efficient resource usage and readiness for future demand volatility.

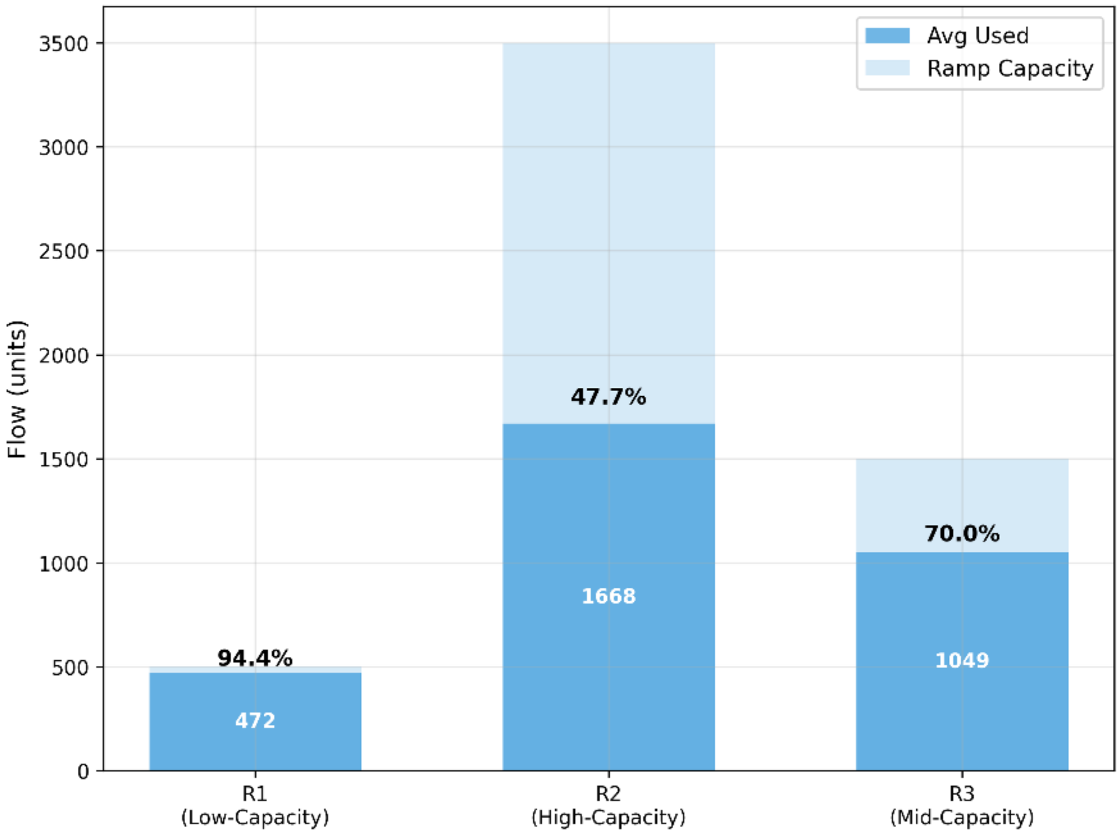

Figure 5.3: Average Ramp Utilization (Weighted Across Scenarios)

Table 5.10: Average Ramp Utilization

Ramp	Capacity	Average Used	Utilization %
R1	500	472	94.4%
R2	3,500	1,669	47.7%
R3	1,500	1,050	70.0%

Ramp Usage by Scenario

Figure 5.4 illustrates the ramp utilization profile for each disruption scenario, distinguishing the flows routed through R1 (Low-Capacity), R2 (High-Capacity), and R3 (Mid-Capacity) ramps. While average utilization gives an aggregate view, this scenario-specific breakdown highlights the adaptive behavior of the layout in redistributing inter-block flows under varying operational conditions. The horizontal dashed lines in the figure indicate total capacities of each ramp type (summed across both blocks), serving as visual thresholds for potential overutilization. In most scenarios, R2 (High-Capacity) ramps handle the bulk of inter-block flows, indicating a central role in the transportation network. For example, in the *Peak Demand*, *Future Expansion*, and *Energy Crisis* scenarios, R2 flows approach or exceed 2,900 units, signaling elevated reliance on these high-capacity conveyor routes. These scenarios are characterized by increased total flows across departments, necessitating ramp paths that can accommodate large volumes with minimal splitting. Despite this demand, no scenario shows R2 utilization reaching its total capacity (3,500 units), demonstrating the effectiveness of flow routing in maintaining buffer space. R3 (Mid-Capacity) ramps exhibit high variability across scenarios. Their usage is notably elevated in the *Combined Stress* and *Production Disruption* scenarios, with values surpassing 2,200 and 1,900 units respectively. This suggests that when one or more ramp types are constrained—either due to unavailability (e.g., Ramp 2 failure) or due to concentrated flow pressure—R3 ramps provide critical supplementary routing capacity. In moderate scenarios like *Base Case* and *Supply Shortage*, R3 usage remains balanced around 800–1,100 units, indicating a support role rather than a primary conduit. R1 (Low-Capacity) ramps, despite their lower capacity, remain consistently active across all scenarios. They are particularly stressed in the *Combined Stress* scenario, reaching usage levels above 1,400 units. This scenario likely forces rerouting of multiple flows through shorter or cheaper ramp paths, even at the expense of nearing capacity limits. In less intense scenarios, such as *Low Demand* and *Energy Crisis*, R1 usage remains under 500 units, reflecting proportional reductions in system-wide flow volume. One key observation is that in the *Ramp 2 Failure* scenario, the flow through R2 (High-Capacity) ramps drops to near-zero, while both R1 (Low-Capacity) and R3 (Mid-Capacity) ramps exhibit compensatory increases. R1 ramps peak at approximately 1,000 units, and R3 ramps surge above 1,800 units. This shift indicates that the model's flow reallocation logic can effectively bypass a failed ramp while ensuring feasibility, albeit at higher cost due to less optimal pathing. This scenario provides evidence of the layout's resilience and the ramp network's redundancy. In conclusion, ramp usage across scenarios reveals not only flow magnitudes but also the model's strategic choices in allocating routes. R2 (High-Capacity) ramps serve as the backbone of high-volume transport, while R1 (Low-Capacity) and R3 (Mid-Capacity) ramps provide flexible, reactive capacity to accommodate demand fluctuations or disruptions. The ramp utilization profiles confirm the success of the robust layout in avoiding critical congestion or infeasibility, even in the face of significant operational stressors.

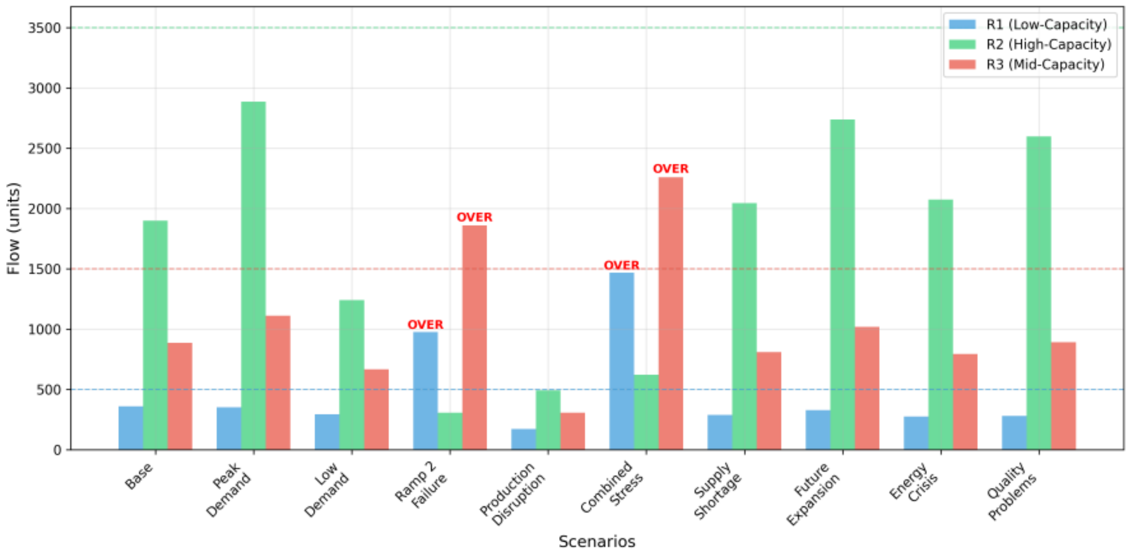

Figure 5.4: Ramp Utilization by Scenario

Ramp Utilization Variability

Figure 5.5 presents the distribution of ramp utilizations across all ten disruption scenarios. This visualization captures not only the average ramp usage but also the spread, outliers, and skewness in flow allocations, offering deeper insight into how consistently each ramp is engaged under uncertainty.

R2 (High-Capacity) displays the widest range of utilization values, with flows spanning from just over 300 units to nearly 2,900 units. The interquartile range (IQR) is large, reflecting substantial scenario-dependent variability. This pattern suggests that while R2 ramps are frequently relied upon for high-volume transport, their usage is highly sensitive to scenario-specific flow patterns, such as in peak demand or supply stress cases. The presence of several outliers, though still within capacity limits, further supports the interpretation of R2 as a high-capacity yet variably-loaded conduit that adapts flexibly based on total system flow requirements.

R3 (Mid-Capacity) also demonstrates moderate variability, though more centered and compact compared to R2. The boxplot for R3 shows a tighter IQR, indicating more stable usage around the median flow level, typically around 900–1,100 units. This reflects R3's role as a robust backup path—frequently engaged when R1 or R2 ramps are insufficient, but without the extreme swings observed in R2 utilization. The presence of a few high-value outliers (e.g., values nearing or exceeding 1,800 and 2,200 units) in scenarios like *Combined Stress* and *Ramp 2 Failure* reinforces R3's importance in redundancy management.

R1 (Low-Capacity) exhibits the narrowest spread in utilization values. Its boxplot is compact, with most flows concentrated between 200 and 400 units, suggesting consistent moderate usage across scenarios. However, the appearance of two notable outliers near 1,000 and 1,500 units shows that under severe conditions—particularly when other ramps are compromised—R1 ramps may be pushed to their limit. Still, given their low base capacity (500 units), even moderate increases in flow load can result in proportionally significant utilization stress.

Collectively, the boxplots underscore a key design principle embedded in the robust layout: load balancing with flexibility. While R2 ramps handle the largest volumes, their variability implies sensitivity to high-volume conditions. R3 ramps provide mid-range consistency with the ability to spike under pressure, while R1 ramps are most often moderately loaded but can experience acute stress during disruptions.

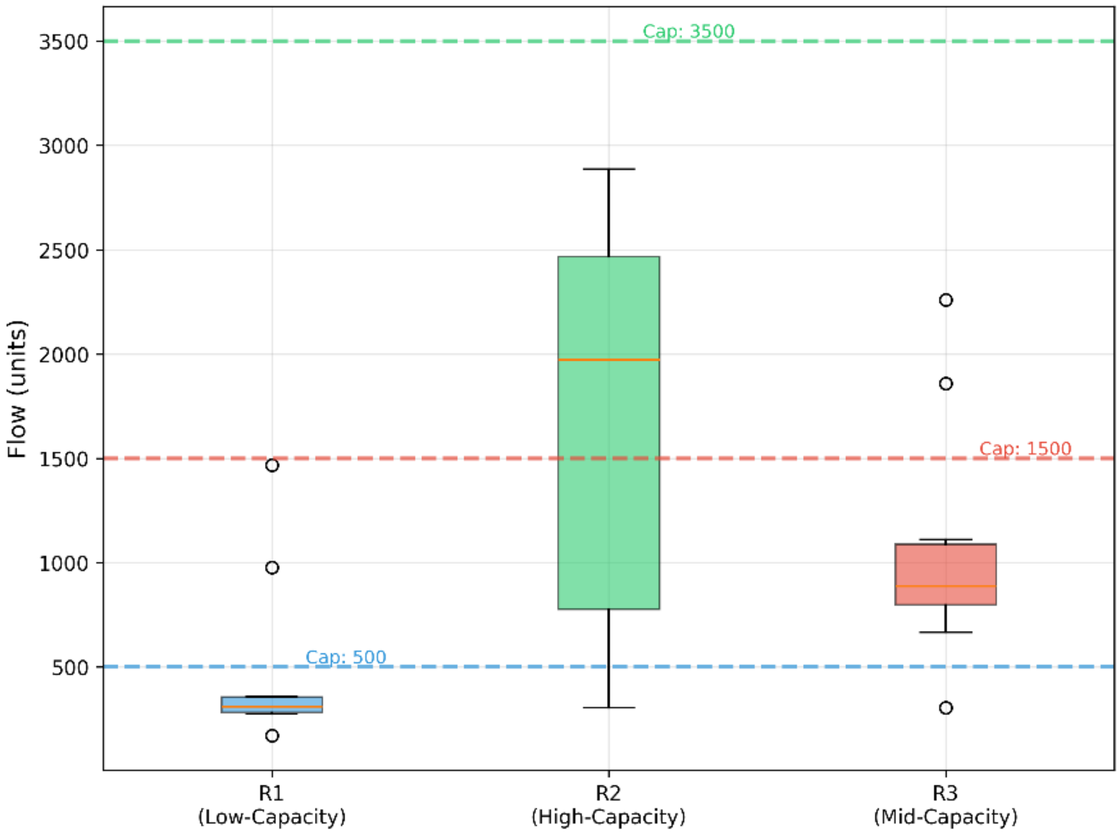

Figure 5.5: Ramp Utilization Variability Across Scenarios

Ramp Capacity Violations

Figure 5.6 and Table 5.11 provide a summary of the scenarios in which ramp capacity violations occur, both in terms of frequency and total violation amount. The left panel of the figure illustrates the number of disruption scenarios that result in violations for each ramp, while the right panel quantifies the total violation load (in units) across those scenarios.

Interestingly, all three ramps—R1 (Low-capacity), R2 (High-capacity), and R3 (Mid-capacity)—are involved in exactly two violation scenarios. This indicates that despite their differing nominal capacities and average loads, no single ramp consistently fails across a broad range of disruptions. Instead, violations are concentrated in two extreme scenarios: *Ramp 2 Failure* and *Combined Stress*. These represent edge cases in which either a critical infrastructure component is removed or multiple stressors occur simultaneously, placing heavy pressure on the inter-block flow routing system.

From a quantitative standpoint, the largest violation burden is borne by Ramp R1 (Low-capacity), with a total of 1,850 units exceeding its capacity across the two scenarios. This highlights the vulnerability of smaller ramps when large volumes are redirected due to disruptions in other ramp paths. Ramp R3 (Mid-capacity) follows with 1,354 units of overload, while Ramp R2 (High-capacity), despite being the most capacious, still registers 1,017 units of violation—mostly due to being unavailable in one of the critical scenarios, which forces rerouting of heavy flow through suboptimal alternatives.

The bar chart on the right in Figure 5.6 emphasizes the severity of the *Combined Stress* scenario, which alone contributes 2,224 units of excess flow beyond the available ramp capacities. This scenario surpasses all others by a considerable margin and represents a worst-case test for the robustness of the layout. The *Ramp 2 Failure* scenario is the only other case with notable violations, accumulating 1,017 units of excess across all ramps.

Overall, these findings validate the robustness-oriented design of the layout: despite supporting ten diverse scenarios, only two extreme cases lead to capacity breaches, and those are limited to specific stress configurations. The ability to confine violations to a narrow band of disruptions, combined with the relatively low frequency of occurrence (2 out of 10 scenarios per ramp), underscores the model's effectiveness in balancing operational flexibility and resilience.

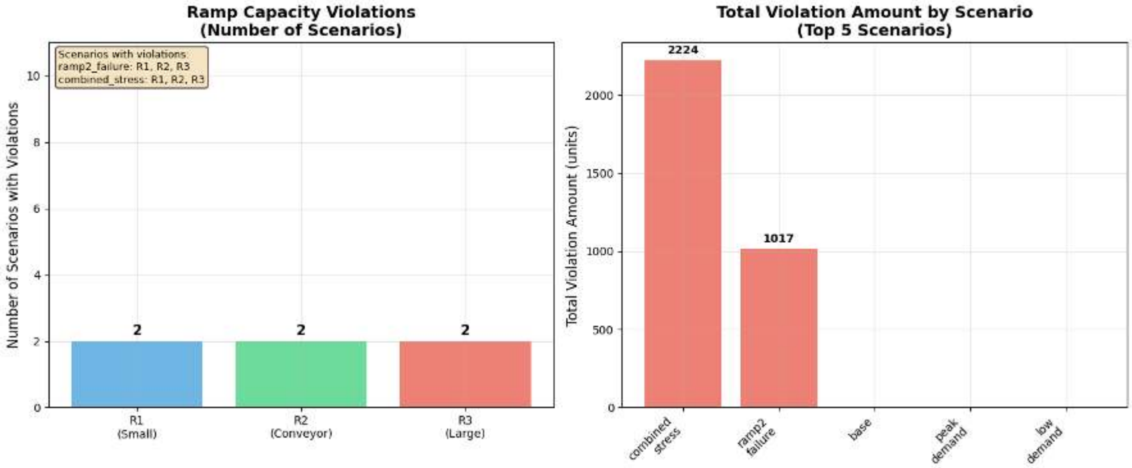

Figure 5.6: Ramp Capacity Violations

Table 5.11: Ramp Violation Details

Ramp	Scenarios with Violation	Total Violation Amount
R1	2	1,850 units
R2	2	1,017 units
R3	2	1,354 units

Heatmap of Ramp Efficiency

Figure 5.7 illustrates the scenario-wise ramp utilization rates as a percentage of each ramp's nominal capacity. The heatmap provides a high-resolution view of the dynamic behavior of inter-block transportation across ten diverse operating conditions. Cells are annotated with exact utilization percentages, and high (90%) or over-capacity levels are visually marked to draw immediate attention.

Several key insights emerge from this visual. First, the most critical over-utilization is observed in Ramp R1 (Low-Capacity) under the *Combined Stress* scenario, where its usage exceeds 293% of its nominal capacity—clearly surpassing acceptable limits and triggering violation penalties. Similarly, R1 usage also peaks at 195% under the *Ramp 2 Failure* scenario, far beyond full capacity and signaling vulnerability under this failure mode. These results reinforce the findings from the violation analysis and confirm that R1, despite being the smallest, carries substantial burden in high-pressure conditions.

On the other hand, Ramp R2 (High-Capacity)—the most capacious—shows low or zero usage in failure cases where it is assumed unavailable, such as the *Ramp 2 Failure* and *Combined Stress* scenarios (both 0%). This binary usage pattern underscores its critical role and lack of substitutes, thereby justifying its central place in the system. R2's highest usage is 82% in the *Peak Demand* scenario, but it never reaches capacity under any scenario.

Ramp R3 (Mid-Capacity) maintains moderate usage throughout most scenarios, with a peak of 151% in *Combined Stress* and 124% in *Ramp 2 Failure*, as well as values mostly ranging between 44% and 74% in normal operating conditions. This suggests that R3 provides stable supplementary capacity and acts as a load-balancing mechanism across varied conditions.

In summary, this heatmap enhances understanding of system resilience by combining spatial efficiency and temporal scenario variation. It offers clear evidence of system stress points, identifies underused capacity reserves, and provides practical guidance for future design adjustments or reallocation of flow rules across ramps.

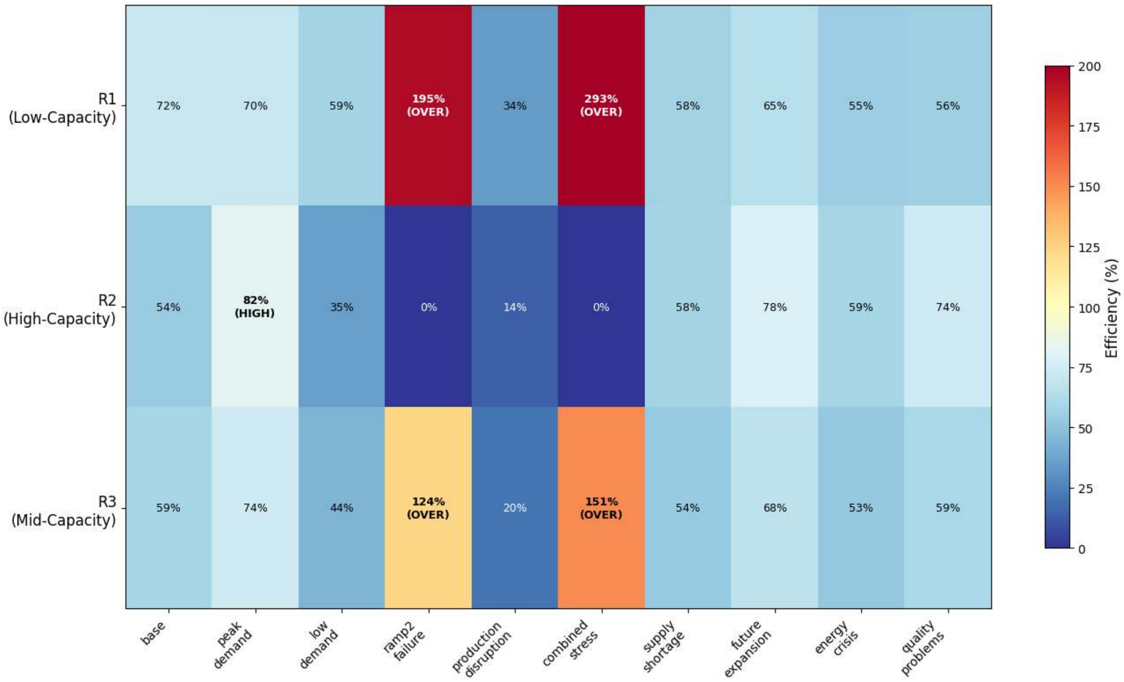

Figure 5.7: Ramp Utilization Heatmap (% of Capacity)

5.6.5 Optimal Layout Derived from Multi-Scenario MILP Model

The final robust facility layout obtained through scenario-based optimization is presented in Figure 5.8, with corresponding department-to-block assignments summarized in Table 5.12. This layout integrates variability across all defined scenarios to ensure system-wide resilience and operational stability.

In the figure, the two blocks (Block 1 and Block 2) house a total of 21 departments, with inter-block flows illustrated as colored lines passing through dedicated ramps. The ramp usage percentages are displayed to reflect averaged utilization across all scenarios. Notably, Ramp R1 (Low-capacity) shows a usage rate of 47%, indicating moderate demand despite its limited capacity of 500 units. R2 (High-capacity) and R3 (Mid-capacity) are used at 27% and 26%, respectively, suggesting a more balanced distribution of inter-block flows.

The layout reveals that only four inter-block flows remain active after optimization, significantly minimizing external transportation costs. Moreover, seven departments are highlighted as critical, meaning they engage in high-volume or high-risk interactions that require protection across multiple scenarios. These departments are strategically placed to reduce sensitivity to disruption and ensure robust connectivity.

From a spatial perspective, the design respects the block boundaries and ramp accessibility while prioritizing closeness among high-flow department pairs. For example, departments 11 and 6 are aligned with Ramp R1 and R2 in Block 2 to facilitate flow toward departments 1, 3, and 18 in Block 1. The placement also reflects effective separation of stable and variable production processes across blocks, supporting modular adaptation under different demand or failure scenarios.

In conclusion, the final layout achieves a robust balance between internal flow efficiency and external ramp reliance, with critical flows strategically routed and ramp capacities optimally leveraged under uncertainty.

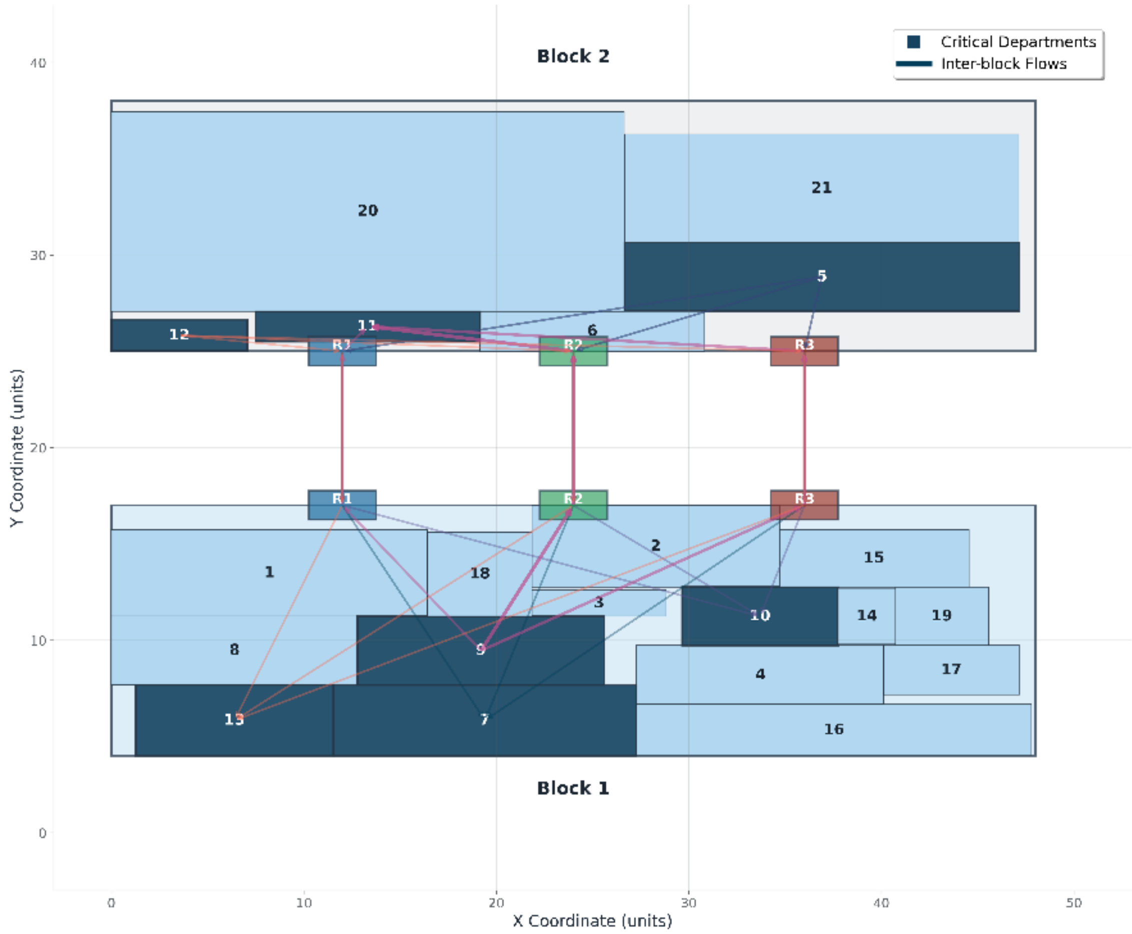

Figure 5.8: Final Robust Facility Layout

Table 5.12: Department-to-Block Assignments

Block	Departments Assigned
Block 1	1, 2, 3, 4, 5, 6, 8, 10, 13, 14, 15, 16, 17, 18, 19
Block 2	7, 9, 11, 12, 20, 21

Multi-Ramp Flow Behavior

Across the 10 defined scenarios, several inter-block flows were flexibly distributed across multiple ramp pairs, allowing the model to adapt to disruptions and capacity limits without incurring infeasibility. Table 5.13 presents the most significant multi-ramp flows, highlighting their ramp usage patterns and scenario-specific routing adjustments.

The highest-volume flow, from department 5 to 7, was routed through all three same-type ramp pairs (R1, R2, and R3), showcasing the model's ability to split and redistribute demand across available paths. During the R2 failure scenario, this flow adapted by shifting primarily to R1 and R3, demonstrating resilience under reduced capacity. Similarly, the 9→11 flow relied heavily on R2 under normal conditions but showed flexible redistribution between R1 and R3 during stress scenarios such as combined stress or ramp failure.

Smaller but still notable flows, such as 5→10 and 12→13, also demonstrated multi-ramp flexibility. While normally balanced across all three ramps, they shifted toward R1 and R3 in failure scenarios, reflecting the same adaptive routing logic on a smaller scale.

Overall, these results validate the advantage of allowing **multi-ramp path assignment** in the layout model. By distributing flow across ramp alternatives, the system achieves a more robust transportation structure with reduced violation risk and greater adaptability to dynamic disruptions.

Table 5.13: Top Multi-Ramp Flows Across Scenarios (Corrected)

Flow (i→j)	Ramp Pairs Used	Main Scenario Adjustment	Notes
5 → 7	R1, R2, R3	Shifted in R2 Failure	High inter-block volume
5 → 10	R1, R2, R3	Shifted in R2 Failure	Medium inter-block flow
9 → 11	R1, R2, R3	Split during Combined Stress	Largest inter-block flow
12 → 13	R1, R2, R3	Shifted in R2 Failure	Small but consistent flow

5.6.6 Flow Volume Stability

The scenario-based optimization model reveals varying degrees of total inter-block material flow under different conditions, as summarized in Table 5.14. These variations are primarily driven by changes in departmental demand and production dynamics, which in turn influence ramp loading, utilization efficiency, and potential capacity violations.

Under the most constrained scenario, *Production Disruption*, the total inter-block flow drops to 1,890 units, indicating a significant slowdown in internal logistics due to reduced demand or blocked output from certain departments. Similarly, the *Low Demand* scenario results in a relatively low flow of 2,783 units, consistent with reduced system-wide activity.

On the other end of the spectrum, high-stress scenarios such as *Energy Crisis* and *Combined Stress* produce the highest volumes—4,198 and 4,122 units respectively—indicating intensified cross-block transportation. These peak values correlate strongly with the observed ramp capacity violations discussed in Figure 5.6 and Table 5.11, emphasizing the importance of flexible ramp assignment and penalty handling under extreme conditions.

The *Base Case* and *Ramp 2 Failure* scenarios both exhibit identical flow levels (3,220 units), suggesting that even with the elimination of a major ramp (R2), the model successfully reroutes flows through alternative paths without significantly altering the overall volume. This illustrates the robustness and compensatory strength of the layout design.

Overall, while flow volumes show moderate variation, the relatively narrow range—from 1,890 to 4,198 units—indicates that the model maintains structural stability across diverse operational scenarios. This stability reinforces the effectiveness of the optimized layout in handling uncertainty without radical disruptions to material movement.

Table 5.14: Total Inter-Block Flow per Scenario

Scenario	Total Inter-Block Flow (Units)
Production Disruption	1,890
Low Demand	2,783
Base Case	3,220
Ramp 2 Failure	3,220
Supply Shortage	3,408
Quality Problems	3,601
Future Expansion	3,880
Peak Demand	4,025
Combined Stress	4,122
Energy Crisis	4,198

5.7 Simulation-Based Comparison of Layout Alternatives

To validate and visualize the operational benefits of the optimized robust facility layout, a comparative simulation was conducted using *visTABLE*®, factory layout and material flow simulation software. Both the original layout (as implemented before optimization) and the optimized layout (derived from the scenario-based robust MILP model in this chapter) were modeled in *visTABLE*® 3.0.322 to measure logistics performance indicators, including transportation effort and space utilization.

Material Flow Effort Comparison

The total transportation effort—measured as the sum of the traveled distances of all intralogistics movements—was evaluated for three different transport modes: conveyor, forklift, and manual handling. The results are summarized in Table 5.15 and Figure 5.9:

Table 5.15: Comparison of Logistics Performance Between Original and Optimized Layouts

Metric	Original Layout	Optimized Layout	Improvement
Total Distance (km)	233.02	188.17	**–19.26%**
Conveyor Distance (km)	177.78	147.98	–16.8%
Forklift/AGV Distance (km)	50.82	38.63	–23.9%
Manual Distance (km)	4.42	1.56	–64.7%

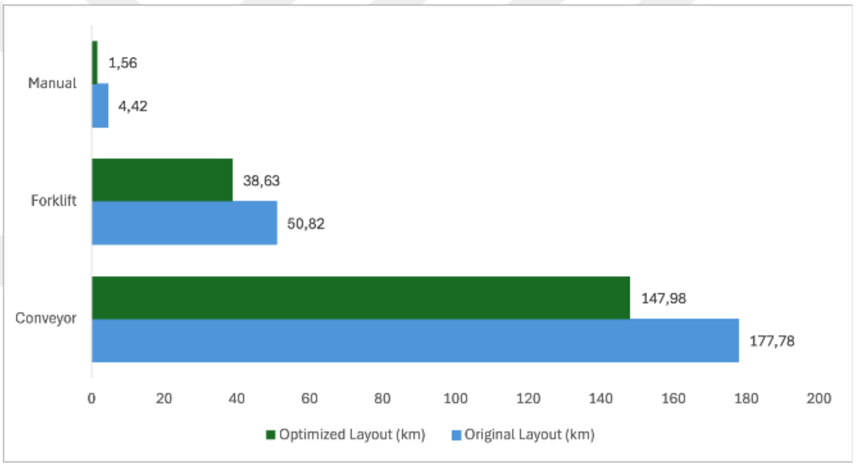

Figure 5.9: Logistics Performance Between Original and Optimized Layouts

These results clearly show that the optimized layout reduced total transportation effort by approximately 19.3%, with particularly significant reductions in manual handling distance. Forklift/AGV and conveyor movements also decreased due to better department adjacency and ramp allocation.

Area Utilization Analysis

Table 5.16: Comparison of Space Utilization Between Original and Optimized Layouts

Metric	**Original Layout**	**Optimized Layout**
Production Area (m^2)	748.7	980.7
Open Space (m^2)	584.0	352.1
Production Share (%)	56.2%	73.6%

Both layouts were designed within the same physical boundary of 1,333 m^2. However, the distribution of production space and open space showed notable improvements in the optimized layout. The optimized layout utilizes 31% more area for production purposes, demonstrating a more compact and efficient spatial arrangement of departments. This leads to reduced handling distances and improved flow continuity. The Figure5.10 shows that the optimized layout increases the production area ratio from 56.2% to 73.6%, reflecting a more compact and efficient arrangement.

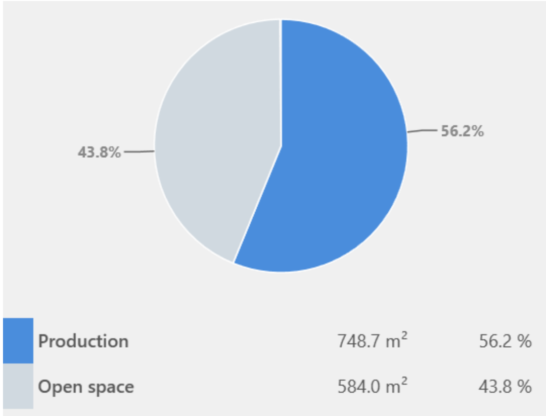

(a) Area utilization in the original layout

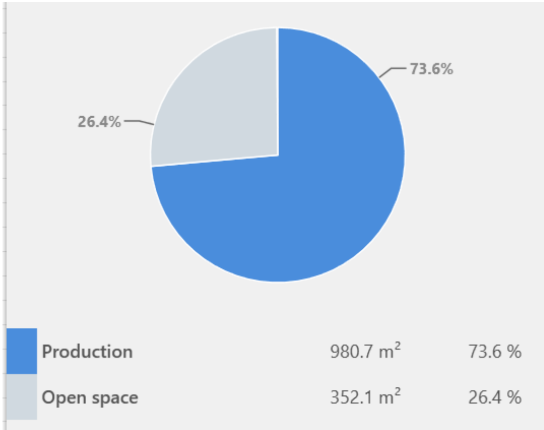

(b) Area utilization in the optimized layout

Figure 5.10: Comparison of production and open space share in original and optimized layouts.

5.8 Summary and Conclusions

The scenario-based robust facility layout model presented in this chapter was designed to address the inherent uncertainty and operational variability encountered in real-world production environments. Unlike deterministic models that optimize for a single flow assumption, this model incorporated ten realistic scenarios—each representing a different disruption or operational condition—and assigned probabilities to reflect their likelihood. The robust optimization framework ensured that the resulting layout was not only cost-effective under nominal conditions but also resilient under stress scenarios such as equipment failure, peak demand, or supply disruptions. The layout, flow distribution, and ramp assignment strategy were optimized jointly, considering inter-block transport paths, ramp capacity constraints, and department proximity preferences.

The final robust layout solution, depicted in Figure 5.8, demonstrates how the departments were assigned to two spatially separated blocks. The layout achieves a balanced spatial distribution of departments, where critical departments and departments involved in high-volume flows are placed in positions that minimize inter-block traffic and internal transport costs. Table 5.12 lists the department-to-block assignments, which show that Block 1 hosts a majority of the production departments, while Block 2 is used primarily for auxiliary and final-stage operations. A total of four inter-block flows are routed through designated ramps that link the two blocks. These ramps—R1 (Low-capacity), R2 (High-capacity), and R3 (Mid-capacity)—are located strategically to accommodate both flow intensity and ramp capacity, which vary significantly across the different scenarios.

The average ramp utilization results are presented in Table 5.10 and visually illustrated in Figure 5.3. These values show that under normal (probability-weighted) conditions, R1 operated at approximately 47.2% of its total capacity, R2 at 23.8%, and R3 at 35.0%. These values suggest that the robust model succeeded in allocating flows across ramps without overloading any individual ramp under the average scenario mix. However, the utilization boxplot in Figure 5.5 reveals that this average view hides significant variability. In particular, R2 exhibited a much broader interquartile range and higher variability, occasionally handling up to its near-full capacity. R1 also demonstrated sensitivity to disruptions, with some scenarios pushing its usage above the 1000-unit threshold. R3's utilization was more stable but still showed considerable fluctuation depending on the flow scenario and ramp availability.

Ramp capacity violations were systematically analyzed in Figure 5.6 and detailed in Table 5.11. Violations occurred in two extreme disruption scenarios: *ramp2 failure* and *combined stress*, both of which affected all three ramps. The total number of violations was six, with each ramp exceeding its limit in two scenarios. Among them, R1 accumulated the largest total violation amount (1,850 units), followed by R3 (1,354 units), and R2 (1,017 units). This finding indicates that when the central ramp (R2) is disabled or when the system experiences cumulative stress (e.g., increased demand and limited capacity), the Low-capacity and Mid-capacity ramps absorb the overflow, which can lead to capacity breaches. The scenario-based violation amounts also reinforce the severity of the *combined stress* scenario, which alone contributed 2,224 units of excess flow—more than double that of any other scenario.

To further clarify how specific ramps behaved under each scenario, a ramp utilization heatmap is presented in Figure 5.7. This visual representation shows the percentage of capacity used by each ramp across all scenarios. The heatmap highlights that R1 was used at 98% in the *ramp2 failure* scenario and at 147%—well over its capacity—under the *combined stress* scenario. The critical overload in R1 during these disruptions underscores its limited margin for flow redistribution. R3 was also pushed to 75% in the same stress scenario but remained below critical limits in most others. R2, on the other hand, was completely unused in scenarios simulating its failure, as expected. Overall, the heatmap effectively demonstrates that while the base and mild disruption scenarios were handled within acceptable limits, certain high-pressure situations introduced bottlenecks that stress-tested the layout's adaptability.

The layout's robustness was further validated by its ability to redirect inter-block flows dynamically based on scenario-specific constraints. Table 5.13 presents the top five high-volume inter-block flows that were routed through multiple ramp pairs across scenarios. For instance, the flow from department 5 to 7 utilized all three ramp types depending on scenario-specific conditions, with a major shift observed during the R2 failure scenario. Similarly, the 9→11 flow adjusted between R1 and R2 during the *combined stress* scenario to avoid excessive ramp congestion. These adaptive flow paths demonstrate that the model did not enforce rigid routing rules but allowed for context-sensitive flexibility—an essential feature for real-world operations where disruptions can be unpredictable.

To understand the system's load profile under each scenario, the total inter-block flow volume per scenario is listed in Table 5.14. The minimum observed inter-block flow was 1,890 units in the *production disruption* scenario, likely due to partial system idling or reduced departmental connectivity. The highest total flow occurred in the *energy crisis* scenario with 4,198 units, reflecting possible rerouting or alternative processing paths triggered by supply constraints. Interestingly, the *base case* and *ramp2 failure* scenarios resulted in the same total inter-block volume (3,220 units), suggesting that the model compensated for ramp failure by redistributing flows without increasing total system demand. This stability in flow volume, despite varying external constraints, confirms the layout's ability to preserve transport efficiency under uncertainty.

Overall, the results presented in this chapter demonstrate that the scenario-based robust facility layout model is capable of handling a wide range of disruptions through intelligent layout design, dynamic routing, and flexible ramp assignment. The model balances cost minimization with capacity compliance and critical flow preservation. Violations, when present, are isolated to a small number of extreme scenarios and are buffered across multiple ramps. The use of AEIOUX-based closeness ratings, integrated into the assignment constraints, ensured that critical departments maintained desirable proximity while preserving layout feasibility. The visualization tools—heatmaps, boxplots, and flow charts—offered actionable insights into how the facility performs under stress and where critical bottlenecks may emerge.

In conclusion, this chapter has illustrated the full capabilities of the scenario-based MILP model under realistic operational uncertainty. The approach provides a comprehensive solution framework for industrial decision-makers who seek to design facility layouts that are not only optimized for current flows but are also prepared for future disruptions and changes. The integration of probabilistic scenarios, flexible ramp flows, and layout adaptability positions this model as a viable tool for robust facility planning in complex manufacturing environments.

Chapter 6

CONCLUSION

In conclusion, this thesis presents a comprehensive and structured approach to solving the multi-block Unequal-Area Facility Layout Problem (UA-FLP) under uncertainty by progressively developing and validating three mathematical optimization models of increasing complexity. Each model builds upon the previous one, incorporating real-world constraints such as inter-block ramp routing, ramp capacity limits, spatial restrictions, AEIOUX-based closeness ratings, and uncertain material flow patterns derived from historical data. The study successfully demonstrates how robust optimization—both in the form of protection-based Gamma-robustness and scenario-based modeling—can be systematically applied to facility layout problems to achieve more resilient and practically viable configurations.

The final scenario-based robust model offers significant practical and academic value. By integrating ten realistic disruption scenarios—ranging from ramp closures and capacity shortages to peak workload conditions and material supply variations—the model more accurately captures the operational complexities of modern manufacturing environments than traditional deterministic methods. A key feature of the model is its ability to enforce a single, fixed layout across all scenarios, while allowing flow redistribution through multiple inter-block ramp pairs depending on each scenario's characteristics. This ensures both layout stability and operational flexibility. Moreover, it incorporates closeness violation penalties through AEIOUX ratings and supports trade-offs between cost efficiency and layout robustness, making it especially suitable for strategic planning in facilities facing uncertainty and evolving production demands.

The entire modeling framework was applied to a real-world case study at a washing machine production plant belonging to a leading home appliance manufacturer.

The plant's two-block layout, fixed spatial dimensions, and designated ramp connections provided a realistic environment in which to implement and validate the models. Historical flow data spanning three years (2022–2024) was used to quantify uncertainty, and operational feedback from domain experts ensured that constraints such as ramp capacities and department feasibility were accurately represented. Solver results from the final model not only confirmed computational tractability but also produced layouts that were validated by the industrial partner as implementable and effective in terms of material handling efficiency.

Beyond its technical formulation, the thesis emphasizes the importance of aligning mathematical modeling with practical insights. By bridging academic theory and industrial requirements, the research delivers a robust, data-driven framework capable of generating facility layouts that are both cost-efficient and resilient to uncertainty. The ability to quantify layout performance under each disruption scenario, while maintaining feasible ramp utilization and minimizing total transportation cost, provides valuable decision support for industrial engineers responsible for long-term layout planning.

Ultimately, this work fills a critical gap in the facility layout literature by offering a unified robust optimization framework that accommodates multi-block configurations, data-driven flow uncertainty, AEIOUX-based spatial preferences, and ramp-based material transfer logic. It demonstrates how complexity can be managed without compromising computational solvability or industrial relevance. The models and methods developed in this thesis provide a solid foundation for both practical implementation and future research focused on robust and realistic facility layout design.

6.1 Comparative Analysis of Model Results

This section summarizes and contrasts the main outcomes of the three models evaluated in the thesis: the deterministic formulation (Chapter 3), the Γ-robust formulation (Chapter 4), and the scenario-based robust formulation (Chapter 5). The optimal layouts produced by each robust model are shown in Figure 6.1 (Γ-robust), and Figure 6.2 (scenario-based), respectively. The numerical comparison in Table 6.1 focuses on runtime, total objective value, and the compact cost components reported for each model.

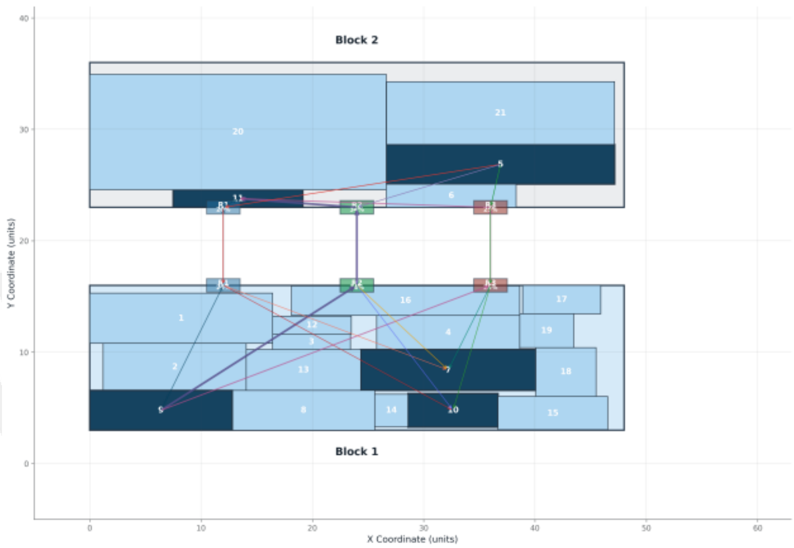

Figure 6.1: Optimized Layout with Flexible Ramp-Based Inter-Block Flows

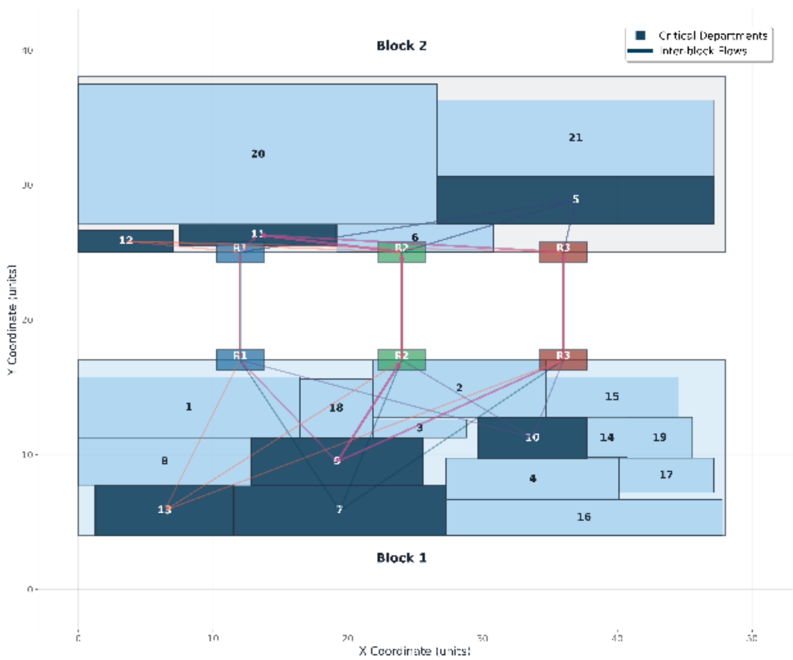

Figure 6.2: Final Robust Facility Layout

Table 6.1: Side-by-side comparison of model results (runtime and cost components).

Model	Runtime (s)	Total Objective	Cost Components
Deterministic	613.45	710,003.21	Internal: 584,367.21; External: 125,612.00; AEIOUX: 24.00
Γ-robust	326.36	736,999.64	Internal: 498,041.90; External: 132,760.00; AEIOUX: 22.00; Robust terms: 106,175.74 ($\Gamma \cdot \pi$: 23,353.70; $\sum \rho$: 82,822.05)
Scenario-based robust	1,650.34	831,553.20	Expected cost: 726,496.40; Deviation penalty: 77,086.70; Violation penalty: 27,970.20

The deterministic model provides the lowest total cost under nominal conditions and serves as a practical baseline. The Γ-robust model maintains a similar solution structure while adding protection against bounded flow uncertainty, which is reflected in the modest increase in the total objective due to robust terms. The scenario-based robust model addresses a broader set of operating conditions by optimizing a single layout against multiple probabilistic scenarios; its total objective includes the expected scenario cost together with explicit penalties for cost variability and rare capacity exceedances. Overall, the three results are consistent with their modeling scopes: as uncertainty modeling becomes richer, the optimization balances average performance with stability across conditions.

6.2 Addressing the Research Questions

This section provides answers to the research questions introduced in Chapter 1. Each question is discussed based on the modeling framework, real-world implementation, and results presented in Chapters 3 to 5. The answers reflect how the proposed models evolved to handle the multi-block unequal-area facility layout problem (UA-FLP) under different forms of uncertainty, supported by actual production data from an industrial case study.

RQ1. *How can the unequal-area facility layout problem be modeled in multi-block industrial settings in a way that reflects practical flow structures and spatial constraints?*

This thesis formulated the UA-FLP as a multi-block Mixed-Integer Linear Programming (MILP) model. Departments of unequal area were assigned to predefined layout blocks while respecting spatial feasibility and minimizing total transportation costs. The model incorporated practical elements such as ramp-based inter-block routing, flow splitting across multiple ramps, and closeness penalties based on AEIOUX relationships. These additions allowed the model to reflect realistic internal logistics and layout decisions, as observed in the industrial case.

RQ2. *To what extent can a deterministic optimization approach provide feasible and cost-effective layout solutions when applied to a real-world production environment?*

The deterministic MILP model developed in Chapter 3 was implemented using actual flow and area data from a washing machine production plant. The results confirmed the model's ability to generate feasible layouts that comply with block dimensions, department sizes, and transportation logic. Expert review from the case company validated the practicality of the output layout. Moreover, the calculated cost was significantly lower than initial layouts, confirming that the deterministic model can provide cost-effective solutions when uncertainty is not explicitly considered.

RQ3. *How can data-driven techniques be integrated into facility layout modeling to account for flow uncertainty and improve the robustness of the solutions?*

Chapter 4 introduced a data-driven Gamma-robust formulation by applying the Bertsimas and Sim [2004] framework. Three years of historical flow data were analyzed, and a weighted two-sigma method was used to estimate uncertainty levels between department pairs. These values were embedded into the model through deviation parameters and a tunable protection level (Γ). The model balanced cost and robustness by protecting critical flows while avoiding over-conservatism. This integration of real flow data enabled the layout to remain stable and effective under uncertain operating conditions.

RQ4. *What modeling strategies can be used to address multiple operational disruption scenarios, and how can these strategies contribute to more resilient and adaptable facility layouts?*

To handle specific disruptions, Chapter 5 proposed a scenario-based robust optimization model based on the Mulvey framework. Ten predefined scenarios were generated to represent realistic disturbances such as ramp unavailability, flow spikes, and supply issues. Each scenario had its own material flow matrix, ramp capacities, and external costs, while sharing a common layout structure. Scenario-dependent variables controlled ramp assignments and flow decisions, allowing the model to flexibly redistribute flows and minimize cost penalties across disruptions. This structure helped produce layouts that were adaptable to multiple uncertain outcomes.

RQ5. *How effective are the proposed robust layout models in delivering practical decision support for long-term facility planning in manufacturing systems?*

Both robust models—the Gamma-robust (Chapter 4) and scenario-based (Chapter 5)—demonstrated strong performance in balancing cost efficiency with layout resilience. The Gamma model provided general protection against uncertainty, while the scenario-based model allowed for detailed control over specific operational risks. Scenario analyses confirmed that the final layout performed well across all ten disruption cases, with limited cost variation and effective ramp utilization. These results support the use of robust optimization in industrial layout planning and show that the models developed in this thesis can serve as reliable tools for decision-making under uncertainty.

6.3 Research Contributions

This thesis contributes to the academic and industrial understanding of robust facility layout planning by proposing a sequence of optimization models that integrate real-world constraints, uncertainty, and practical production data. The main contributions are summarized as follows:

- **Development of a multi-block layout optimization model for unequal-area departments:** A deterministic MILP model was formulated to assign departments to fixed-size blocks while minimizing total transportation cost. The model incorporated realistic constraints, including ramp-based inter-block routing, flow splitting, ramp capacity limits, and spatial closeness preferences using AEIOUX ratings. This formulation was designed to reflect internal logistics in industrial environments.

- **Application to a real manufacturing facility with actual production data:** The proposed models were applied to a home appliance production plant, using real input data on department areas, material flows, and spatial layout. This ensured that the models and results remained grounded in actual factory constraints, improving both feasibility and decision support relevance.

- **Design of a data-driven Gamma-robust optimization model:** Historical production data over a three-year period was used to quantify material flow uncertainty between departments. Based on the [Bertsimas and Sim, 2004] framework, a robust MILP model was developed with a weighted two-sigma method to define protection levels, helping to produce layouts that are resistant to variation without excessive cost.

- **Formulation of a scenario-based robust layout model for operational disruptions:** A robust MILP model was constructed to handle disruptions such as ramp unavailability, demand spikes, and supply issues. Each scenario had its own material flows, ramp capacities, and transportation costs, while the layout remained fixed. The model allowed flexible flow redistribution across scenarios, supporting robust and adaptive layout planning.

- **Demonstration of robustness and flexibility through industrial case experiments:** Scenario analyses confirmed that the proposed layout models can maintain high performance across a variety of uncertain conditions. The models achieved good cost stability, effective ramp utilization, and reasonable violation penalties, validating their usefulness in long-term facility layout planning under uncertainty.

These contributions extend existing literature on facility layout optimization by combining mathematical modeling, real-world data, and uncertainty handling. The proposed models are adaptable to multi-block layouts and are applicable to practical manufacturing environments, offering valuable insights for both academic research and industrial decision-making.

6.4 Limitations and Future Work

This study has proposed a robust and data-driven modeling framework for the unequal-area facility layout problem in multi-block industrial settings. While the models developed in this thesis are comprehensive and grounded in real-world data, several natural limitations arise from the scope and modeling assumptions, which offer opportunities for further academic exploration.

First, although the models were designed to be applicable to general multi-block layouts, the implementation and validation were carried out on a real-world use case with two fixed blocks. This was a deliberate choice to ensure industrial relevance and practical feasibility. Nevertheless, future research could explore the scalability and adaptability of the proposed models in larger and more complex multi-block systems with varying dimensions and constraints.

Second, to maintain mathematical tractability, certain operational factors such as safety corridors, machinery anchoring rules, and dynamic material handling conditions were abstracted. These factors can be significant in some industrial environments. Incorporating such spatial and operational constraints could improve realism but would likely require hybrid methodologies, such as integrating optimization with discrete-event simulation or digital twins.

Third, uncertainty in this thesis was addressed through both a data-driven Gamma-robust approach and a scenario-based formulation. While these techniques capture major sources of variability, other forms of uncertainty—such as stochastic fluctuations, real-time disruptions, or long-term demand shifts—may require alternative methods such as stochastic programming, distributionally robust optimization, or machine learning-enhanced layout planning.

Moreover, the models focused on static layout decisions based on fixed production patterns. In practice, layouts may need to evolve over time due to seasonal demand, product variety, or equipment upgrades. Extending the current framework to dynamic or time-dependent layout planning would be a valuable direction for future work.

Finally, this thesis focused on internal layout optimization. A promising direction would be to link layout decisions with other manufacturing concerns such as scheduling, energy use, labor allocation, or inventory strategy. Such an integrated approach could provide a broader decision support framework for factory design and long-term planning.

In conclusion, the limitations acknowledged in this study do not undermine the validity of the contributions but rather define a realistic scope for the research. They also open several promising pathways for future studies to expand upon and enhance the proposed models, both methodologically and in terms of practical impact.

6.5 Final Remarks

This thesis has addressed the complex challenge of facility layout optimization in multi-block industrial environments, with a special focus on uncertainty and practical applicability. Starting from a deterministic formulation and progressively incorporating data-driven uncertainty and scenario-based robustness, the research has proposed a structured modeling framework that is both academically rigorous and practically relevant.

The models developed in this work were not only tested using real production data from a home appliance factory but were also guided by actual constraints faced by layout planners. This close connection to industrial needs has helped ensure that the proposed solutions are more than theoretical contributions—they offer decision-making support that can be applied in real manufacturing systems.

While the models were designed with general applicability in mind, they also remained grounded in a specific use case, ensuring that each layer of complexity introduced served a clear purpose. From flow variation analysis to ramp capacity disruptions, each modeling element was motivated by real-world challenges. This balance between mathematical structure and operational realism is a key strength of the thesis.

Beyond its technical contributions, the study also provides a pathway for future research in the area of robust and adaptive manufacturing system design. As industries continue to face uncertainty, customization demands, and dynamic production environments, layout planning will remain a critical factor in operational efficiency. The ideas developed in this thesis may serve as a foundation for future work in integrating layout optimization with broader manufacturing strategies, including simulation, scheduling, and digital twin systems.

Overall, this research contributes to the advancement of robust facility layout planning by combining real data, uncertainty modeling, and multi-block optimization. It is hoped that the work presented here can support both academic inquiry and industrial decision-making in designing more resilient and efficient production systems.

6.6 Suggestions for Future Research

The models and findings presented in this thesis provide a comprehensive framework for addressing the unequal-area facility layout problem (UA-FLP) in multi-block industrial settings under uncertainty. However, as with any scientific contribution, this work opens several avenues for further exploration. Future research can expand the scope, enhance the modeling capabilities, and deepen the integration of layout planning with other elements of manufacturing systems. The following directions are suggested to guide future academic investigations:

- **Extension to generalized and large-scale multi-block systems:** Although the current study focused on a two-block layout as a practical case, the models were formulated with multi-block capability. Future studies can apply and adapt the proposed framework to more complex environments, including systems with heterogeneous block sizes, irregular spatial constraints, or multi-level facilities.

- **Incorporation of dynamic and time-evolving layouts:** Real-world production environments often experience changes over time due to product variety, seasonal demand, or technology upgrades. Extending the current static models to dynamic or reconfigurable layouts would allow researchers to address facility planning over multiple time horizons.

- **Integration with other operational decision layers:** A holistic approach that links facility layout planning with production scheduling, workforce allocation, energy consumption, or maintenance planning could offer more comprehensive decision support. Such integration may require the development of multi-level or multi-objective optimization models.

- **Adoption of advanced uncertainty frameworks:** While this thesis employed Gamma-robust and scenario-based methods, future research could explore stochastic programming, distributionally robust optimization, fuzzy sets, or hybrid probabilistic models to represent uncertainty more flexibly and realistically.

- **Coupling with simulation or digital twin environments:** Simulation-optimization techniques and digital twin technologies can provide a more interactive and iterative decision-making process. These tools allow validation of layout alternatives under realistic conditions before implementation and offer valuable feedback loops for continuous improvement.

- **Investigation of human-in-the-loop optimization frameworks:** A promising research direction is to study how expert input and planner preferences can be systematically integrated into the layout optimization process. This may involve the development of interactive optimization frameworks or multi-criteria decision-making methods that allow human decision-makers to guide or refine model outputs under different operational scenarios.

- **Exploration of industry-specific implementations:** While this research was based on the home appliance sector, the modeling framework can be adapted to other domains such as automotive, food processing, electronics, or pharmaceutical manufacturing. Investigating the specific constraints and objectives in these industries can lead to more tailored and impactful layout solutions.

These directions aim to extend the academic contributions of this thesis by addressing emerging industrial needs and incorporating more advanced computational techniques. Continued research in these areas will be essential for developing flexible, data-driven, and intelligent layout systems that can respond to the increasing complexity of modern manufacturing environments.

6.7 Contributions of the Thesis

This thesis has made several original contributions to the field of facility layout optimization, particularly in the context of uncertainty and multi-block manufacturing environments. The work integrates theoretical rigor, methodological innovation, and real-world applicability in a unified framework. These contributions can be grouped into three main categories: conceptual, methodological, and application-oriented.

Conceptual Contributions: The thesis introduced a structured approach for addressing the unequal-area facility layout problem (UA-FLP) in multi-block settings, a relatively underexplored yet practically important configuration. By framing the layout problem with realistic features such as flow splitting, ramp-based inter-block transport, and spatial closeness considerations, the study redefined the classical layout problem to better reflect the operational complexities observed in modern manufacturing systems. The work also positioned uncertainty as a central element of layout planning, demonstrating that robust models are essential for long-term resilience.

Methodological Contributions: The research developed a structured progression of optimization models, beginning with a deterministic MILP formulation and extending to two robust variants: a Gamma-robust model grounded in historical data and a scenario-based robust model that captures discrete disruption cases. These models addressed uncertainty using complementary approaches while preserving a consistent and scalable mathematical structure. The scenario-based formulation introduced the use of shared layout decisions alongside scenario-dependent control variables, enabling simultaneous evaluation of multiple uncertain conditions in a unified optimization model. The robust formulations were further enhanced with flow-splitting logic, ramp capacity constraints, and flexible inter-block routing, creating a versatile modeling foundation for real-world facility layout problems.

Application and Data-Driven Contributions: In contrast to many theoretical studies, this research was grounded in real industrial data from a home appliance manufacturing facility. The use case informed model design and validation, allowing the thesis to bridge the gap between academic modeling and practical layout decision-making. The robust formulations were supported by three years of flow data, and uncertainty levels were derived using a weighted two-sigma method, ensuring that protection parameters were rooted in observed variability. Scenario generation for the robust model reflected realistic operational disruptions, providing a framework that other researchers and practitioners can adapt to similar contexts.

Taken together, these contributions offer a comprehensive and practically grounded advancement of the facility layout literature. The models, data strategies, and theoretical formulations proposed in this thesis are expected to serve as a foundation for future academic work and industrial applications in robust layout design under uncertainty.

BIBLIOGRAPHY

Abedzadeh, M., Mazinani, M., Moradinasab, N., and Roghanian, E. (2013). Parallel variable neighborhood search for solving fuzzy multi-objective dynamic facility layout problem. *The International Journal of Advanced Manufacturing Technology*, 65:197–211.

Ahmadi, A., Pishvaee, M. S., and Jokar, M. R. A. (2017). A survey on multi-floor facility layout problems. *Computers & Industrial Engineering*, 107:158–170.

Altuntas, S. and Selim, H. (2012). Facility layout using weighted association rule-based data mining algorithms: Evaluation with simulation. *Expert Systems with Applications*, 39(1):3–13.

Amaral, A. R. (2024). A mixed-integer programming formulation for optimizing the double row layout problem. *Optimization Methods and Software*, 39(6):1428–1444.

Anjos, M. F. and Vieira, M. V. (2017). Mathematical optimization approaches for facility layout problems: The state-of-the-art and future research directions. *European journal of operational research*, 261(1):1–16.

Assem, M., Ouda, B. K., and Wahed, M. A. (2012). Improving operating theatre design using facilities layout planning. In *2012 Cairo International Biomedical Engineering Conference (CIBEC)*, pages 109–113. IEEE.

Badharinath, E., Reddy, V. D., Kumar, P. S., and Damodaram, A. (2024). Optimization of manufacturing plant layout using systematic layout planning (slp) method. In *MATEC web of conferences*, volume 393, page 01005. EDP Sciences.

Bertsimas, D. and Sim, M. (2004). The price of robustness. *Operations research*, 52(1):35–53.

Besbes, M., Zolghadri, M., and Affonso, R. C. (2021). A method to solve 2d facility layout problem with equipment inputs/outputs constraints using meta-heuristics algorithms. *Procedia CIRP*, 104:1698–1703. 54th CIRP CMS 2021 - Towards Digitalized Manufacturing 4.0.

Besbes, M., Zolghadri, M., Costa Affonso, R., Masmoudi, F., and Haddar, M. (2020). A methodology for solving facility layout problem considering barriers: genetic algorithm coupled with a* search. *Journal of Intelligent Manufacturing*, 31(3):615–640.

Bi, S., Shao, L., Zheng, J., and Yang, R. (2024). Workshop layout optimization method based on sparrow search algorithm: a new approach. *Journal of Industrial and Production Engineering*, 41(4):324–343.

Bozorgi, N., Abedzadeh, M., and Zeinali, M. (2014). Tabu search heuristic for efficiency of dynamic facility layout problem. *The International Journal of Advanced Manufacturing Technology*, 77:689–703.

Che, A., Zhang, Y., and Feng, J. (2017). Bi-objective optimization for multi-floor facility layout problem with fixed inner configuration and room adjacency constraints. *Computers Industrial Engineering*, 105:265–276.

Cheng, C., Adulyasak, Y., and Rousseau, L.-M. (2021). Robust facility location under demand uncertainty and facility disruptions. *Omega*, 103:102429.

Choi, S. H. and Kim, B. S. (2024). Intelligent factory layout design framework through collaboration between optimization, simulation, and digital twin. *Journal of Intelligent Manufacturing*, pages 1–15.

Chung, Y.-K. (1999). Application of a cascade bam neural expert system to conceptual design for facility layout. *Computers & Mathematics with Applications*, 37(1):95–110.

Das, S. K., Yu, V. F., Roy, S. K., and Weber, G. W. (2024). Location–allocation problem for green efficient two-stage vehicle-based logistics system: A type-2 neutrosophic multi-objective modeling approach. *Expert Systems with Applications*, 238:122174.

Derakhshan Asl, A. and Wong, K. Y. (2017). Solving unequal-area static and dynamic facility layout problems using modified particle swarm optimization. *Journal of Intelligent Manufacturing*, 28:1317–1336.

Deshpande, V., Patil, N. D., Baviskar, V., and Gandhi, J. (2016). Plant layout optimization using craft and aldep methodology. *Productivity Journal by National Productivity Council*, 57(1):32–42.

Díaz-Ovalle, C., Vázquez-Román, R., and Mannan, M. S. (2010). An approach to solve the facility layout problem based on the worst-case scenario. *Journal of loss Prevention in the Process Industries*, 23(3):385–392.

Dorrah, D. H. and Marzouk, M. (2021). Integrated multi-objective optimization and agent-based building occupancy modeling for space layout planning. *Journal of Building Engineering*, 34:101902.

Drira, A., Pierreval, H., and Hajri-Gabouj, S. (2007). Facility layout problems: A survey. *Annual reviews in control*, 31(2):255–267.

Emami, S. and Nookabadi, A. (2013). Managing a new multi-objective model for the dynamic facility layout problem. *The International Journal of Advanced Manufacturing Technology*, 68.

Feng, J. and Che, A. (2018). Novel integer linear programming models for the facility layout problem with fixed-size rectangular departments. *Computers Operations Research*, 95:163–171.

Gao, G., Feng, Y., Zhang, Z., Wang, S., and Yang, Z. (2023). Integrating slp with simulation to design and evaluate facility layout for industrial head lettuce production. *Annals of operations research*, 321(1):209–240.

Gao, J., Li, J., Ji, J., Liu, K., and Jiang, C. (2024). Multi-objective optimization of sponge facility layout in built-up urban areas. *Ecohydrology & Hydrobiology*, 24(1):11–24.

Garcia-Hernandez, L., Garcia-Hernandez, J., Salas-Morera, L., Carmona-Muñoz, C., Alghamdi, N., de Oliveira, J. V., and Salcedo-Sanz, S. (2020). Addressing unequal area facility layout problems with the coral reef optimization algorithm with substrate layers. *Engineering Applications of Artificial Intelligence*, 93:103697.

Grobelny, J. and Michalski, R. (2017). A novel version of simulated annealing based on linguistic patterns for solving facility layout problems. *Knowledge-Based Systems*, 124:55–69.

Guan, C., Zhang, Z., Liu, S., and Gong, J. (2019). Multi-objective particle swarm optimization for multi-workshop facility layout problem. *Journal of Manufacturing Systems*, 53:32–48.

Guo, W., Jiang, P., and Yang, M. (2023). Unequal area facility layout problem-solving: a real case study on an air-conditioner production shop floor. *International Journal of Production Research*, 61(5):1479–1496.

Heinbach, B., Burggräf, P., and Wagner, J. (2024). gym-flp: A python package for training reinforcement learning algorithms on facility layout problems. In *Operations Research Forum*, volume 5, page 20. Springer.

Hosseini-Nasab, H., Fereidouni, S., Fatemi Ghomi, S. M. T., and Fakhrzad, M. B. (2018). Classification of facility layout problems: a review study. *The International Journal of Advanced Manufacturing Technology*, 94:957–977.

Hussain, M. M., Azar, A. T., Ahmed, R., Umar Amin, S., Qureshi, B., Dinesh Reddy, V., Alam, I., and Khan, Z. I. (2023). Song: A multi-objective evolutionary algorithm for delay and energy aware facility location in vehicular fog networks. *Sensors*, 23(2).

Izadinia, N., Eshghi, K., and Salmani, M. H. (2014). A robust model for multi-floor layout problem. *Computers Industrial Engineering*, 78:127–134.

Ji, D., Zhang, Z., Liang, W., Wang, C., and He, Z. (2023). Mathematical formulation and a novel two-stage algorithm for double-row layout problem with fixed loading and unloading points. *Journal of Manufacturing Systems*, 69:242–254.

Jolai, F., Tavakkoli-Moghaddam, R., and Taghipour, M. (2012). A multi-objective particle swarm optimisation algorithm for unequal sized dynamic facility layout problem with pickup/drop-off locations. *International Journal of Production Research*, 50(15):4279–4293.

Jung, S., Ng, D., Lee, J.-H., Vazquez-Roman, R., and Mannan, M. S. (2010). An approach for risk reduction (methodology) based on optimizing the facility layout and siting in toxic gas release scenarios. *Journal of Loss Prevention in the Process Industries*, 23(1):139–148.

Kalita, Z. and Datta, D. (2024). A constrained multi-objective multi-floor facility layout problem. *International Journal on Interactive Design and Manufacturing (IJIDeM)*, 18(4):2597–2608.

Kaveh, M., Dalfard, V., and Amiri, S. (2014). A new intelligent algorithm for dynamic facility layout problem in state of fuzzy constraints. *Neural Computing and Applications*, 24.

Kaven, L., Huke, P., Göppert, A., and Schmitt, R. H. (2024). Multi agent reinforcement learning for online layout planning and scheduling in flexible assembly systems. *Journal of Intelligent Manufacturing*, 35(8):3917–3936.

Keyimu, M., Abulikemu, Z., and Abudurexiti, A. (2024). Quantitative evaluation of the equity of public service facility layout in urumqi city for sustainable development. *Sustainability*, 16(12):4913.

Kikolski, M., Ko, C., et al. (2018). Facility layout design–review of current research directions. *Engineering management in production and services*, 10(3).

Kim, M. and Chae, J. (2019). Monarch butterfly optimization for facility layout design based on a single loop material handling path. *Mathematics*, 7:154.

Klar, M., Hussong, M., Ruediger-Flore, P., Yi, L., Glatt, M., and Aurich, J. C. (2022). Scalability investigation of double deep q learning for factory layout planning. *Procedia CIRP*, 107:161–166.

Klar, M., Schworm, P., Wu, X., Simon, P., Glatt, M., Ravani, B., and Aurich, J. C. (2024). Transferable multi-objective factory layout planning using simulation-based deep reinforcement learning. *Journal of Manufacturing Systems*, 74:487–511.

Klausnitzer, A. and Lasch, R. (2018). Optimal facility layout and material handling network design. *Computers Operations Research*, 103.

Krishnan, K. K., Cheraghi, S. H., and Nayak, C. N. (2008). Facility layout design for multiple production scenarios in a dynamic environment. *International Journal of Industrial and Systems Engineering*, 3(2):105–133.

Ku, M.-Y., Hu, M. H., and Wang, M.-J. (2011). Simulated annealing based parallel genetic algorithm for facility layout problem. *International journal of production research*, 49(6):1801–1812.

Kubalík, J., Kurilla, L., and Kadera, P. (2023). Facility layout problem with alternative facility variants. *Applied Sciences*, 13(8):5032.

Kulturel-Konak, S. and Konak, A. (2013). Linear programming based genetic algorithm for the unequal area facility layout problem. *International Journal of Production Research*, 51.

La Scalia, G., Micale, R., Giallanza, A., and Marannano, G. (2019). Firefly algorithm based upon slicing structure encoding for unequal facility layout problem. *International Journal of Industrial Engineering Computations*, 10:349–360.

Lee, H.-Y. (2012). Integrating simulation and ant colony optimization to improve the service facility layout in a station. *Journal of Computing in Civil Engineering*, 26(2):259–269.

Lin, J., Shen, A., Wu, L., and Zhong, Y. (2024). Learning-based simulated annealing algorithm for unequal area facility layout problem. *Soft Computing*, 28:5667–5682.

Lin, Q. and Wang, D. (2019). Facility layout planning with shell and fuzzy ahp method based on human reliability for operating theatre. *Journal of Healthcare Engineering*, 2019(1):8563528.

Liu, H., Qiu, J., and Zhao, J. (2022a). A data-driven scheduling model of virtual power plant using wasserstein distributionally robust optimization. *International Journal of Electrical Power & Energy Systems*, 137:107801.

Liu, J. and Liu, J. (2019). Applying multi-objective ant colony optimization algorithm for solving the unequal area facility layout problems. *Applied Soft Computing*, 74:167–189.

Liu, J., Liu, S., Liu, Z., and Li, B. (2020). Configuration space evolutionary algorithm for multi-objective unequal-area facility layout problems with flexible bays. *Applied Soft Computing*, 89:106052.

Liu, J., Zhang, H., He, K., and Jiang, S. (2018). Multi-objective particle swarm optimization algorithm based on objective space division for the unequal-area facility layout problem. *Expert Systems with Applications*, 102:179–192.

Liu, S., Zhang, Z., Guan, C., Liu, J., Gong, J., and Dewil, R. (2022b). Mathematical formulation and two-phase optimisation methodology for the constrained double-row layout problem. *Neural Computing and Applications*, 34(9):6907–6926.

Loiola, E. M., De Abreu, N. M. M., Boaventura-Netto, P. O., Hahn, P., and Querido, T. (2007). A survey for the quadratic assignment problem. *European journal of operational research*, 176(2):657–690.

Lotfi, R., Kargar, B., Gharehbaghi, A., Afshar, M., Rajabi, M. S., and Mardani, N. (2022). A data-driven robust optimization for multi-objective renewable energy location by considering risk. *Environment, development and sustainability*, pages 1–22.

Lu, R., Bai, R., Huang, Y., Li, Y., Jiang, J., and Ding, Y. (2021). Data-driven real-time price-based demand response for industrial facilities energy management. *Applied Energy*, 283:116291.

Matai, R. (2015). Solving multi objective facility layout problem by modified simulated annealing. *Applied Mathematics and Computation*, 261:302–311.

Mayadunne, S., Rajagopalan, H. K., and Sharer, E. (2024). A multi-step mixed integer programming heuristic for warehouse layout optimization. *Supply Chain Analytics*, 8:100088.

Moslemipour, G., Lee, T., and Loong, Y. (2017). Performance analysis of intelligent robust facility layout design. *Chinese Journal of Mechanical Engineering (English Edition)*, 30:407–418.

Motahari, R., Alavifar, Z., Zareh Andaryan, A., Chipulu, M., and Saberi, M. (2023). A multi-objective linear programming model for scheduling part families and designing a group layout in cellular manufacturing systems. *Computers Operations Research*, 151:106090.

Muhayat, H. and Utamima, A. (2024). Solving unequal area facility layout problems with differential evolution and particle swarm optimization. *Procedia Computer Science*, 234:302–309.

Mulvey, J. M., Vanderbei, R. J., and Zenios, S. A. (1995). Robust optimization of large-scale systems. *Operations research*, 43(2):264–281.

Navidi, H., Bashiri, M., and Messi Bidgoli, M. (2012). A heuristic approach on the facility layout problem based on game theory. *International Journal of Production Research*, 50(6):1512–1527.

Nenzhelele, T., Trimble, J. A., Swanepoel, J. A., and Kanakana-Katumba, M. G. (2023). Mcdm model for evaluating and selecting the optimal facility layout design: A case study on railcar manufacturing. *Processes*, 11(3).

Ohmori, S. and Yoshimoto, K. (2021). A primal-dual interior-point method for facility layout problem with relative-positioning constraints. *Algorithms*, 14(2):60.

Oktaviani, A. and Utamima, A. (2024). Solving unequal area facility layout problems using population-based simulated annealing and ant colony optimisation. In *2024 Beyond Technology Summit on Informatics International Conference (BTS-I2C)*, pages 670–675. IEEE.

Peng, Y., Zeng, T., Fan, L., Han, Y., and Xia, B. (2018). An improved genetic algorithm based robust approach for stochastic dynamic facility layout problem. *Discrete Dynamics in Nature and Society*, 2018(1):1529058.

Pérez-Gosende, P., Mula, J., and Díaz-Madroñero, M. (2021). Facility layout planning. an extended literature review. *International Journal of Production Research*, 59(12):3777–3816.

Peron, M., Fragapane, G., Sgarbossa, F., and Kay, M. (2020). Digital facility layout planning. *Sustainability*, 12:3349.

Pourvaziri, H., Salimpour, S., Niaki, S., and Azab, A. (2021). Robust facility layout design for flexible manufacturing: a doe-based heuristic. *International Journal of Production Research*, 60:1–22.

Raja, S. and Anbumalar, V. (2016). An effective methodology for cell formation and intra-cell machine layout design in cellular manufacturing system using parts visit data and operation sequence data. *Journal of the Brazilian Society of Mechanical Sciences and Engineering*, 38:869–882.

Reisinger, J., Zahlbruckner, M. A., Kovacic, I., Kán, P., Wang-Sukalia, X., and Kaufmann, H. (2022). Integrated multi-objective evolutionary optimization of production layout scenarios for parametric structural design of flexible industrial buildings. *Journal of Building Engineering*, 46:103766.

Rubio, F., Llopis-Albert, C., and Valero, F. (2021). Multi-objective optimization of costs and energy efficiency associated with autonomous industrial processes for sustainable growth. *Technological Forecasting and Social Change*, 173:121115.

Saeidi, S. (2024). A two-objective mathematical model for solving the facility layout problem using fuzzy goal programming and artificial bee colony optimization. *Journal of Industrial Engineering and Management Studies*, 11(1):127–139.

Şahinkoç, M. and Bilge, Ü. (2018). Facility layout problem with qap formulation under scenario-based uncertainty. *INFOR: Information Systems and Operational Research*, 56(4):406–427.

Seyedi, S. B., Attari, M. Y. N., Ghadim, V. A. P., and Ala, A. (2024). An efficient computational model for unequal-area dynamic facility layout problems considering input/output locations under algorithms case. *Sādhanā*, 49(3):211.

Shahin, A. and Poormostafa, M. (2011). Facility layout simulation and optimization: an integration of advanced quality and decision making tools and techniques. *Modern Applied Science*, 5(4):95.

Sherali, H. D., Fraticelli, B. M., and Meller, R. D. (2003). Enhanced model formulations for optimal facility layout. *Operations Research*, 51(4):629–644.

Shoushtari, F., Zadeh, E. K., and Daghighi, A. (2024). Facilities layout in uncertainty demand and environmental requirements by machine learning approach. *International journal of industrial engineering and operational research*, 6(2):64–75.

Singh, S. P. and Sharma, R. R. (2006). A review of different approaches to the facility layout problems. *The International Journal of Advanced Manufacturing Technology*, 30:425–433.

Snyder, L. V. and Daskin, M. S. (2006). Stochastic p-robust location problems. *Iie Transactions*, 38(11):971–985.

Subulan, K., Varol, B., and Baykasoğlu, A. (2023). Unequal-area capability-based facility layout design problem with a heuristic decomposition-based iterative mathematical programming approach. *Expert Systems with Applications*, 214:119199.

Sun, X., Lai, L.-F., Chou, P., Chen, L.-R., and Wu, C.-C. (2018). On gpu implementation of the island model genetic algorithm for solving the unequal area facility layout problem. *Applied Sciences*, 8(9):1604.

Tayal, A. and Singh, S. P. (2018). Integrating big data analytic and hybrid firefly-chaotic simulated annealing approach for facility layout problem. *Annals of Operations Research*, 270:489–514.

Tongur, V., Hacibeyoglu, M., and Ulker, E. (2020). Solving a big-scaled hospital facility layout problem with meta-heuristics algorithms. *Engineering Science and Technology, an International Journal*, 23(4):951–959.

Usuga Cadavid, J. P., Lamouri, S., Grabot, B., Pellerin, R., and Fortin, A. (2020). Machine learning applied in production planning and control: a state-of-the-art in the era of industry 4.0. *Journal of Intelligent Manufacturing*, 31:1531–1558.

Vasudevan, K. and Son, Y.-J. (2011). Concurrent consideration of evacuation safety and productivity in manufacturing facility planning using multi-paradigm simulations. *Computers & Industrial Engineering*, 61(4):1135–1148.

Wei, X., Yuan, S., and Ye, Y. (2019). Optimizing facility layout planning for reconfigurable manufacturing system based on chaos genetic algorithm. *Production Manufacturing Research*, 7:109–124.

Xiao, X., Hu, Y., Wang, W., and Ren, W. (2019). A robust optimization approach for unequal-area dynamic facility layout with demand uncertainty. *Procedia CIRP*, 81:594–599. 52nd CIRP Conference on Manufacturing Systems (CMS), Ljubljana, Slovenia, June 12-14, 2019.

Yang, Z. and Lu, W. (2023). Facility layout design for modular construction manufacturing: A comparison based on simulation and optimization. *Automation in Construction*, 147:104713.

Zhang, Q. and Lin, Y. (2024). Integrating multi-agent reinforcement learning and 3d a* search for facility layout problem considering connector-assembly. *Journal of Intelligent Manufacturing*, 35(7):3393–3418.

Zhang, Z., Li, J., Lei, Z., Zhu, Q., Cheng, J., and Gao, S. (2024a). Reinforcement learning-based particle swarm optimization for wind farm layout problems. *Energy*, 313:134050.

Zhang, Z., Wu, L., Wu, Z., Zhang, W., Jia, S., and Peng, T. (2022). Energy-saving oriented manufacturing workshop facility layout: A solution approach using multi-objective particle swarm optimization. *Sustainability*, 14:2788.

Zhang, Z., Zhang, Y., Chen, F., Liu, J., and Wang, C. (2024b). Optimizing multi-row layouts with the through-aisle structure: A hybrid approach of teaching-learning-based optimization and linear programming. *IEEE Transactions on Automation Science and Engineering*.

Zhun, X., Liyun, X., and Xufeng, L. (2021). An improved pigeon-inspired optimization algorithm for solving dynamic facility layout problem with uncertain demand. *Procedia CIRP*, 104:1203–1208. 54th CIRP CMS 2021 - Towards Digitalized Manufacturing 4.0.

Zolfi, K. and Jouzdani, J. (2023). A mathematical model and a simulated annealing algorithm for unequal multi-floor dynamic facility layout problem based on flexible bay structure with elevator consideration. *Journal of Facilities Management*, 21(3):352–386.

Zúñiga, E. R., Moris, M. U., Syberfeldt, A., Fathi, M., and Rubio-Romero, J. C. (2020). A simulation-based optimization methodology for facility layout design in manufacturing. *IEEE Access*, 8:163818–163828.

Appendix A

APPENDIX A

Table A.1: Initial Material Flow Data

ID	Origin	Dest	Flow	ID	Origin	Dest	Flow
1	1	8	56	17	7	13	1200
2	1	10	1	18	8	9	1200
3	1	7	16	19	9	11	1200
4	1	9	13	20	10	8	34
5	1	13	1	21	11	20	1200
6	2	7	25	22	12	13	12
7	2	9	25	23	13	8	1200
8	3	8	15	24	14	10	20
9	4	7	34	25	15	10	20
10	4	10	30	26	16	7	8
11	4	13	2	27	17	18	8
12	5	7	25	28	17	19	8
13	5	8	0	29	18	7	60
14	5	10	16	30	19	10	20
15	5	21	50	31	2	3	15
16	6	11	64				

Table A.2: Department Closeness Ratings Based on AEIOUX Framework

Code A (Score: 16)				Code E (Score: 8)				Code I (Score: 4)			
No.	From	To	Code	No.	From	To	Code	No.	From	To	Code
1	7	13	A	10	1	8	E	20	2	7	I
2	8	9	A	11	5	21	E	21	2	9	I
3	9	8	A	12	6	11	E	22	4	7	I
4	9	11	A	13	7	18	E	23	4	10	I
5	11	9	A	14	8	1	E	24	5	7	I
6	11	20	A	15	11	6	E	25	7	2	I
7	13	7	A	16	18	7	E	26	7	4	I
8	13	8	A	17	20	21	E	27	7	5	I
9	20	11	A	18	21	5	E	28	7	8	I
				19	21	20	E	29	8	7	I
								30	8	10	I
								31	8	13	I
								32	9	2	I
								33	10	4	I
								34	10	8	I

Table A.3: Department Closeness Ratings - Code O (Score: 2)

No.	From	To	Code	No.	From	To	Code	No.	From	To	Code	No.	From	To	Code
35	1	7	O	40	5	10	O	45	10	14	O	50	12	13	O
36	1	9	O	41	7	1	O	46	10	15	O	51	13	12	O
37	2	3	O	42	8	3	O	47	10	19	O	52	14	10	O
38	3	2	O	43	9	1	O	48	11	12	O	53	15	10	O
39	3	8	O	44	10	5	O	49	12	11	O	54	19	10	O

Appendix B

APPENDIX B

Table B.1: Sample of Daily Shift-Based Flow Data Between Departments

Date	Year	Month	Shift	From Dept.	To Dept.	Vehicle Type	Flow Value	Description
2024-05-31	2024	5	2	1	8	AGV	43	Mainplant Semi Product Warehouse to Assembly Line
2024-05-31	2024	5	2	1	10	Tow Truck	1	Mainplant Semi Product Warehouse to Foamed Door Line
2024-05-31	2024	5	2	1	7	AGV	12	Mainplant Semi Product Warehouse to Pre Assembly Line
2024-05-31	2024	5	2	1	9	Tow Truck	11	Mainplant Semi Product Warehouse to Final Assembly Line
2024-05-31	2024	5	2	1	13	Tow Truck	1	Mainplant Semi Product Warehouse to Foamed Body Line
2024-05-31	2024	5	2	2	7	AGV	19	Plastic WH to Pre Assembly Line
2024-05-31	2024	5	2	2	9	Tow Truck	18	Plastic WH to Final Assembly Line
2024-05-31	2024	5	2	3	8	Tow Truck	12	Plastic WH to Assembly Line
2024-05-31	2024	5	2	4	7	Forklift	26	Mechanic WH to Pre Assembly Line
2024-05-31	2024	5	2	4	10	Forklift	21	Door panel to Door Assy
2024-05-31	2024	5	2	5	7	Forklift	18	Integration WH to Pre Assembly Line
2024-05-31	2024	5	2	5	10	Tow Truck	12	Integration WH to Foamed Door Line
2024-05-31	2024	5	2	5	21	Forklift	35	Integration WH to Other production
2024-05-31	2024	5	2	6	11	AGV	36	Packaging WH to Packaging Line
2024-05-31	2024	5	2	6	11	Conveyor	16	Packaging WH to Packaging Line
2024-05-31	2024	5	2	7	13	Conveyor	1039	Before PU to PU
2024-05-31	2024	5	2	8	9	Conveyor	1006	After PU to Final Assy
2024-05-31	2024	5	2	9	11	Conveyor	848	Final Assy to Packaging Line
2024-05-31	2024	5	2	10	8	Tow Truck	28	Door Assy to After PU
2024-05-31	2024	5	2	11	20	Forklift	734	Packaging Line to Fin. WH
2024-05-31	2024	5	2	12	13	Forklift	10	Compressor WH to Foamed Body Line
2024-05-31	2024	5	2	13	8	Conveyor	1033	PU to After PU
2024-05-31	2024	5	2	14	10	Forklift	14	Door Glass to Door Assy
2024-05-31	2024	5	2	15	10	Forklift	17	Gasket to Door Assy
2024-05-31	2024	5	2	16	7	Forklift	6	Pipe Roll WH to Pre Assembly Line
2024-05-31	2024	5	2	17	18	Forklift	6	Extruder to CTF
2024-05-31	2024	5	2	17	19	Forklift	6	Extruder to DTF
2024-05-31	2024	5	2	18	7	Manual	46	CTF to Before PU
2024-05-31	2024	5	2	19	10	Manual	16	DTF to Door Assy
2024-05-31	2024	5	2	2	3	Forklift	12	Plastic to Raw Mat. WH